T.R.
ONDOKUZ MAYIS UNIVERSITY
INSTITUTE OF GRADUATE STUDIES
DEPARTMENT OF ANATOMY

THE MORPHOMETRIC ANALYSIS OF CRANIAL STRUCTURES RELATED TO THE TRANSSPHENOIDAL APPROACHES TO SELLA TURCICA BY NEUROIMAGING

Doctoral Dissertation

Haidar ALHAMADANI

Supervisor

Assoc. Prof. Dr. Mennan Ece PIRZIRENLI

SAMSUN
2021

THESIS ACCEPTANCE AND APPROVAL

This study entitled **"The Morphometric Analysis of Cranial Structures Related to the Transsphenoidal Approaches to Sella Turcica by Neuroimaging"**, prepared by **Haidar ALHAMADANI** and supervised by **Assoc. Prof. Dr. Mennan Ece PIRZIRENLI**, was found successful and unanimously accepted by committee members as Ph.D. thesis of the Department of Anatomy, following the examination on the date 13.08.2021

Committee members		Signature	Final decision
Chairman **(supervisor)**	Doç.Dr. Mennan Ece PİRZİRENLİ Ondokuz Mayıs Üniversitesi Anatomi Anabilim Dalı		☒ Accept ☐ Reject
Member	Prof. Dr. Aymen WARILLE Ondokuz Mayıs Üniversitesi Histoloji ve Embriyoloji Anabilim Dalı		☒ Accept ☐ Reject
Member	Doç. Dr. Aslı TANRIVERMİŞ SAYİT Ondokuz Mayıs Üniversitesi Radyoloji Anabilim Dalı		☒ Accept ☐ Reject
Member	Doç.Dr. Zülal ÖNER Ondokuz Mayıs Üniversitesi Anatomi Anabilim Dalı		☒ Accept ☐ Reject
Member	Dr. Öğr. Üyesi Murat GÖLPINAR Hitit Üniversitesi Tıp Fakültesi Anatomi Anabilim Dalı		☒ Accept ☐ Reject

This thesis has been approved by the committee members that already stated above and determined by the Institute Executive Board.

CONFIRMATION

… / … / …

Prof. Dr. ALİ BOLAT
Head of Institute of Graduate Studies

ETHICAL STATEMENT

I have prepared this research work in accordance with the rules of the Institute of Graduate Studies, Ondokuz Mayis University for Doctorate’s Degree Thesis. It contains correct and complete information which was gathered at different stages of the thesis. I also adhered to scientific ethics and all information sources from which I benefited are indicated in the reference section.

Signature
13/ 08 /2021
Haidar ALHAMADANI

DECLERATION OF THESIS ORIGINALITY REPORT

Thesis title: The Morphometric Analysis of Cranial Structures Related to The Transsphenoidal Approaches to Sella Turcica by Neuroimaging.

As a result of the originality report taken by me from the plagiarism detection program on 12/ 07 /2021 for the thesis mentioned above, it was found as follows;

Similarity rate : 17%

Single resource rate : 2%

Signature
13/ 08 /2021
Prof. Dr. Mennan Ece PİRZİRENLİ

ÖZET

SELLA TURCICA BÖLGESİNE TRANSSFENOİDAL GİRİŞİMLERLE İLGİLİ KRANİYAL YAPILARIN NÖROGÖRÜNTÜLEME TEKNİĞİ İLE MORFOMETRİK ANALİZİ

Haidar AlHAMADANI
Ondokuz Mayıs Üniversitesi
Lisansüstü Eğitim Enstitüsü
Anatomi Anabilim Dalı
Doktora tezi, August / 2021
Danışman: Doç. Dr. Mennan Ece PİRZİRENLİ

Sinus sphenoidalis, transsfenoidal prosedürde Sella Turcica a doğru önemli bir koridordur, ancak pnömatizasyon modelindeki yüksek değişkenliği, kemik işaretlerinin şeklini değiştirerek preoperatif yol haritasını oldukça önemli bir konuma taşımaktadır.

Tezin amacı, nazal açıklıktan Sella turcica'ya kadar olan en kısa yol ile ilgili yer işaretlerini belirlemede bilgisayarlı tomografi (BT) taraması fizibilitesini test etmektir.
RAdiant DICOM yazılımı kullanılarak, 100 denek (transsfenoidal operasyon geçirmiş 26 erkek ve 24 kadın olmak üzere hipofiz adenomlu 50 hasta) ve diğer 50 kişinin (normal paranazal sinüs BT'si olan 27 erkek ve 23 kadın) Multiplan BT taraması analiz edildi. Katılımcıların yaşları 21 ile 85 arasında ortalama 50 idi. Verileri 2014-2020 yılları arasında OMÜ Tıp Fakültesi hastanesinin elektronik arşivinden alınmıştır.

Radyolojik ve istatistiksel analizler, Sella'yı işaret eden temporal bölgeye ait landmark niteliğindeki yapıların koordinatlarının belirlenmesinin önemini ortaya koydu. Columella'dan Sella tabanına olan ortalama mesafe karşılaştırılabilir bir ölçüm değeriydi. Bu çizgi hastalarda ön sfenoidal duvarı 7 cm sonra kesmekteydi.

Bu kesişme, hastalarda daha yüksek ortalama ile planum sphenoidale'nin 1.5 ila 2.5 cm altındaydı. Hastalarda %66, her iki grupta da %83 oranında doğal ostium bu çizginin değişik derecelerde ve concha nasalis superior ve cellula ethmoidale'nin üzerindeydi. Omurga benzeri gelişmiş bir ön duvar, vakaların çoğunda kaydedilirken, posterior imklinasyon vakaların dörtte birinden fazla olmadığı bildirildi. Sella'ya açılan septa, vakaların %40 ila %60'ından fazlasında bulunmaktaydı. Optik ve karotislerde şişkinlik vakaların ancak dörtte birinde rapor edilmiştir. Optikokarotid girintileri, processus clinoidalis anterior pnömatizasyonu ile yüksek oranda ilişkiliydi. Son olarak, interkarotid mesafe hasta grubunda anlamlı olarak daha yüksekti.

Buna göre, radyolojik raporu navigasyon rotasıyla ilgili ayrıntılarla zenginleştirmek için transsfenoidal müdahale için üzerinde anlaşmaya varılmış bir yol haritası oluşturmak üzere BT taramasının kullanılmasını önermekteyiz. Bu, herhangi bir ameliyat zorluğuna ilişkin ameliyat öncesi farkındalığı artırır ve işlemin güvenliğini ve etkinliğini artırmaya yardımcı olur.

Anahtar Sözcükler: Transsfenoidal Yaklaşım, Cerrahi Işaretler, Operatif Anatomi.

ABSTRACT

THE MORPHOMETRIC ANALYSIS OF CRANIAL STRUCTURES RELATED TO THE TRANSSPHENOIDAL APPROACHES TO SELLA TURSICA BY NEUROIMAGING

Haidar AlHAMADANİ
Ondokuz Mayıs University
Institute of Graduate Studies
Department of Anatomy
PhD., August /2021
Supervisor: Assoc. Prof. Dr. Mennan Ece PİRZİRENLİ

Sphenoid sinus is an important corridor toward the Sella Turcica in transsphenoidal surgery but its high variability in pneumatization pattern changes the shape of its bony landmarks making preoperative road map highly indicated. The objective of the study is testing feasibility of CT scan in identifying landmarks related to the shortest path from the nasal aperture to the Sella tursica.

Using Radiant DICOM software, multiplanner CT scan of 100 individuals (50 pituitary adenomas patients subjected to transsphenoidal surgery ;26 men and 24 females, and another 50 control cases having normal paranasal sinus CT, 27 males and 23 females. Participants ages were between 21 to 85 average 50. Their data retrieved from the electronic archive of OMU teaching hospital between 2014 and 2020. Radiological and statistical analysis revealed that coordinates of temporal marker refereeing to Sella were ready to specify .Mean distance from columella to the sellar floor was comparable .That line intersected with the anterior sphenoidal wall at an average 7cm in patients .This intersection was below the planum sphenoidale 1.5 to 2.5 cm with higher average in patients.Natural ostium was above this line in varying degrees a well as above superior concha and ethmoid cell in 66% in patients and 83 in both groups. Advanced keel-like anterior wall was registered in majority of cases while the posterior inclination was reported not more that one fourth of cases. Septa leading to the Sella extended between 40 to more than 60% of cases. Bulging of optic and carotids where reported not more than one fourth of cases. Optico-carotid recesses was highly correlated with the pneumatization of the anterior clinoid process. Finally, the inter-carotid distance was significantly higher in patients' group. Accordingly, we recommend using CT scan to create an agreed upon road map for transsphenoidal intervention and to enrich the radiological report with details related to navigation route that increases preoperative awareness of any operative difficulty and helps raising the procedure's safety and effectiveness.

Keywords: Transsphenoidal Approach, Surgical Landmarks, Operative Anatomy.

ACKNOWLEDGEMENT

I am deeply grateful to associate prof. Mennan Ece, Prof. Aymen, prof. Mehmet head of anatomy department and prof. Cengiz head of neurosurgical department OMU and all the professors and colleagues in anatomy, radiology, neurosurgery and statistics departments for their invaluable assistance and genuine support. Moreover, I would like to offer my special thanks to my lovely wife for her unwavering support and belief in me.

Haidar AL-HAMADANI

TABLE OF CONTENTS

ABBREVIATIONS

ACP	Anterior Clinoid Process
CSF	Cerebrospinal Fluid
CT scan	Computed Tomography Scan
3D MPR mode	Multiplanar Reformatting Mode
DICOM	Digital Imaging And Communications In Medicine
ICA	Internal Carotid Artery
MPCT	Multiplanar Computerized Tomography
MRI	Magnetic Resonance Imaging
OCR	Opticocarotid Recess
SPSS	Statistical Package For The Social Scienses
SS	Sphenoid Sinus
ST	Superior Turbinate
TSA	Transsphenoidal Approach

LIST OF FIGURES

LIST OF TABLES

1. INTRODUCTION

1.1. Background

Pituitary gland tumors represent up to 15% of intracranial neoplasms. Although most of them are benign but their abnormal hormonal effect or enlarging mass effect may lead to grave complications, systematic as in acromegaly in response to abnormal hormonal secretion or local as blindness due to local compression of optic nerves or chiasm (Laws et al., 2017).

Surgical removal of pituitary adenomas has been considered of pivotal role in treating these adenomas. Intracranial sub frontal approach was considered routine route to reach the pituitary. However, the continuous search for a safer approach avoiding brain retraction with the rapid refinement of the visualizing technology and the instrumentations have led to reconsidering an old previously abandoned approach. That was the trans-nasal trans-sphenoidal approach to the Sella Turcica (Laws et al., 2017).

The Sella Turcica and the residing pituitary gland lie in the midline projecting partially inside the sphenoid sinus. This sinus is the aerated sphenoidal body that lies posterior and superior to the nasal cavity acting as a transition between the Sella and the nose (Rhoton, 2002).

The critical understanding of this relationship and its limitations, with the proper magnification and illumination and well-designed instruments have made the transsphenoidal approach to Sella turcica relatively safe and feasible route. With continuous refinement sphenoid sinus has become a corridor for an expanding list of indications to reach the skull base extending from the planum sphenoidale above to the foramen magnum below (Arbolay et al., 2009).

Moreover, surgeons are shifting their favor from the trans-septal trans-nasal to endonasal approach with the use of endoscopes. This allows surgeon to see landmarks while making his way through the anterior wall of the sphenoid to reach the seller floor. Recognitions of landmarks throughout the procedure is an absolute requirement to recognize the surgical targets and to avoid dreadful complications (Kabil et al., 2005; Bora et al., 2020).

Any ways, the instruments commonly used in endonasal transsphenoidal approach to the Sella are straight and need a straight line stretching from the exterior passing the nasal cavity and then through the anterior wall of the sphenoid to reach the Sellar floor and the pituitary beyond (Palmer and Chiu, 2013).

Making our way through this corridor urges us to present the relevant anatomy from a new perspective like that encountered by the surgeon making it handy at the disposal of the operating team to use it for operative navigation even without expensive technology (Ismail et al., 2018).

1.2. The Problem

Transsphenoidal approach to Sella Turcica is a challenging endeavor from anatomical point of view to mention the least. Therefore, variations in nasal and sphenoidal path should be addressed preoperatively otherwise using long instruments in a limited space to reach a deeply seated target would be loaded with difficulties and potential complications (Dasar and Gokce, 2016).

Bolger et al (1999) found that lack of orientation and unfamiliarity with the regional anatomy is a prominent risk factor that may lead to serious complications. Medico-legal litigation showed an increase in claims related to anatomical errors which is strongly linked to insufficiency in mastering relevant surgical anatomy (Ellis, 2002).

Although CT scan has been around for decades, radiologists and surgeons do not reach an agreement upon the best way to evaluate the surgical path in this type of operations. It seems that reports offered little in terms of management decisions. Moreover, standard list of relevant surgical landmarks is lacking, although this list would ease much the task of mapping out a safe journey toward the Sella (Deutschmann et al., 2013). But unfortunately, a concise consistent template focusing on clinically relevant information, even addressing relevant negative findings, tailored to a specific patient in question has yet to be produced (García-Garrigós et al., 2015).

Optimizing the quality of reporting with checklists would improve interdisciplinary communication and identification of critical variations for surgeons in training (Error et al., 2018). This practice would eventually improve the outcome (Ahmadipour et al., 2016; Peris-Celda et al., 2013; Guo et al., 2018).

1.3. The Trend in Presenting Sphenoidal Morphometry

During our literature review, we realized that the sets of measurements related to the sphenoid sinus, chosen by researchers, followed no specific pattern. the researchers did not show why they picked up some of the measurements while leaving others. Even the correlation with the surgical need was not clearly specified.

1.4. Purpose of the Study

Therefore, we took this opportunity to examine the basic relevant landmarks related to the shortest path available between the anterior nostril and the sellar floor. This path is the same one taken by the endoscope and other instruments used in transsphenoidal approach to excise a pituitary adenoma.

We want to show if multiplanar CT could reveal relevant basic surgical nasal and sphenoidal landmarks for endonasal transsphenoidal approach to Sella turcica. Morphometrically analyzing these landmarks and establishing their baseline data would construct a clearer picture for the path towards the sphenoid sinus and surrounding structures.

Moreover, clarifying the relation between intra-sphenoidal landmarks and the intracranial structures, will pave the road towards Sella with accurately oriented trajectory and the safest working angles, without inflicting any additional damage.

We think that this initiative would aid in formulating preop CT protocol to standardize the work of inter-disciplinary radiologist-surgeon team and improve level of communication between its members. Using this knowledge intraoperatively may make it feasible to accomplish the job even without expensive intraoperative navigation tool. This goal is of utmost importance for making the work of beginners easier, by using multiplanar CT as a powerful tool for teaching surgically oriented anatomy.

2. GENERAL INFORMATION AND LITERATURE REVIEW

2.1. The Importance of Sphenoid Sinus in Skull Base Surgery

The sphenoid bone is of central importance to skull base surgery. As it is lying at the interface between the nasal cavity anteriorly and the Sella Turcica posteriorly, it allows approaching the pituitary gland inside Sella Turcica and the surrounding structures at the skull base using the trans-nasal trans-sphenoidal air-filled natural corridors (Solari et al., 2012).

2.2. Development of Sphenoid Sinus

The skull base structures are clustered together in the early stages of development. During fetal development, the paranasal sinuses originate as invagination of the nasal mucosa into facial and cranial bones. The sphenoid sinus presents as minute cavities at birth, develops postnatally and changes continuously during childhood starting from the first year of life. Anterior pneumatization of the anterior site of the sphenoid sinus would be obvious at the 4th year of life. It also extends backward into the presellar area and subsequently expands into the area below and behind the Sella Turcica. The pneumatization process progresses slowly in a temporal-posterior direction (Hiyama, 2015) Reaching its full adult size during adolescence usually by the age of 12, although the exact age is still under debate. Skull base development is a slow, gradual, age-dependent, sex-independent process. Although one study has shown that the male sphenoid is larger than the female's counterpart (Budu et al., 2013; Zolar et al., 1994; Kikuchi et al., 2015; Pirinc et al., 2019; Banu et al., 2014).

2.3. Why it is Variable?

As the sphenoid sinus is created by pneumatization of the sphenoid body anterior and inferior to the Sella, it is subjected to considerable variation in degree of pneumatization resulting in variable sizes, shapes, and patterns of septation.

The recesses and the prominences seen inside the sphenoid sinus are related to the neurovascular structures embedded around the sphenoid sinus (Pirinc et al., 2019). The pattern of location of these landmarks may be considered conventional but it also varied probably because of the pattern of sphenoid pneumatization (Unlu et al., 2008). In contrast to that, an article by Kim et al (2013) showed that although pneumatization may change the shape of the sphenoid sinus when seen from inside but the relative location of the surrounding structures remains the same.

Pneumatization and septation variability could make the identification of sphenoidal bony landmarks during surgery more difficult when the pneumatization is not well developed around the structure so its bulge inside the sinus cavity would not be easily recognized.

2.4. Enlargement of the Sinus

As mentioned above, the sinus enlarges by the extension of the pneumatization. As such it may extend to the roots of the pterygoid processes or greater wing of the sphenoid and even to the basilar occipital bone. Absorption of bone may occur with advancing age enlarging the sinus even more. These changes significantly alter the corridors used by surgeons to reach lesions in and above the skull base (Pirinc et al., 2019).

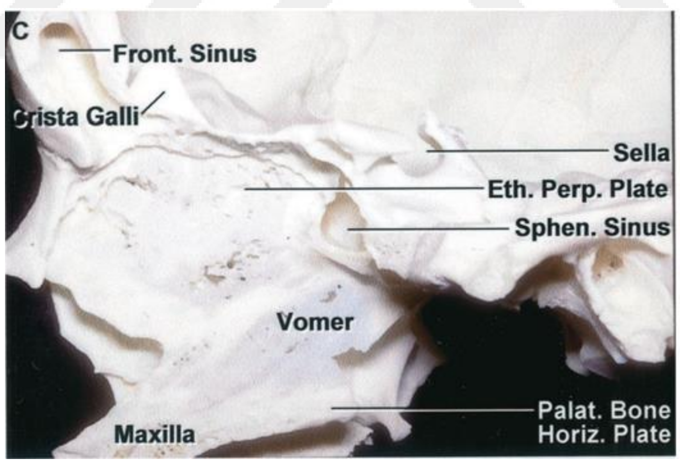

Figure 2. 1. Nasal septum leading to anterior wall of sphenoid sinus (Rhoton, 2002)

2.5. Surgical Anatomy of Sphenoid Related to Transsphenoidal Approach

Being relatively deep behind a restricted door, reaching the Sella Turcica at the skull base by passing the sphenoid sinus requires a roadmap. This map should identify the relevant milestones that guide the intervention.

In this way, the operator would be equipped with detailed knowledge of anatomy of the area in question, before starting the surgical adventure.

Fortunately, the new versions of neuroimaging like CT scan can perfectly reveal these relevant anatomical features thanks to its ability to show the contrast between bones, air and soft tissue. The surgeon should seize the opportunity in using this technology to meet the requirements for preoperative planning on individual basis (Guo et al., 2018). Bear in mind that intraoperative stereo taxis and navigation device is no way a substitute to knowledge in detailed relevant surgical anatomy (Wei et al., 2013).

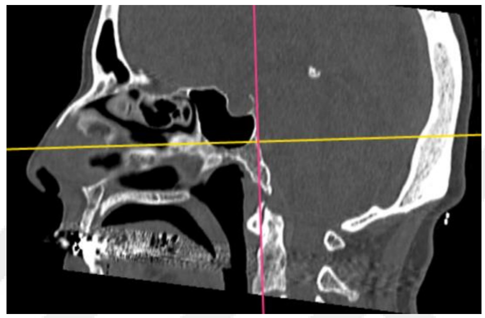

Figure 2. 2. Mid-sagital revealing the Sella bulging inside the sphenoid sinus

2.6. Does Detailed Anatomy Really Matters?

For interventions with endoscopy or surgical microscopy, anatomical details, especially minor individual variations, have become significant to the success rate of operations. Detailed knowledge in anatomy would decrease time of the operation and limit the chance to injure critical structures by mistake (Palmer and Chiu, 2013).

It is crucial to take into consideration that avoidable errors occurring due to lack of anatomical knowledge are met with little public tolerance nowadays and are increasingly associated, now more than ever, with more public claims (Ellis, 2002).

2.7. Related Nasal Anatomy

2.7.1. The Anterior Nares

The anterior nares are the external portion of the nostrils (nose). They open into the nasal cavity and allow the inhalation. It is usually wide enough to allow the passage of instrumentation for sellar surgery (Uzun and Ozdemir, 2014).

2.7.2. Nasal Bones

These are bilateral symmetrical paired bones that form the bridge of nose. They articulate superiorly with the frontal bone at the nasofrontal suture, laterally with the maxillary bones and in front with the upper lateral nasal cartilage. The nasofrontal angle create a depression called nasion.

2.7.3. Columella

It is the central column that extends between the tip of the nose to just in front of the nasal spine. It is composed by the two cartilaginous medial crura and the anterior edge of the nasal septum with the skin covering.

2.7.4. Piriform Aperture

The passages created by the nasal cartilages will soon lead to the piriform aperture which is the bony opening created by the lateral and inferiorly situated maxillary bones and the superiorly situated nasal bones. It is wider below than above and divided at the midline by a bony nasal septum. Anterior nasal spine lies at the base of the piriform aperture in the midline and could be considered a reference for the midline (Palmer and Chiu, 2013).

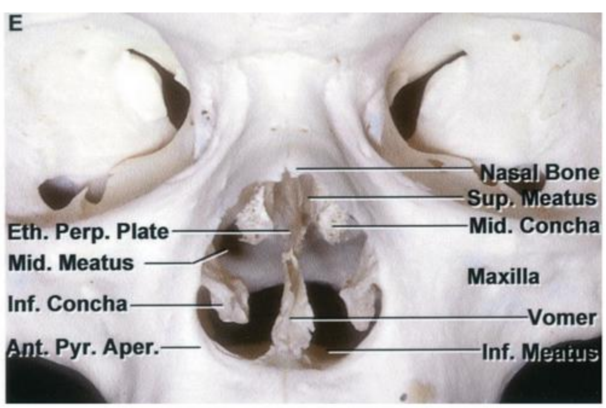

Figure 2. 3. Piriform aperture (Rhoton, 2002)

The two nasal cavities are wider below than above and enclosed by the cribriform plate as a roof, while the floor is formed by the hard and soft palate. The hard palate is made up of two bones of the facial skeleton, located in the roof of the mouth. The bones are the palatine process of the maxilla and the horizontal plate of palatine bone. The hard palate spans the alveolar arch formed by the alveolar process that holds the upper teeth. Nasal septum forms the medial wall of the two nasal cavities, while ethmoid, maxillary bones, and inferior nasal turbinate constitute the lateral wall. The anterior wall of the aerated body of the sphenoid bone forms the posterior wall of the nasal cavity. But inferior to the posterior wall, the nasal cavity is continuous with the nasopharynx through the posterior nasal aperture which is called the choana.

2.7.5. The Septum

The nasal septum is the key midline support structure of the nose and is composed of the quadrilateral cartilage anteriorly, perpendicular plate of the ethmoid bone, and vomer bone posteriorly.

This septum extends posteriorly leading to the choana inferiorly and the anterior wall of sphenoid superiorly. Choana is the aperture that leads from the nasal cavity toward the nasopharynx immediately below the sphenoid sinus (Twigg et al., 2017).

Quick and efficient endoscopic access can be impeded by factors like a deviated nasal septum and/or very narrow nasal cavity (Cusimano et al., 2013).

The anterior septal cartilage develops as the unossified portion of the perpendicular plate of the ethmoid. This cartilage attaches posteriorly to the perpendicular plate, posteroinferiorly to the vomer, and superiorly to the nasal bones and upper lateral cartilages. Antero inferiorly, the cartilage resides within a canal extending anteriorly towards the anterior nasal spine and maxillary crest.

2.7.6. The Perpendicular Plate of the Ethmoid Bone

This plate represents the posterior and superior part of the septum. It articulates posteriorly with the sphenoidal crest. The posterior septum and sphenoid keel attached to it make a consistent midline reference. The perpendicular plate is attached superiorly to the ethmoidal cribriform plate at the narrow roof of the nasal cavity.

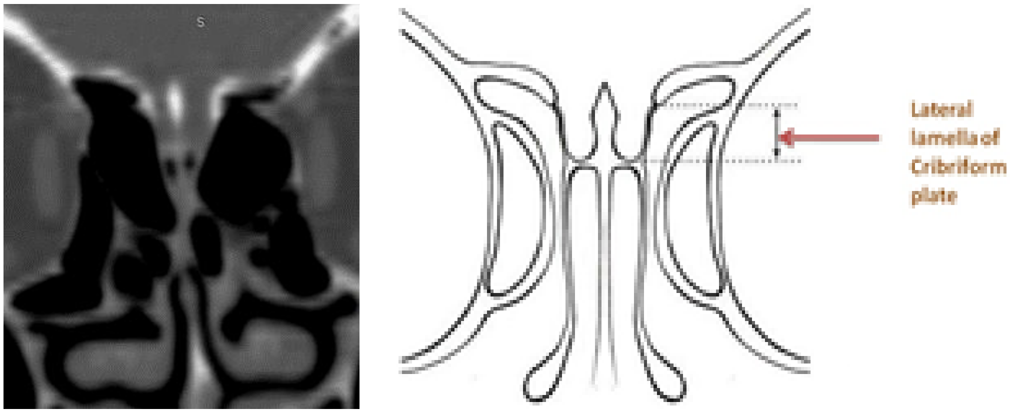

Figure 2. 4. Perpendicular plate of ethmoid and its lateral lamella

At the cranial side of the cribriform plate lie the olfactory bulbs separated only by the dura. The word cribriform means with multiple fenestrations. These tiny foramina transmit the olfactory nerves wrapped by dural sleeves from the bulb to the olfactory mucosa that lines the nasal part of the cribriform plate and adjacent nasal septum and lateral walls on either side.

The cribriform plate has a thin lateral lamella that could easily be fractured from manipulating olfactory mucosa or bone with resultant CSF leak (Palmer and Chiu, 2013).

2.7.7. Lateral Lamella of the Cribriform Plate and the Risk of CSF Leak

Nasal roof has two components: thick lateral frontal and thin medial ethmoidal. The latter is called lateral lamella of the cribriform plate. This thin lamella could descend to lie in the confined area between the ethmoidal cells posteriorly. This descent brings with it the base of the frontal lobes and makes the skull base closer thus increasing the chance of iatrogenic injury with potential CSF leak (Halil Arslan el al., 1999; Zufiría et al., 2015).

Superior or supreme turbinate is attached to the lateral lamella of ethmoid. These turbinates in addition to the posterior ethmoid cells cover the anterior face of the sphenoid. With well pneumatized sphenoidal rostrum the ostium of the sphenoid sinus, which is the natural opening of this air cell, can be situated more laterally covered more by the turbinate. In such a situation, the only way to expose the ostium is to lateralize or remove the turbinate. This very act could put the lateral lamella into danger of fracture with resultant anosmia and CSF leak.

Low cribriform plate is more prone to injury during surgical interventions (Twigg et al., 2017). Also, age-related global loss of bone density should add to this problem (Ganjaei et al., 2019).

2.7.8. Vomer

Vomer is the diagonal rectangle that stretches between the rostrum of the sphenoid posteriorly and the maxilla infero-anteriorly and the palatine bone infero-posteriorly. It is a separate bone representing part of the nasal septum. It has two posterior wings that embrace the rostrum of sphenoid. The whole circumference of this joint is called Spehno-vomerine suture. Uygun et al. considered this suture a landmark for safe entry into the sphenoid as its removal is used to step into sphenoidal stage where sellar base becomes clearly visible (2016).

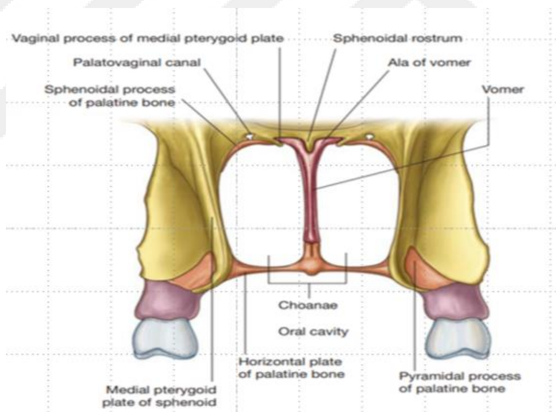

Figure 2. 5. Vomer articulation with the sphenoid rostrum (Drake, et al, 2009)

2.7.9. The Lateral Wall of Nasal Cavity

The lateral walls have irregular surfaces due to the presence of 3 pairs of bony extensions called turbinate. These turbinates are useful as orientation landmarks during surgery. Below each turbinate is a space called meatus that contains the communication apertures between the paranasal cavities and the nasal one. The paranasal cavities are air filled sinuses that develop inside the cranial and facial bones.

The inferior concha (turbinate) is an independent bone, it is the most inferior and anterior turbinate. It could be recognized while the endoscope is still in the nasal vestibule before entering piriform aperture.

Advancing the endoscope posteriorly parallel to the inferior concha, lateral to the nasal septum would lead us to the choana; the posterior nasal aperture acting as a gate leading to the nasopharynx.

The upper limit of the choana represents a well-defined line for the lower limit of the anterior sphenoidal wall. The predetermined path toward the Sella is somewhere above the choana immediately lateral to the nasal septum and medial to the medial wall of the posterior ethmoidal cell which cover most of the anterior face of the sphenoid sinus.

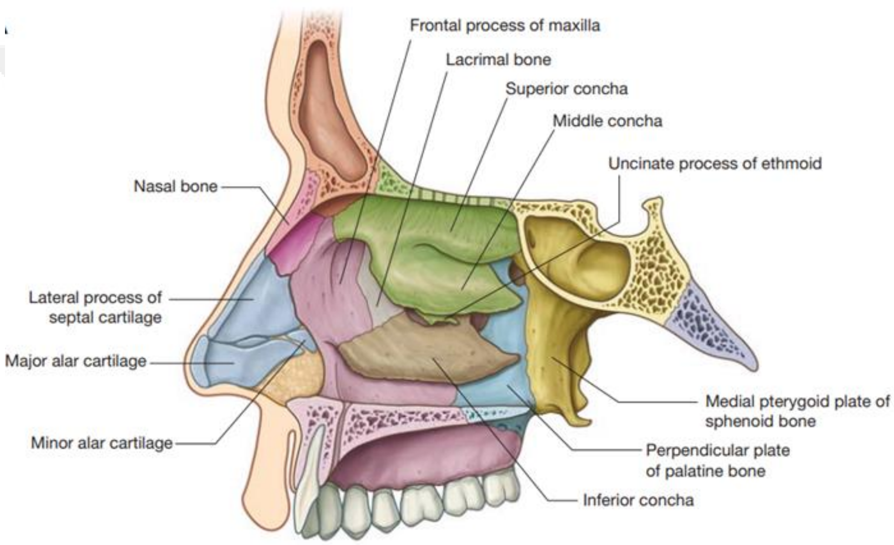

Figure 2. 6. Lateral wall of the nasal cavity (Drake et al., 2009)

2.7.9.1. Middle Turbinate (concha)

The middle turbinate, as the superior one, is a part of the ethmoid bone. Its anterior margin is about 2 cm behind that of the inferior turbinate. Its head could be pneumatized defined as a concha bullosa. A wide concha bullosa can severely narrow the nasal cavity, precluding the further progression of the endoscope (Twigg et al., 2017; Banu et al., 2014; Halil Arslan et al., 1999).

2.7.9.2. The Tail of Middle Turbinate

Moving posteriorly, the tail of the middle turbinate would lead to the sphenopalatine foramen. This foramen is located at the superior aspect of the vertical plate of the palatine bone (Palmer and Chiu, 2013).

2.7.9.3. Sphenopalatine Artery and Blood Supply of Nasal Cavity

The pterygopalatine fossa lying behind the posterior wall of the maxillary sinus has the maxillary artery and its terminal branches as sphenopalatine artery (Karkas et al., 2020). This artery branches before passing through the sphenopalatine foramen. Its medial branch, the posterior septal, passes above the choana, below the sphenoidal ostium reaching towards the nasal septum (Dutta, 2020). On the other hand, the lateral branch; the posterior lateral nasal artery reaches the lateral wall of the nasal cavity supplying middle and inferior conchae. These branches supply blood to up to 90% of the nasal mucosa and could be injured if the anterior wall of sphenoid is tackled (Pádua and Voygels, 2008; Wei et al., 2013).

Eordogh et al found that sphenopalatine foramen is at large lies at the transition of the superior and middle nasal meatus (2018) transmitting the above-mentioned branches of the sphenopalatine artery into the nasal cavity. There were no cases with a single artery at the plane of the sphenopalatine foramen.

The nasal cavity is supplied from external carotid artery via sphenopalatine branch mentioned above with an addition from the labial artery, a branch of facial artery supplying the nasal vestibule. The branches of the greater palatine artery also contribute by supplying the inferior anterior septum.

There are also branches from internal carotid artery contributing to the blood supply to the nasal cavity. They are the anterior and posterior ethmoid arteries, branches of the ophthalmic artery. They contribute significantly to nasal blood flow. The anterior is larger and is the major blood supply to the anterior third of both the septum and lateral nasal wall while the posterior ethmoid artery supplies a small area on the superior turbinate and adjacent septum, and it may be absent.

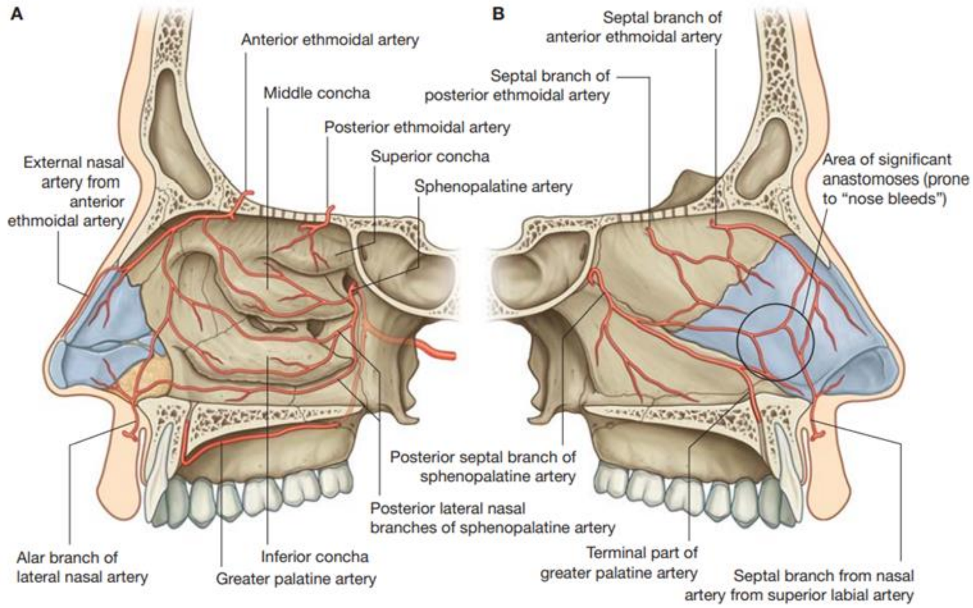

Figure 2. 7. Arterial supply to the nasal cavity (Drake et al., 2009)

Little area on the anterior septum has a network of vessels from anterior ethmoid and sphenopalatine artery called Kiesselbach plexus. There is another plexus located posteriorly on posterior nasal floor and middle turbinate irrigated mainly by sphenopalatine artery which is called Woodruff plexus (Palmer and Chiu, 2013).

2.7.9.4. Superior Turbinate (concha)

This ethmoid bony projection is located both posterior and superior to the middle turbinate; sometimes accompanied by a small upper fold called the supreme turbinate. It lies between the posterior ethmoidal cell and the nasal septum in a narrow gutter that is bounded superiorly by the lamina cribrosa at the cranial floor and opened inferiorly towards the posterior part of nasal cavity (Eweiss et al., 2012).

Because of its close relation with the natural ostium of the sphenoid sinus it was suggested as a reference point to identify that ostium whether medial or lateral to its posterior inferior end (Kim e al., 2001).

2.7.9.5. The Supreme Turbinate (concha)

This fold was usually ignored since it is the smallest between the conchae, rarely seen intraoperatively and thought to be rather insignificant. The posterior ethmoid cell may open under it and the sphenoid ostium may lie medial to it (Gotlib et al., 2018).

2.7.9.6. Ethmoid sinuses

Lying in front of the anterior wall of sphenoid sinus these cells block the excess to the sphenoid sinus leaving only an extremely limited gutter between the medial wall of the cell laterally and the nasal septum medially. The superior concha being an extension from the ethmoid blocks the access even more as it should be lateralized to reveal the ostium of the sphenoid sinus. Sometimes, if additional working room is required in transsphenoidal skull base surgery, bilateral ethmoidectomies must be done to pave the road for the instruments (Cusimano, 2013).

2.7.9.7. Onodi Cells (cellula spheno-ethmoidalis)

More than 100 years ago Onodi described the possible posterior extension of the posterior ethmoid sinus toward the posteriorly-situated sphenoid sinus occupying its superior and lateral aspect. He called this air-filled space cellula spheno-ethmoidalis of Onodi cell. When present, the sphenoid would be pushed downward away from the optic nerve which may show itself hanged inside this space. It is found in up to 8%–14% of patients. It may disorient the operator as it may guide him wrongly towards the orbital apex and the middle cranial fossa (Halil Arslan et al., 1999; Kaplanoglu et al., 2013; García-Garrigós et l., 2015; Hiyama et al., 2015).

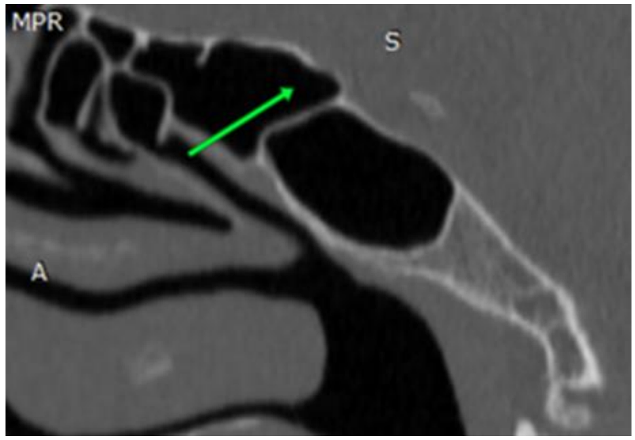

Figure 2. 8. Posterior inclination of the anterior wall of the sphenoid as a diagnostic feature for Onodi cell

2.7.10. Spheno-Ethmoid Recess

There is a space at the most posterior and superior aspect of the nasal cavity. This space is lying between the posterior ethmoid cell laterally and the nasal septum medially and the anterior face of the sphenoid posteriorly. It is guarded anteriorly by the superior turbinate. The sphenoidal ostium usually opens into this space (Dutta, 2020).

2.7.10.1. Anterior Wall of Sphenoid

The anterior wall of the sphenoid resembles the prow of a boat seen from the front (Eweiss et al., 2012). This bulge of anterior wall of sphenoid was considered by Wei et al the best place for entry to sphenoid sinus (2013).

2.7.10.2. Narrow Gate Toward the Sphenoid

The posterior part of the lateral nasal wall, carrying the posterior ethmoid cell, with the posterior wall of the nasal cavity is a major obstacle in transsphenoidal surgery because although it is a confined area, it is the only area available for direct access to sphenoidal sinus. Sometimes lateralizing the structures related to the lateral wall is enough to pass towards the sphenoid. Otherwise, some of these structures should be removed to create the required space to reach the inside of the sphenoid in moving towards the sellar floor (Mutlu, 2001).

2.7.10.3. Sphenoidal Ostium

The sphenoid sinus drains via a natural ostium(opening) into the sphenoethmoidal recess. Less frequently the sinus drains into the posterior ethmoid cell. The ostia are in a superior position related to the floor of the sinus, about 1.5 cm above the choana at each side of the midline (Dutta, 2020).

Several studies have shown that the posteroinferior end of the superior turbinate is the most reliable endonasal landmark for identification of the natural ostium of the sphenoid sinus. As it is located superior and medial to this end of the superior turbinate (Gupta et al., 2013; Nesibe Yilmaz, 2015; D'Souza et al., 2013; Eweiss et al., 2012; Gotlib et al., 2018; Kim et al., 2001)

If the sphenoid sinus and the sphenoid rostrum are well pneumatized, the ostium may also lie lateral to the posterior end of the superior turbinate partially covered by its lower part. In these cases, ostium may not be readily recognizable, so lateralization of the superior turbinate must be performed (Kim et al., 2001). The operator should be careful in protecting the lateral lamella of the cribriform plate on which these turbinates are inserted because pushing the turbinate laterally may fracture the cribriform plate leading to iatrogenic rhinorrhea (Dutta, 2020).

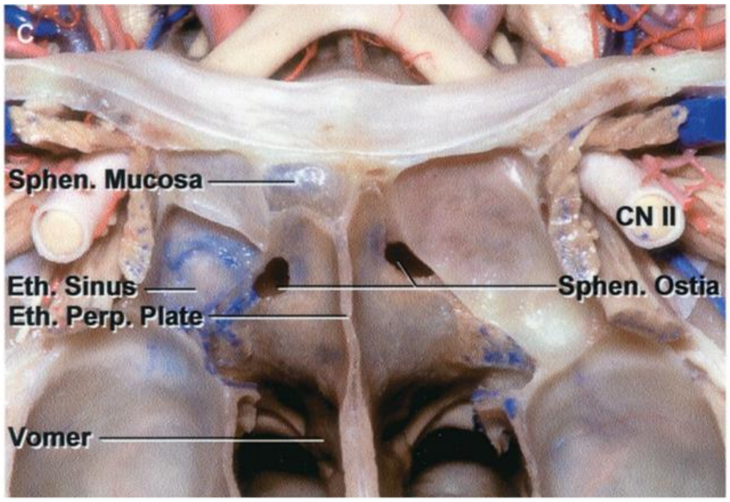

Figure 2. 9. Ostia of sphenoid (Rhoton, 2002)

D'Souza et al stated that it was not easy to locate the ostium during endoscopy (2013). So, they suggested that the ostium could be found by ascending with the endoscope from the superior aspect of the choana for 1.5 cm along the spheno-ethmoid recess on each side of the perpendicular ethmoid plate. The angulation degree of the instruments was at 34.3° \ 62.7 mm from nasal sill (Rhoton, 2002).

2.7.10.4. Opening the Anterior Wall of The Sphenoid in Transsphenoidal Approach to Sella Turcica

The opening may be tailored to extend predominantly to either side 1 to 1.5 cm, depending on the size, shape, and location of the tumor. The opening is enlarged to allow passage of instruments of sufficient size and angle to remove the tumor. The level of the ostia is marked as the upper limit of the opening into the sphenoid sinus (Rhoton, 2002).

Cappabianca et al. pointed out that there is no need to identify the ostium to do sphenoidotomy so it may be unnecessary to take the risk of pushing the superior concha (2012). Also, Dutta stated that manipulating the superior turbinate could be avoided by ignoring the localization of the ostium for sphenoidotomy (2020). Despite that, our literature review revealed that the articles still revolving around the concept of identifying the ostium as a prerequisite in transsphenoidal process.

2.7.11. Sphenoid Bone

This bone composes part of the anterior and middle fossae of the skull base. Lying between temporal and occipital bones posteriorly and frontal and ethmoid bones anteriorly. It has a central body with laterally outstretched 2 lesser wings, and another two greater wings, which spread upward from the lower part of the body. The medial end of the lesser wing in represented by the anterior clinoid process. Another 2 processes are projecting downwards from the body. They are called pterygoid processes. Each one has medial and lateral pterygoid plates. The lesser wing forms the posterior part of the orbital roof. While the greater wing composes the lateral orbital wall. The solid cubical body, resting immediately above the nasopharynx, would change with time to an aerated room called sphenoid sinus. Its anterior face forms the upper posterior limit of the nasal cavity. The sinus is communicating bilaterally with the nasal cavity via a pair of openings lying at a level higher than the sphenoidal floor called the ostia (Rhoton, 2002).

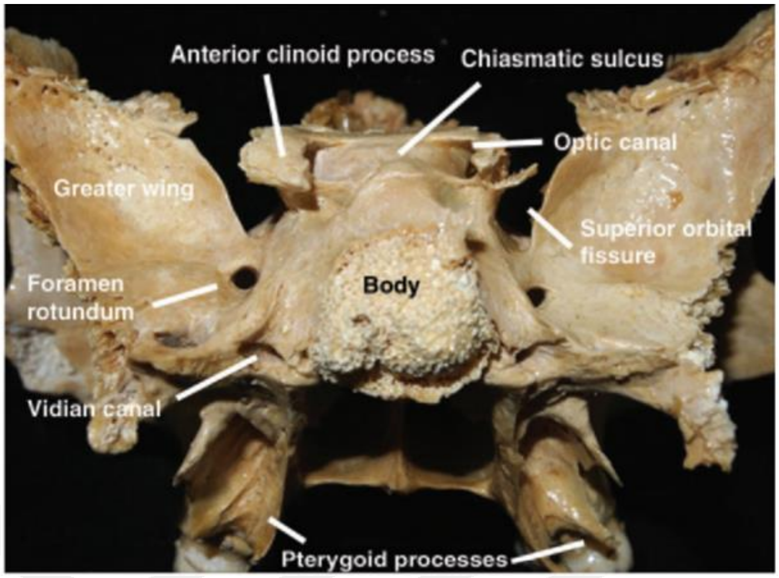

Figure 2. 10. Sphenoid bone parts and extensions (García-Garrigós et al., 2015)

Intracranially, the upper posterior aspect of the body has a nest occupied by the pituitary gland which extends inferiorly from the basal side the brain. This nest is called sella turcica. It is bounded anteriorly by the tuberculum sellae and posteriorly by the dorsum sellae. There is a shallow groove in front of the tuberculum sellae called the chiasmatic sulcus for the optic chiasm that connects both optic nerves as soon as they exit the optic foramina. The dorsum acts as a bony bridge that limits the sella posteriorly. It is also continuous with the downward slope of the clivus towards the foramen magnum. The upper clivus is formed by the sphenoid bone while the lower part is a part of the occipital bone (Rhoton, 2002).

With gradual pneumatization of this body of the sphenoid the sellar site would leave a bulge inside the sinus indicating its location. Eventually only a thin bone would be in between the dural pouch surrounding the pituitary gland and the mucosa of the sphenoid sinus. Having a midline sellar bulging, inside the centrally located sphenoid sinus that faces the nasal cavity, the nasal approach to the pituitary turned to be feasible. But despite this feasibility, using this relatively deep and limited corridor needs improvement in our understanding of the local anatomy using the available imaging modalities and also improvement in the instrumentations (Rhoton, 2002).

2.7.11.1. Relations

Brain lobes and related cranial nerves and major vessels are intimately related to the cranial surface of the sphenoid bone as it forms part of the anterior fossa, posterior orbit, middle fossa, the roof of the nasal cavity, sphenoid sinus, pterygopalatine and infratemporal fossae. Its bony plates not only provide barriers between various locations, but they also transmit nerves and vessels between the extra and intracranial spaces and vice versa (Hiyama et al., 2015).

2.7.11.2. Neural Relations

The basal surface of the frontal lobes, with the olfactory tracts and the gyri and recti, lies over the body and the smooth upper surface of the lesser wing. While the temporal lobes are embraced by the greater wings which separate them from the contents of the orbital cavities. The optic chiasm is located at the midline posterior to the planum sphenoidale which represents the roof of the sphenoidal body. The upper aspect of the brain stem lies just behind the posterior surface of the sphenoid, behind the Sella and the upper part of the clivus. The sphenoid has bilateral sets of foramina that transmit the second down to the sixth cranial nerves (Hiyama et al., 2015).

2.7.11.3. Arterial and Venous Relationships

The body of the sphenoid has 2 lateral grooves for the internal carotid arteries. Intracranial groove appears as bulging inside a well aerated sphenoid sinus. They lie anterolateral to the sellar bulge coming out of the posterior wall of the sinus. On the other hand, the basilar artery lies behind the posterior wall of the sinus as well as behind and below the Sella. The cavernous sinuses also lie lateral to the cranial side of the lateral wall of the body, enclosing the internal carotid arteries and the third to the 6^{th} cranial nerves heading toward the orbit. Moreover, anterior and posterior inter-cavernous sinuses stretch between the two cavernous sinuses in front and behind the pituitary (Farımaz et al, 2019).

2.7.11.4. Sphenoid Bone Foramina

Superior orbital fissure is a cleft between the superior lesser wing and the inferior greater wing. The oculomotor, trochlear, abducent and ophthalmic nerves enter the orbit through this fissure.

The optic strut is a bridge of bone that separates between the superior orbital fissure inferiorly and the optic canal medially and superiorly. The strut extends between the base of anterior clinoid process and the side of sphenoid sinus body. With adequate pneumatization the base of that strut may appear as a dimple if seen from within the sinus (Meybodi et al., 2018; Hiyama et al, 2015).

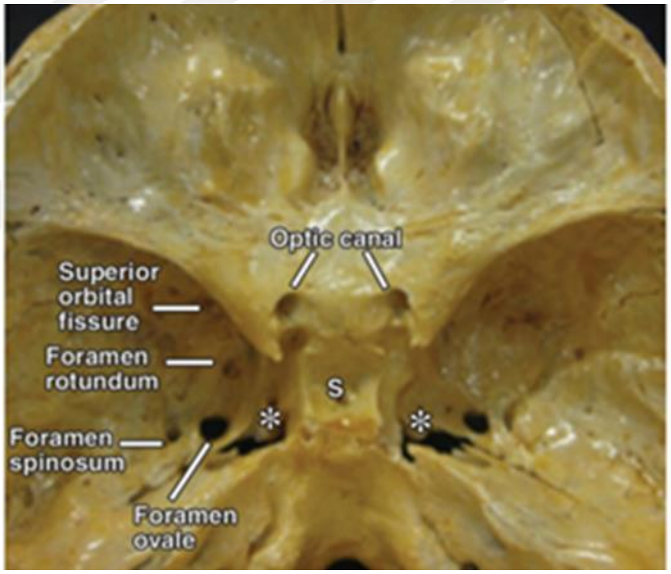

Figure 2. 11. Sphenoidal foramina (García-Garrigós et al., 2015)

The optic canal is only half a centimeter long and its medial wall is the longest one (Peng-Fei et al., 2015). Optic canal may bulge inside the sphenoid sinus at the posterolateral corner (Dessi et al., 1994). Optic canal bulging inside the sinus may put the nerve at risk of injury taking into consideration that this part of the optic nerve has a relatively vulnerable blood supply. Even Güler et al found that shear and compressive injury would be more harmful on the medial and inferior proximal portions of the optic nerves (2019). Unfortunately, this is the area adjacent to the sphenoid sinus (DeLano et al., 1996).

The foramen rotundum, ovale, and spinous are located from anterior to posterior near the junction of the body and greater wing. The maxillary and mandibular nerves and the middle meningeal artery pass through these foramina in precisely the same given order (Hiyama et al, 2015).

The pterygoid (vidian) canal courses inside the floor of the sphenoid sinus extending between the internal carotid artery canal that conveys the petrous part of this artery posteriorly and the upper aspect of the pterygopalatine fossa anteriorly, just posterior and superior to the sphenopalatine foramen (Hiyama et al, 2015).

2.7.11.5. Types of Sphenoid Sinus Pneumatization

Sphenoid pneumatization begins around the first year of age with a period of significant enlargement between 3 and 6 years of age. As it is advancing posteriorly with time, it reaches the anterior sellar wall around the age of 7 (Banuet al., 2014). Recent data demonstrates that the sinus continues to pneumatize through the third decade of life (Pirinc et al., 2019).

Pneumatization of sphenoid is classified according to the posterior limit of the aerated site seen by in a sagittal plane. In the present study, the classification proposed by Hammer and Radberg was adopted which classified the sphenoid sinus into three types: conchal, presellar, and sellar (Hammer and Radberg, 1961).

The conchal type is when the area in front and below the Sella is a solid bone and found mostly in children before complete pneumatization. In presellar type, the cavity of the sphenoid does not extend passing the coronal plane of the anterior sellar wall. It represents 24% according to Locatelli (2017). The sellar is the most common one where the cavity extends to variable extent below the anterior face of the Sella. It may reach as far as the dorsum sellae and the posterior plate of the Clivus. It is found to represents 74% of case (Hamberger et al., 1961; Hamid et al., 2008; Renn and Rhoton, 1975; Kim, 2013; Perondi et al., 2013; Carrabba et al., 2013; Lazaridis et al.,2010; Ismail et al., 2018).

2.7.11.6. Surgical Importance of Pneumatization

There is a positive correlation between the degree of pneumatization of sphenoid with the easiness of executing the transsphenoidal surgical intervention. The greater the extend of air-filled space inside sphenoid sinus, the higher the possibility of having an obvious intra-sphenoidal landmark. So, the sellar type is the most favorable for this type of surgery (Locatelli et al., 2017).

2.7.11.7. Pneumatization and Operative Complication

Preoperative critical evaluation of the degree of pneumatization has been associated with lesser incidence of operative complications as cerebrospinal fluid (CSF) leak (ELKammash et al., 2014).

2.7.11.8. Lateral Pneumatization

The sphenoid sinus cavity may extend also towards the greater wing laterally or the pterygoid process inferiorly. In doing so, the cavity must pass a line extending between the medial edge of foramen rotundum and that of vidian canal. In case of lateral pneumatization the maxillary or vidian nerves may bulge inside the sinus (Kikuchi, 2015; Secchie al., 2018; Terra et al., 2006; Sildiroglu et al., 2015).

2.7.11.9. Another Types of Classifications

More detailed classifications describing the extension of air into multiple directions, have been suggested by new researchers addressing the increasing need to evaluate the sphenoid as a common corridor toward more extended list of adjacent structures at the skull base other than the Sella itself. However, previously mentioned classification is still applicable for approaching a pituitary tumor (Jian et al., 2010; Güldner et al., 2012; Wiebracht and Zimmer, 2014; Pirinc et al., 2019; Hiyama et al., 2015; García-Garrigós et al., 2015).

2.7.11.10. Lesser Wing Pneumatization

The sinus cavity may extend from the base of optic strut reaching the lesser wing and the anterior clinoid process. This type of pneumatization tends to make the optic canal protrude inside the posterolateral angle of the sinus sometimes with dehiscent thin bone and exposed optic nerve. This phenomenon would increase the vulnerability of the optic nerve to iatrogenic injury, especially in case of complex anatomy as in having Onodi cell (Dessi et al., 1994; Rahmati et al., 2016; Sildiroglu et al., 2015; DeLano et al., 1996).

2.7.11.11. Width and Depth

The depth of the sphenoid sinus is around 2cm while the thickness of the anterior sellar wall and sellar floor is expected to be 0.4 mm in sellar type (Rhoton, 2002), while the largest width of sphenoid is less than 4 cm (Mutlu et al., 2001; Wiebracht and Zimmer, 2014; Carrabba et al., 2013; Sildiroglu et al., 2015; Kajoak et al., 2013).

2.7.11.12. The Interior Design of the Sphenoid Sinus

2.7.11.13. The Septa of Sphenoid Sinus

Variable patterns of pneumatization leave behind a variable pattern of septation. Sphenoidal septa usually show variable pattern of ramification, thickness, attachment site and number of septa.

Even with one major sagittal septum that separates the sinus into at least two major cavities, this septum is usually deviated to one side producing asymmetrical cavities. No more than 20 % sinuses have shown midline septum. Moreover, there may be minor septa orienting in multiple directions creating multiple small cavities. Or may be there is no septum, and the sinus shows one major cavity. When the inter-sinus septum is there, 20% of cases its posterior attachment ends on the carotid protuberance. If there was more than one, 87% of cases would have at least one septum inserted on the carotid (Sildiroglu et al., 2015; Secchi et al., 2018; Carrabba et al., 2013; Fernandez-Miranda et al., 2009; Zada et al., 2011; Nesibe, 2016).

2.7.11.14. The Interior of the Sinus After Removal of Septa

The endoscopic approach to the sphenoid has made it possible to examine the landmarks of the sinus from inside. These landmarks usually associated with the intracranial structures (Hiyama et al., 2015; Palmer and Chiu, 2013; Ismail et al., 2018).

The roof of the sinus is represented by the anterior smooth surface of the planum sphenoidale lying at the midline, behind the cribriform plate of ethmoid. Its posterior limit is the anterior limbus of a shallow depression usually evident only on the intracranial side. This depression is the chiasmatic sulcus that extends between the two optic foramina housing the optic chiasm above and in front of the sellar bulge. The sulcus is limited posteriorly by another limbus. The sulcus usually has no remarks on the intrasinus side of the bony roof. Therefore, the planus is seen extending posteriorly toward the transverse depression lying between the roof and the upper limit of the sellar bulge. In that case, the chiasmatic sulcus can only be referenced from inside above the tuberculum recess between both optic prominences (Solari et al., 2012; DeLanoet al., 1996; Unlu et al., 2008).

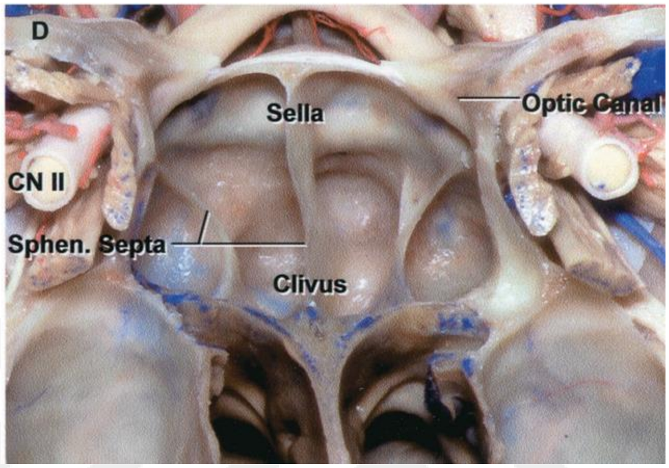

Figure 2. 12. The interior of the sphenoid sinus showing the septa and the sellar bulge (Rhoton,2002)

The above-mentioned transverse depression between the roof and the sellar bulge is called the tuberculum recess. Its lateral ends are called medial optico-carotid points. Calculating the site of these points is important in case of suprasellar exposure (Nunes et al., 2016).

Diaphragma sellae, covering the pituitary gland inside the Sella, is attached anteriorly to the tuberculum sellae which is represented by tuberculum recess if seen from within the sinus. The shortest inter-carotid distance is usually at this level. Protuberances of the optic nerves diverge anteriorly from the posterolateral angles of the roof (Peris-Celda et al., 2013; Solari et al., 2012).

2.7.11.15. The Posterior Wall

The sellar bulge is evident at the superior aspect of the posterior wall of the sphenoid sinus separated from the roof only by tuberculum recess. The smooth sellar bulge would be obvious only in sellar type and would be ill-defined in the conchal or presellar types. Sella is the site where the pituitary gland resides in, extending from the basal surface of the brain. From the intracranial perspective, the Sella is bounded anteriorly, posteriorly, and inferiorly by bony plates. The roof and lateral walls of the sella are formed by dural folds. The dura of the roof is called the diaphragm sellae, attached anteriorly to the tuberculum sellae and stretches laterally between the anterior and posterior clinoid processes. It has a central opening for the stalk of the pituitary with its blood supply. An arachnoid pouch filled with CSF may also extend inferiorly through the diaphragm toward the Sella. The sellar bulge creates an angle above it with the planum and below it with the clivus. Parasellar carotids, bulging in a C shape anterior and lateral to the sellar face, embrace the sellar prominence bilaterally (Farımaz et al., 2019; Carrabba et al., 2013; Zada et al., 2011; Peris-Celda et al., 2013; Solari et al., 2012). The right and left carotid arteries are at the closest distance at the tuberculum recess. Paraclival carotids guard the clivus in between, below the level of sellar bulge (Yeung et al., 2018; Marcati et al., 2018; Carrabba et al., 2013).

2.7.11.16. Clivus

Aktas and colleagues in their cadaveric study identified clival recess more that half of the samples. Basilar plexus lines the internal surface of the clivus and forms an extensive inter-cavernous venous connection across the midline. The abducent nerve enters the cavernous sinus close to the inferior segment of the paraclival intra-cavernous carotid artery at the upper clivus. Both are tightly surrounded by dense collagenous tissue (Aktas et al., 2013). The basilar artery in the basal cistern with its branches, and the lower neighboring cranial nerves with the midline brain stem, all lie immediately behind the clivus (Perondi et al., 2013; Jian Wang et al., 2010; Peris-Celda et al., 2013; Solari et al., 2012).

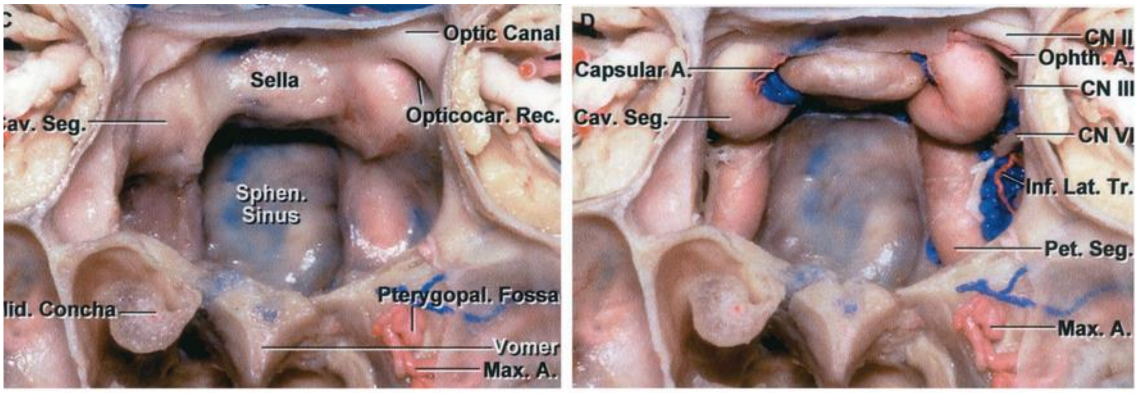

Figure 2. 13. The interior of the sphenoid sinus showing the sellar, optic and carotid bulges and the opticocarotid recess in between. The picture on the right shows the neurovascular structures behind the bulges of the sinus (Rhoton, 2002)

2.7.11.17. The Floor of Sphenoid Sinus

The floor separates it from the nasopharynx below. This bony floor allows the vidian nerve to run inside the pterygoid canal. This canal is located off the midline and when the pneumatization extends downward the canal would protrude to a variable extent inside this air cavity (Adin et al., 2019; Hiyama et al., 2015; Sildiroglu et al., 2015).

Shkarubo et al. showed that this canal usually appears as a gutter (2018) and Palmer have used vidian bundle to indicate the site of the petrous internal carotid artery (2013).

Maxillary nerves lie where the floor meets the lateral walls of the sphenoid sinus. They are exiting the cranial base through foramina rotundum. Just peripheral to the foramen rotundum these nerves frequently produce prominent bulge up to 15 mm into the inferolateral sinus wall below the sellar level (Budu et al., 2013; Meloni et al., 1992; Sildiroglu et al., 2015; Vuksanovic-Bozaric et al., 2019; Dasar and Gokce, 2016; Solari et al., 2012).

2.7.11.18. Lateral Wall of the Sinus

Cavernous sinuses rest on the cranial side of the lateral wall of the sphenoid sinus. The cavernous part of the internal carotid artery passes bilaterally through these venous sinuses and leaves right and left impressions inside the sphenoid air cell on the lateral walls. This impression takes a C shape where the convexity faces anterolaterally. The front of the C shape is usually lie in a more anteriorly placed coronal plane unless the Sella is hugely expanded by a tumor. The carotid sulcus that occupies the loop of the intracranial portion of the internal carotid artery may be dehiscent in about 20 % of cases studied (Yeung et al., 2018; Solari et al., 2012).

Lateral to this C shape, the cranial nerves that pass through the superior orbital fissure could leave their own impressions on the lateral wall of the sphenoid sinus. At the posterior aspect of the lateral wall, the optic nerve may leave another prominence. It may also be dehiscent but less frequently than that of the carotid (Sildiroglu et al., 2015).

The degree of pneumatization would dictate how obvious the protuberances are when examined from inside the sinus using an endoscope (Rahmati et al., 2016; Hiyama et al., 2015; Dessi et al, 1994).

The close relevance of the optic nerve to the posterior ethmoid and sphenoid sinuses is a risk factor that increases the risk of iatrogenic injury and even blindness (Daniel et al., 1990; Jian Wang et al., 2010; DeLano et al., 1996).

The optic and the carotid bulge would create a depression between them called optico-carotid recess representing exactly the base of the optic strut. It is triangular dimple located under the optic bulge lateral to the protuberance of the clinoid segment of internal carotid artery. This recess would be of varying degree of depth and may be quite deep extending to the anterior clinoid process (Meybodi et al., 2018; Solari et al., 2012; Halil Arslan et al, 1999).

2.7.11.19. Segments of Internal Carotid Artery In Relation to the Sphenoid

From caudal to rostral the internal carotid artery (ICA) could be divided as follows:

1. The paraclival segment: This can be subdivided into an extracavernous lacerum segment and intra-cavernous trigeminal segment, related to Gasserian ganglion and the first two trigeminal branches (Marcati et al., 2018).

2. The parasellar segment of the intracavernous ICA: The origin of the inferior hypophyseal artery would lie medial to this segment while intra-cavernous nerves lie laterally. Meckle’s cave with Gassarian ganglion and the first and second trigeminal divisions are separated from the lateral wall of the sphenoid sinus by the internal carotid

artery prominence. The abducent nerve would be sandwiched between internal carotid artery medially and ophthalmic nerve laterally. These superior orbital fissure contents produce a smooth wide prominence in the midlateral wall of the sphenoid sinus below the optic canal (Wang et al., 2010; Farımaz et al., 2019; Carrabba et al., 2013; Newman et al., 2020; Yeung et al., 2018; Perondi et al., 2013).

3. Clinoid segment of the intra-cavernous ICA lies medial to the optico-carotid recess, between the proximal and distal dural rings (Meybodi et al., 2018; Peris-Celda et al., 2013).

2.7.11.20. Thin Bone or Dehiscence

Variable percentage of studied cases shows absence of visible bone between the mucosal lining of the sinus and the dura at the skull base. Even without dehiscence the bone may be half a millimeter or less, even described by Unlu et al as a translucent membrane giving minimal protection from surgical trauma (2008). The possibility of having these weak gaps would increase when intra sinus protrusions are detected. Loss of bony protection leaves the nerves and vessels around the sphenoid sinus with only mucosal and dural coverings which would make the vigorous curetting of the sinus mucosa riskier to these delicate structures. This may explain the reason behind some cases of vascular injury and cranial nerves deficit encountered during transsphenoidal surgeries. This is a clear indication to use the CT scan preoperatively to identify cases with dehiscence and be prepared for it (Renn and Rhoton, 1975; Johnson et al., 1985; Twigg et al., 2017; Solari et al., 2012).

2.8. In Summary

Taking into consideration that sphenoid sinus is surrounded by numerous important neurovascular structures underling its bony prominences and recesses which are seen from inside, structures as internal carotid arteries, optic nerves must be preserved using available bony landmarks to create a roadmap to reach the Sella safely.

2.9. Sugery

Ahmed et al. have studied the impact of surgical intervention by one specialized surgeon and found that surgery was preferable over other types of treatment modalities

(1999). That study and those of others have concluded that surgery has been the first line of treatment ever since.

2.9.1. The Evolution of Transsphenoidal Approach

At the beginning of the twentieth century, neurosurgeons faced high percentage of mortality during their attempt to operate on the pituitary gland using transcranial approach. That was the drive behind using the nasal route as a safer alternative. A report of successful transsphenoidal operation was published in 1906. Although the procedure went into multiple refinements and developments it was overshadowed with time by its old transcranial counterpart, as the latter became more favorable in removing pituitary tumors and preserving the optic apparatus (Liu et al., 2001).

With the emergence of modern microscope or endoscope, better illumination of the operative field, as well as magnification and depth appreciation have been experienced by these visual aids. These capabilities allow reaching deep structures as pituitary gland at the skull base with minimal disturbance of normal tissues. Moreover, with the invention of sophisticated neuroimaging modalities mainly CT scan and MRI the gradual improvement in navigation along the operative field using at least the intraoperative fluoroscopy with specialized instrumentations, transsphenoidal approach has been increasingly become the preferred approach for midline pituitary tumors since it fulfills the premise that dictates surgical dissection, which is preserving normal tissue and using the safest and shortest route to reach a surgical target (Laws et al., 2017).

Experience in using this corridor to reach the Sella at the skull base with deep understanding of the detailed relevant surgical anatomy has widen the horizon of transsphenoidal approach by using this air cell as a window to reach more laterally placed lesions from planum sphenoidale above to the dense of C2 below (Arbolay et al, 2009).

2.9.2. Why Choosing the Transsphenoid Over the Transcranial Approach?

The major potential advantage of endonasal technique compared with the transcranial approach is that it does provide minimal invasion as it does not require skin incision and external craniotomy. Instead, it uses the natural air-filled spaces as corridors to reach the surgical target safely and effectively. It also avoids retracting brain tissue and provides direct and adequate access to the lesion since it does not traverse any major neurovascular structures thereby offering the advantages of fewer complications, less discomfort and quicker recovery (Lekgwara et al., 2019).

However, transnasal transphenoidal approach has its own set of limitations other than the tumor characteristics, that may favor a transcranial approach. Firstly, it is associated with a steep learning curve (in a popular sense) as it provides relatively restricted exposure and higher risk of CSF leak. Studies noted an increased complication rate during surgeons' early experience with this technique (Komotar, 2012).

Several routes through the nasal cavity have been suggested to reach the sphenoid. The sublabial approach starts from under the upper lip to reach the submucosal space along one side of the nasal septum (Albano et al., 2019; Koren et al., 1999). While the transseptal approach avoids the oral cavity and starts with a small incision along one side of the columella to reach the same submucosal path along the septum towards the sphenoid (Rhoton, 2002).

The endonasal approach takes the advantage of having the nasal cavity itself being a natural corridor connecting the sphenoid with the exterior. While avoiding any disruption of the mucosal lining, instruments pass between the concha laterally and the nasal septum medially till reaching the anterior face of the sphenoid (Kabil et al, 2005).

2.9.3. Endoscopy or Microscopy?

Starting from early nineties a shift has been unfolding from microscopic to endoscopic transsphenoidal surgery. In reviewing relevant data from 1952 to 2010 Goudakos et al (2011) revealed that both had comparative rate of complete tumor excision and remission. Li et al. presented a result that contradicted with the previous study regarding the feasibility of tumor excision emphasizing that it was better using the endoscope, adding that even the complication rate was less with this modality (2017). Frank et al. specified that the excision rate was better with the use of endoscope only in cases of lateral extension of the tumor and in the incidence of approach phase complications (2006). Bora et al. also supported the superiority of endoscopy in ensuring total removal of the microadenoma in cases of Cushing’s disease (2020).

This comparative superiority of the endoscope partly attributed to its ability to provide better visualization of the anatomical details including those in laterally situated blind corners that can not be seen by the magnification device as the endoscopy and to its more flexible trajectory (Koren et al., 1999; Unlu et al., 2008).

The diameter of the endoscope makes the use of bulky retractor unnecessary. This last advantage makes the anatomical landmarks more obvious since the bulky retractor would not cover the path towards the Sella (Wei et al., 2013).

So, in using a low-profile endoscope, there would be no major anatomical barrier to move between the nasal vestibule and the Sella apart from the anterior wall of the sphenoid. This would make endoscopic transsphenoidal approach more direct, less traumatic, and generally safe and effective modality (Nasrin et al., 2008; Goudakos et al., 2011; Li et al., 2017; Wei et al., 2013; Frank et al., 2006; Bora et al., 2020; Koren et al., 1999).

Moreover, with the use of a canula, the operator could reach the anterior wall of sphenoid avoiding any maneuver around normal tissue that may end up with trauma (Cusimano, 2013).

2.9.4. Transsphenoidal Approach to Sella Turcica

2.9.4.1. Positioning

Positioning for the operation is a critical step. The head needs to be fixed in a comfortable (supine to almost sitting) position avoiding extreme hyperextension or any kink that endanger the patency of airways or cervical vessels. Different aeration of sphenoid dictates the degree of flexion or extension required for introduction of instruments via the nostril. Up to 15-degree extension of the head is enough to ensure that the instruments would not hit the thorax during insertion into the nose (Laws, 2017). A spheno-nostril line has been suggested to guide the head positioning for transsphenoidal approach.

Furthermore, establishing an external skull point at the temporal bone as suggested by Campero et al (2009). claimed to aid in directing the instrument to the proper angle from the entry at the nostril till reaching the sellar floor, obviating the need for an expensive intraoperative navigation tool as the same above group explained. This external point is referencing a calculated internal point intimately related to the sphenoid and Sella they call it spheno-sellar point. On the other hand, Wang et al (2010) calculated the approach angle using another set of external and internal points.

2.9.4.2. Surgical Landmarks

As surgery aims to do less harm with minimal invasion, minor anatomical details have become significant in executing safe operations. In every surgical route a specific set of milestones should be recognized along the path. Localizing these landmarks is considered essential to avoid confusion, time consumption and endangering normal anatomy inadvertently (Ahmadipour et al., 2016).

Along the trajectory toward the Sella bony landmarks could be recognized. These are comparatively stable and related to soft tissue structures. In case of sphenoidal anatomy, the bony landmarks get its shape from pneumatization around neurovascular structures behind. For example, the carotid protuberance is hiding the carotid artery behind (Unlu et al., 2008).

Based on identifieble landmarks the surgeon can successfully reach the surgical target even without an assistance from intraoperative CT scan navigation. In fact, the presence of these landmarks sometimes overcomes the need for navigation, spares it only for complex anatomy with recurrent surgeries (AyguelMert el et al., 2014).

So, searching for these landmarks by evaluating preoperative CT is well justified. But, although CT scan is a routine work for diagnosing pituitary tumor and evaluating its extent, studying the surgical roadmap is a comparatively forgotten act (Hiyama et al., 2015).

During the first stage of the endonasal transsphenoidal approach, the endoscope can be advanced through one nostril, passing between the nasal septum medially and nasal conchae laterally to reach the sphenoid face lateral to the sphenoid crest where it articulates with the posterior edge of perpendicular plate of ethmoid bone and vomer. Rostrum is the inferior continuation of the sphenoid crest. No incision is needed in the anterior part of the nasal cavity and removal of the conchae is not required (Cusimano et al., 2013).

Uygun et al. pointed out that removing sphenovomerine joint will remove the anterior and inferior walls of the sphenoid sinus thereby exposing the hypophysial fossa with opticocarotid recesses as well as the carotid and optic protuberances (2016). In this article Uygun and colleagues did not pay attention to the ostium in passing through the anterior wall of sphenoid. She argued that removing the sphenovomerine suture would be enough to pave the way toward the interior of the sphenoid.

Posteroinferior end of the superior turbinate is used as a reliable guide to obtain a straightforward trajectory towards the sphenoid ostium without any need of any other internal or external guidance (Laws et al., 2017; Ismail et al., 2018).

As Gupta et al., explained, the sphenoid ostium could be identified in the spheno-ethmoid recess (2013). The posterior portion of the nasal septum should be separated from sphenoid face and displaced medially towards the opposite side. Also, the mucosa on the sphenoidal face should be detached away and then dissected laterally. The whole anterior wall of the sphenoid sinus is thus exposed which is projected and pointed at the midline like a prow (Wei et al., 2013).

A pedicle flap may be constructed from the septal mucosa below the olfactory mucosa above and based on the posterior septal artery which is a branch of sphenopalatine artery running on the anterior wall of sphenoid below the corresponding ostium (Phillip and Nix, 2016).

Then the anterior wall of the sphenoid is removed to create a midline opening extending bilaterally well enough to allow for visualization of the sellar protuberance and for the passage of required instruments. Koren et al. described how to start removing bone from the anterior wall of sphenoid starting from the natural ostium (1999). It is not advisable to extend the bony removal too far in the inferolateral direction, behind the tail of the middle turbinate where the sphenopalatine artery and its principal branches are located. As this artery is the major obstacle for lateral and inferior enlargement of the opening on the anterior wall of the sphenoid sinus, therefore raising a mucosal flap would push the artery aside without damaging it (Jane et al., 2005).

After all the final exposure should allow for a wide binasal access to the anterior sellar wall and its floor passing through the sphenoid sinus (Phillips and Nix, 2016).

2.9.4.3. Danger of Misalignment

Deviation away from the required angle in the sagittal plane may cause a drift of the instrument toward the skull base at the anterior fossa, or downward towards the clivus. Surgeon may go down below the hard palate to a maximum of 22 mm (Lega et al., 2011) using transnasal route. Such misalignment is loaded with the possibility of inflicting neural and vascular damage (Campero et al., 2009). This was the cause behind the suggestion of Wang et al. in using external landmarks to check for the angle of work (2010).

2.9.4.4. Landmarks for the Midline for Nasal Phase

The surgeon should keep himself aware of the midline throughout the approach. The midline of the upper teeth and philtrum can be considered reliable midline markers, whereas the nasal septum cannot be used for this purpose since its deviation is frequent. At the depth of the surgical corridor, the junction of vomer as part of the nasal septum, with anterior sphenoidal crest is the most reliable anatomical landmark for reference at any stage of the operation to avoid risking the adjacent critical paramedian neurovascular structures (Rhoton, 2002).

2.9.4.5. Landmarks for the Midline In Sphenoidal Phase

With adequate pneumatization of the sphenoid sinus, sellar bulge, bilateral parasellar carotid protuberances, optic carotid recesses, clival carotid prominences could be seen and used to calculate the exact location of the midline (Wang et al., 2010; Yeung et al., 2018; Farımaz, et al., 2019; Perondi et al., 2013; Carrabba et al., 2013; Sacher et al., 1986; Newman et al., 2020; Zada et al., 2011; Hiyama et al. 2015; Peris-Celda et al., 2013; Solari et al., 2012).

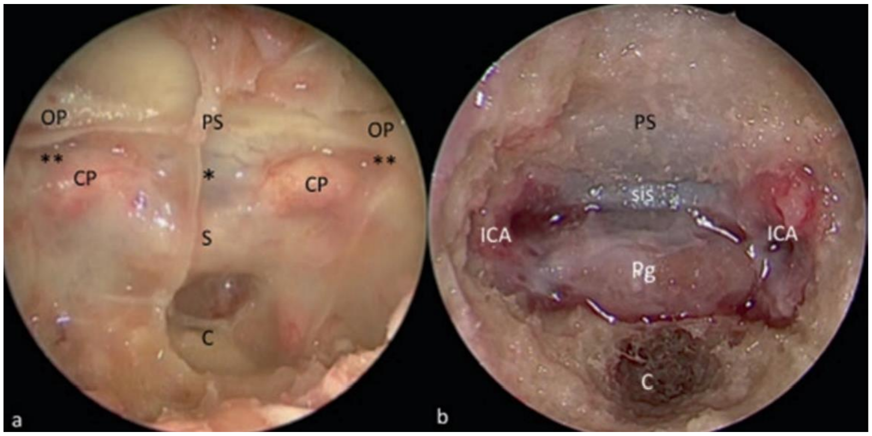

Figure 2. 14. Surgical view of sphenoid sinus posterior wall. S sella, C clivus, PS planum sphenoidale, sis superior intercavernous sinus, ICA internal carotid artery, Pg pituitary gland (Laws et al., 2017)

The identification of these landmarks would be feasible only after removing all the intrasphenoid septations to get the full exposure of the internal features. Creating a single room inside the sinus would allow more free space for instruments and identify more easily the key anatomical landmarks (Unlu et al., 2008).

Intra-sinus septa are not a reliable indicator of the midline but with careful study of the preoperative CT pictures one could predict where the septum is heading and to what structure it is attached. A septum may lead to the Sell, the optic or carotid protuberance (DeLano, 1996). Its potential relation to the ICA could lead to vascular injury if utmost care is not exercised while removing this septum (Phillips and Nix, 2016; Twigg et al., 2017; Carrabba et al., 2013; Fernandez-Miranda et al., 2009; Sildirogluet al., 2015; Hiyama et al., 2015; Solari et al., 2012).

2.9.5. Summary for the Surgical Intervention

To reach the Sella, the angle of the instruments should be carefully maintained and bony structure must be removed from the anterior wall and the inside of the sphenoid sinus. The intimate contact of the sinus walls, roof, and the floor with intracranial neuro-vascular structures could lead to inadvertent CSF leak and injuries to these critical structures. Therefore, we should resort to the preop CT roadmap to determine in advance the proper angle for approaching the Sella and the exact location of the landmarks that indicate the site of the critical structures lying along the path.

2.10. Medical Imaging

2.10.1. The Indication for Pre-Operative Radiological Assessment

The declared aim of the preoperative imaging is to study the characteristics of the pathology and its stereotactic localization. High degree of precision is required to study the relationship of the pathology with the adjacent normal structures. However, another set of details should be included in the radiological report for a patient with pituitary adenoma which are related to the best possible surgical paths. Since the transsphenoidal approach is a routine now, preoperative surgical planning should include studying the surgical corridor that instruments should pass to reach the Sella from below the skull base and identifying its landmarks. In doing so, a roadmap for safe passage would be created preoperatively. That would work to reduce the intraoperative complications to the minimum (Lubbe et al., 2008; Naim-Ur-Rahman et al., 1996).

This type of detailed preoperative assessment needs a comprehensive knowledge in relevant anatomy since high magnification reveals new critical details and relations between neurovascular structures at the skull base. So, surgeons should master microscopical and endoscopic anatomy as an essential skill before embarking upon this type of surgery as appreciating the details of the magnified field revealed by the endoscope would increase safety and effectiveness of the intervention (A. Neubauer, et al., 2005).

2.10.2. The Advantage of Using CT

Computed tomography scanning is the imaging technique of choice in the examination of the paranasal sinuses and adjacent structures because it is more feasible to access, compared with MRI, and furthermore because of its ability to display and distinguish between bone, soft tissue, and air (Chumnanvej et al., 2019). It accurately depicts anatomy and clearly shows the extent of disease in and around the paranasal sinuses (KSievers et al., 2000).

Preoperative computed tomography is the preferred in showing the following:

1. The degree of aeration and integrity of bony plates.

2. The location and insertion of inter-sinus septa.

3. The position of anterior skull base vessels, especially when combined with CT Angio.

4. The exact location of neural foramina at the skull base.

5. The presence of anatomical variations, such as Onodi cells.

6. Safe limits of dissection powered by its ability to depict what Chumnanvej called it the approach workspace (2019).

Guo et al (2018) have added that preoperative CT could improve quality.

2.10.3. Correlating the Pre- and Intra-Operative Visual Clues

Surgeons must correlate all the available visual information pre and intraoperatively to take the best decision regarding the safest operative steps with the best possible trajectory, thereby reducing possible complications (Schulze et al., 2010).

With the preoperative axial, coronal, and sagittal CT images, the treating team could identify the necessary landmarks and important structures surrounding sphenoid sinus, as well as any problematic anatomical variant. Even without expensive navigation tool, this correlation provides the surgeon with a three-dimensional visual road map that improves the surgeon’s sense of direction inside the surgical field and reveals the position of the surgical instruments in relation to the patient’s anatomy (Campero et al., 2009).

Although intraoperative imaging guidance may be used to facilitate safe delineation of relevant anatomy, it is expensive, time consuming, not always available, and even may not be reliable (Achey et al., 2019).

2.10.4. 3D Reconstruction

There has been considerable interest in rendering 2D images of CT or MRI into 3D images closely resembling surgical field. Image reconstruction has been used for surgical training and preoperative planning including that for transsphenoidal surgery. If this technology is absent, multiplanar reconstruction is used. In this modality, axial coronal and sagittal pictures are correlated to create a meaningful 3D picture in the mind of the surgeon (Schulze et al., 2010).

2.10.5. Radiant DICOM Viewer

Specialized software applications as Radiant DICOM Viewer deal with DICOM files to handle medical imaging to produce multiplanar CT pictures. Variable pictures from endless angles and perspectives could be displayed. Measurements of distances and angles are feasible with this software. It is easy to use, free for limited time, with user friendly interface. The exportation of images and even videos is possible in multiple picture formats (Agbetoba et al., 2017).

3. MATERIALS AND METHODS

3.1. Ethical Approval

This study was conducted after being approved by the Medical Research Ethics Committee of the Ondokuz Mayis University with document number B.30.2.ODM.0.20.08/1023-1072 on first of January 2020.

As this was a retrospective study using only deidentified data following extraction of requisite information, patients were not involved beyond the scope that described in this study. Written informed consent from the participants was not necessary. Furthermore, patient's name was preserved confidential not published or shared with a third party.

3.2. Source of Data

With this approval, CT scan imaging of 100 patients were collected from the electronic medical data base of the teaching hospital of Ondokuz Mayis Medical Faculty archived via Nucleus software application. This software harbors electronic medical archive of patients that received medical care in the above-mentioned hospital.

3.3. Inclusion and Exclusion Criteria

Inclusion criteria: the individuals were male and female adults older than 20 years of age up to the age of 90. We have chosen our patients' sample from 300 patients admitted to the neurosurgery department in OMU teaching hospital with pituitary adenomas between 2014 and 2020 and subjected to transsphenoidal surgery to remove the pituitary adenoma.

The control group was chosen from another set of patients subjected to paranasal sinuses CT scan for multiple rhino logical indications without having a pituitary disease.

Exclusion criteria: Any gross pathology that destroyed the bony architecture of the body of the sinus was excluded from the study. CT scan of patients with previous surgeries or significant sinus disease were excluded. Moreover, the present work did not account for extreme anatomical variations, as for example in acromegalics where bone changes are to be expected. Patients younger than 20 years old were excluded from the study, as were patients with bone diseases.

3.4. Participants

Taking into consideration the exclusion criteria, our set of patients and control represent a subgroup from the larger sample obtained from the statistics department in the above-mentioned hospital. having the inclusion criteria studied between 2014 and 2020, our participants were selected consecutively from the list.

Statistical power analysis via Cochran's Sample Size Formula has reached upon a conclusion that the minimum acceptable number for both groups were 44 participants. That was in accordance with the alike published literature. Therefore, 50 patients with pituitary adenoma that have been subjected to transsphenoidal surgery in that very hospital whose consecutive CT scans of the brain fulfilled the inclusion criteria were chosen to be analyzed.

Another set of imaging data taken from different 50 patients devoid from any pathologies of the sellar region, was considered the control 'normal 'group.

3.5. Study Design

This is controlled prevalence monocenter retrospective Cross-Sectional study.

3.6. CT Protocol Specifications

As bony tissues, air filled spaces and distances are clearly defined in the brain CT, the latter has been used for the direct visualization and the determination of the bony structures in nasal and sphenoidal regions.

CT examinations were performed at our institution at OMU teaching hospital in Samsun with a 16-channel multi-slice CT scanner using local protocol.

Patients were in Supine position taking axial CT scan using the following parameters; 120 kV tube voltage, effective 150 mAs, 1 mm slice thickness, and image matrix 768 × 768with coronal and sagittal reformation.

CT pictures should reveal the whole nasal area extending from above the frontal sinus to below the nasal floor including posteriorly the whole picture of the clivus from above the posterior clinoid process to the foramen magnum.

3.7. Technique for Images Processing

The sequential CT data sets were analyzed using Radiant DICOM 2020.2.2 trial version downloaded from radiant viewer.com as it is it the same software used in neurosurgical department of OMU teaching hospital. This is a dedicated workstation image processing software produced by small polish company created by a radiologist aiming to pursuing simplicity in handling medical imaging. CT scan pictures are stored in files with DICOM format. It provides the following basic tools for the manipulation and measurement of images as zooming, brightness and contrast adjustments. Many modes are available as bone and mixed skin bone windows. Unfortunately, the 3D pictures created by this software are not useful enough to study the details of sphenoid.

Based on the images acquired by the tomography scans, multiple variables were assessed in succession as they appear during the advancement of the endoscope passing from the nose to the sphenoid posteriorly. Nonenhanced bone algorithm pictures were used for the identification of the landmarks and taking their various measures.

Measurements were performed on a median sagittal image in which the nasal septum is visible. Using this software, the initial midline sagittal plane is determined using a reference line linking the anterior nasal spine and sphenoidal crest.

All measurements were performed independently by the student and his supervisor and confirmed by a staff neuroradiologist. The axial images are taken parallel to the hard palate. Depth was measured parallel to the planum sphenoidale, and height was measured perpendicular to planum plane. The sagittal midline images pass through the center of the odontoid posteriorly and the mental spine anteriorly. The coronal plane was perpendicular to the sagittal one. After scanning, the coronal, axial, and sagittal images were reconstructed with a slice thickness of 1.00 mm, and the raw data were reconstructed using bone algorithms.

The following anatomical landmarks and distances were identified and measured using multiplanar mode in Radiant viewer software:

1.Site of Sella projected on external surface of skull at the temporal bone away from Tragus and the distance above the level of the tragus.

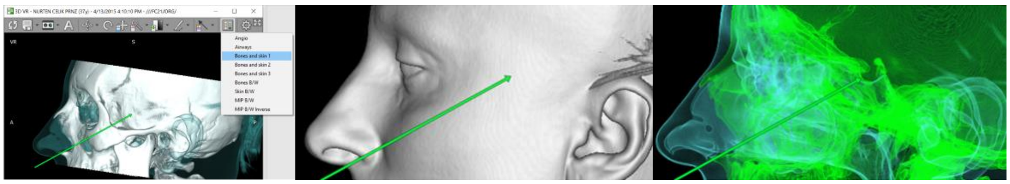

Figure 3. 1. Projecting the site of the Sella on the temporal area

2.Choosing 3D MPR mode for analysis with bone window

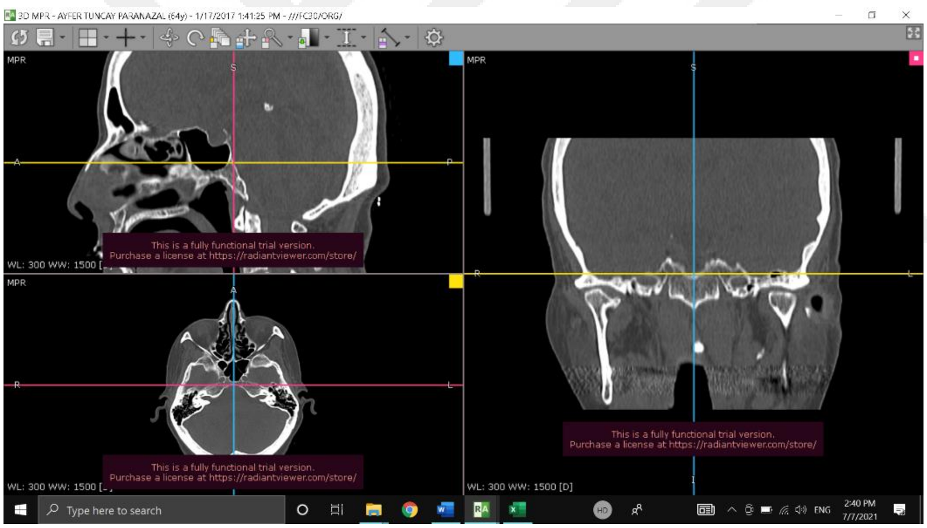

Figure 3. 2. 3D MPR mode to study the area in multiple planes

3.Measuring Distance from the base of columella to anterior wall of sphenoid at midline

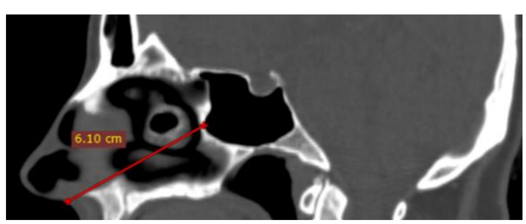

Figure 3. 3. Columella anterior sphenoidal wall distance

4. Measuring distance from columella to the lowest point in anterior seller wall

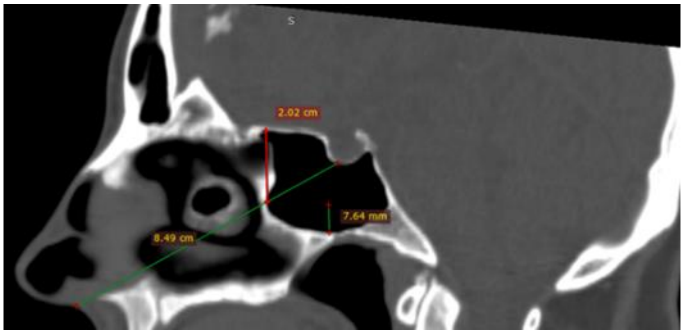

Figure 3. 4. Columella sellar wall distance and intersection area to skull base distance

5. Measuring perpendicular distance from entry point at ant sphenoidal wall to planum sphenoidale

6. Measuring distance from intersection point to lower edge of right and left ostium.

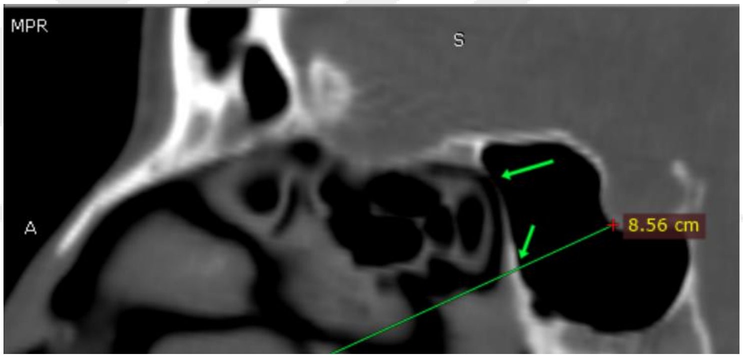

Figure 3. 5. Distance from the intersection to the ostium.

7. measuring the sellar bulge from the posterior wall of the sphenoid sinus.

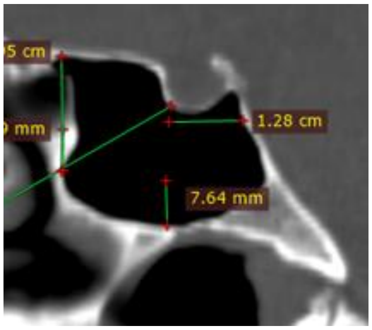

Figure 3. 6. Seller bulge from the posterior wall

8.Sellar enlargement has been registered in the patient's group whether it was present or absent depending on the know criteria that define normal Sella.

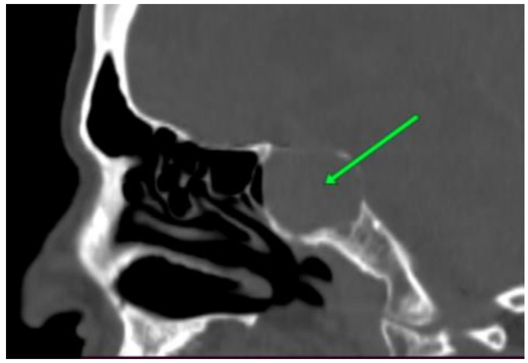

Figure 3. 7. Ballooned Sella by a pituitary adenoma

9.Inter-carotid distance at the sellar face floor level measured from the medial rim of the carotid sulcus to the contralateral medial rim.

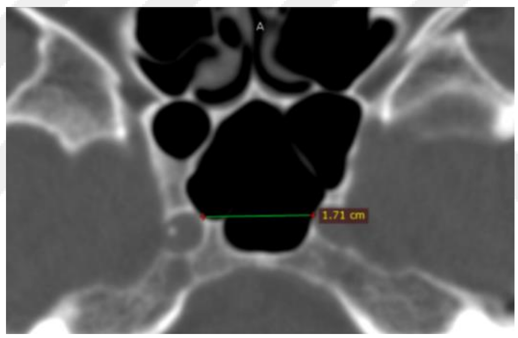

Figure 3. 8. Intercarotid distance measurement

10.Entry site relation to middle and superior concha level and ethmoid cell.

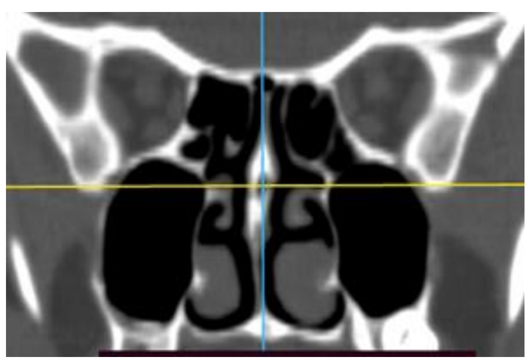

Figure 3. 9. Relation of intersection site at the anterior wall of sphenoid to the conchae and ethmoid cell.

11.Sphenoid crest whether Beaked or no

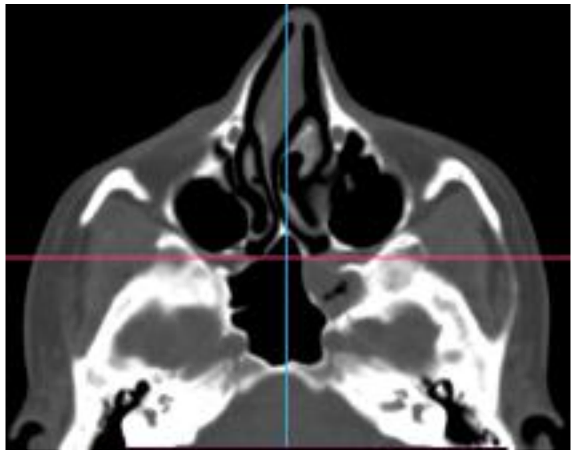

Figure 3. 10. Advanced anterior wall of the sphenoid with a keel line protrusion

12.Anterior wall orientation whether vertical or inclined posteriorly with identification of Onodi cell.

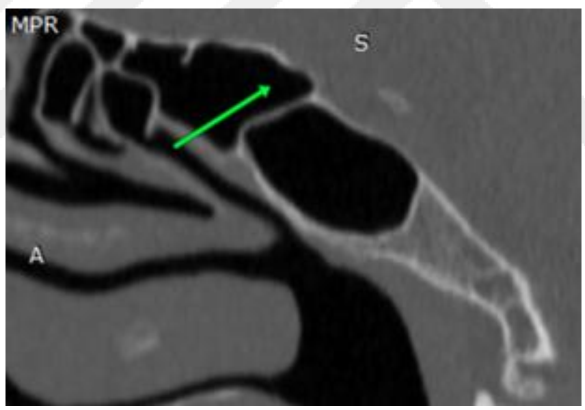

Figure 3. 11. posteriorly overriding sphenoethmoid Onodi cell.

13.Septal attachment to sella or laterally to carotid or optic bulge.

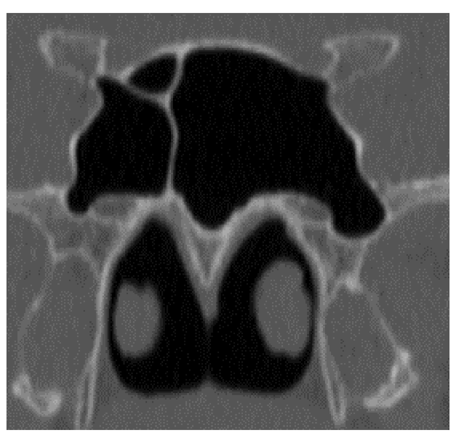

Figure 3. 12. lateral attachment of sphenoidal septum

14. lateral optico-carotid recess whether obvious or no.

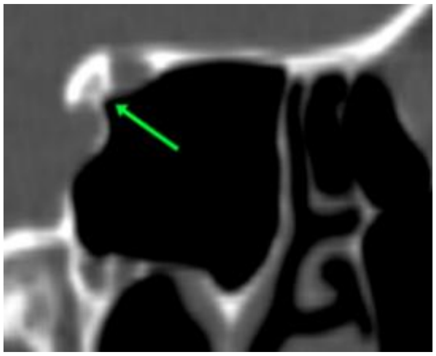

Figure 3. 13. Lateral opticocarotid recess at the base of optic strut.

15.Type of Sphenoid pneumatization.

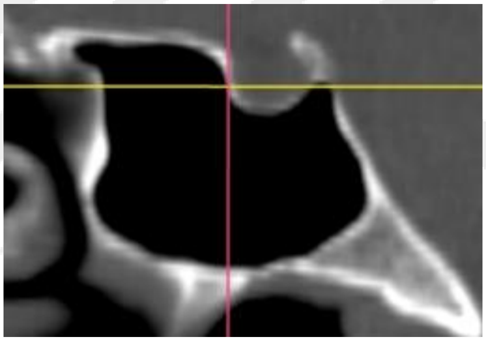

Figure 3. 14. Pneumatization beyond the anterior face of the sella in sellar type.

16.Optic nerve bulging.

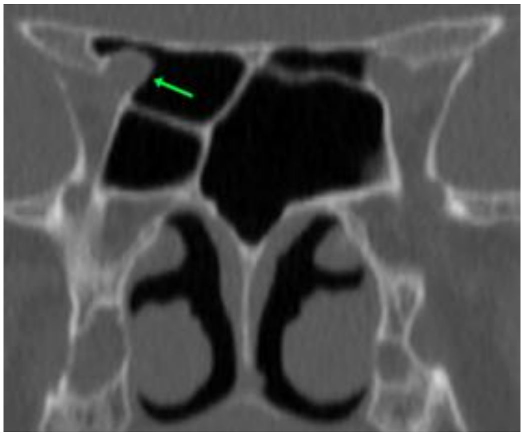

Figure 3. 15. Bulging of the optic nerve inside the sinus.

17.Carotid bulging.

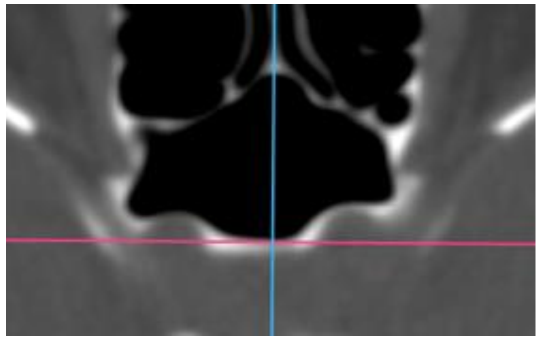

Figure 3. 16. Carotid bulging inside the sinus (Teddy bear sign)

18.Pneumatization of anterior clinoid.

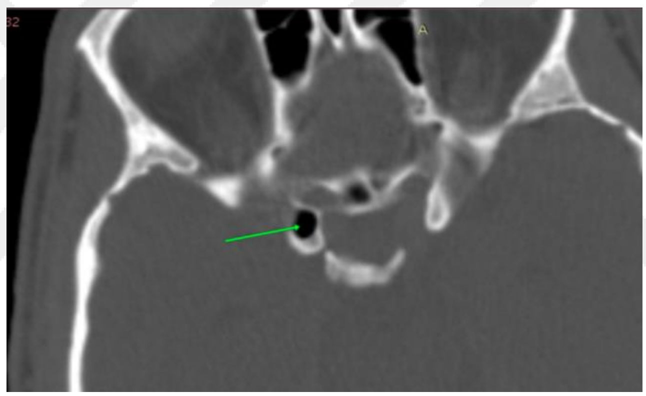

Figure 3. 17. Pneumatization of the anterior clinoid process.

The sequence in the list was set in accordance with the sequence of the transsphenoidal approach to the pituitary.

3.8. Protocol for Reviewing Literature

Google scholar and OMU library electronic databases were searched from 1990 till March 2021. Drawing reproduced anonymously from the same CT scan data. No further permission was required.

3.9. Statistical Analysis

The data were analyzed by the SPSS V25 program (SPSS Inc., IBM Corporation, USA). Gender subpopulation is used to rule out intersexual differences and impact of gender on each specific measurement.

For every interval variable we calculated the following: the average, mean, median, standard deviation and min-max values. For categorical nominal values were presented with frequency and Prevalence.

Shapiro–Wilk and the Kolmogorov–Smirnov tests were used to check for normality of distribution of variables.

After using Levene's test for homogeneity (equality) of variance, the continuous variables were described as mean and SD and analyzed by T test to investigate for the comparison between means for every interval variable in the major groups and the subgroups. On the other hand, Mann Whitney U test was used for comparing non-normally distributed variables.

The computed significance in T test was two tailed which means that the mean was considered significantly different (whether greater or lesser i.e. the test statistic is in the top 2.5% or bottom 2.5% of its probability distribution) resulting in a p-value less than 0.05.

To know the linear relationships between continuous numerical variables we have tested how certain measurements impact each other by calculating the Pearson bivariate correlation test. A correlation coefficient of 0.1 represented a weak correlation, while coefficient of 0.3 was considered a moderate correlation and a correlation coefficient of 0.5 and above represented a strong correlation. Spearman correlation coefficient was used as the nonparametric alternative to Pearson test for non-normally distributed continuous variables. Like Pearson's, it also showed the direction and strength of correlation.

Discrete Categorical variables were described as frequency (% of total) and analyzed using Pearson's chi-square X2 test. The chi-square test was used for comparing the observed frequencies to the frequencies that we might expect to obtain purely by chance. It helps you to find the relationship between two variables but has no direction and size of the relationship in other word it does not tell you how much the significance is. Adding Phi coefficient to Chi square, we can measure the strength of this significance as it extends between 0 and 1 where 1 indicates an extraordinarily strong correlation. Values of $p < 0.05$ were considered statistically significant. If these characteristics were not significantly different between the observation group and the control group ($p>0.05$), therefore groups would be considered comparable.

Eta association coefficient between nominal and interval variables measures the strength of association between an interval and a nominal value. Eta square represents the size of effect. For example, 0.25 Eta square means that the percentage of effect of the independent variable on the dependent variable is 25%.

4. RESULTS AND DISCUSSION

4.1. Results

4.1.1. Normality and Comparison Between Mean Values of the Continuous Variables

After doing Shapiro Wilk test to check normality of distribution of variables, the decision to choose between statistical tests to compare between two independent variables was made. According to the results of Shapiro Wilk test, we chose independent sample T test for normally distributed values to investigate for any differences between means in the same group based upon gender or between the two major groups. For non-normally distributed values we have chosen Mann whitney test to investigate for any significant differences in the medians between genders in the same group or between the two major groups. This latter test is the nonparametric counterpart of independent samples T test used as we mentioned for non- normally distributed continuous values.

Note that before using T test for normally distributed values we had used Levene test to investigate for the homogeneity of variances. That was to show how far the scores were distributed around the means of the tested samples.

P value of .05 is our defined threshold of the significance level. However, statistical significance indicates only that you have sufficient evidence to conclude that an effect exists. It is a mathematical definition that does not know anything about the subject area and what constitutes an important effect. Instead, we need to apply knowledge and expertise to determine whether the effect is big enough to be meaningful in the real world. In other words, not all statistically significant differences are interesting.

4.1.2. Age and Sex Distribution

Table 4. 1. Description of gender and age distribution in both control and patients

Groups and subgroups	Control group	patients
	Number / Mean(SD)	
overall	(N50) 53(15)	(N50) 47(16)
male	(N27) 54(14)	(N 26) 47(17)
female	(N23) 52(17)	(N24) 47(14)

N indicates number of cases, while SD is the standard deviation.

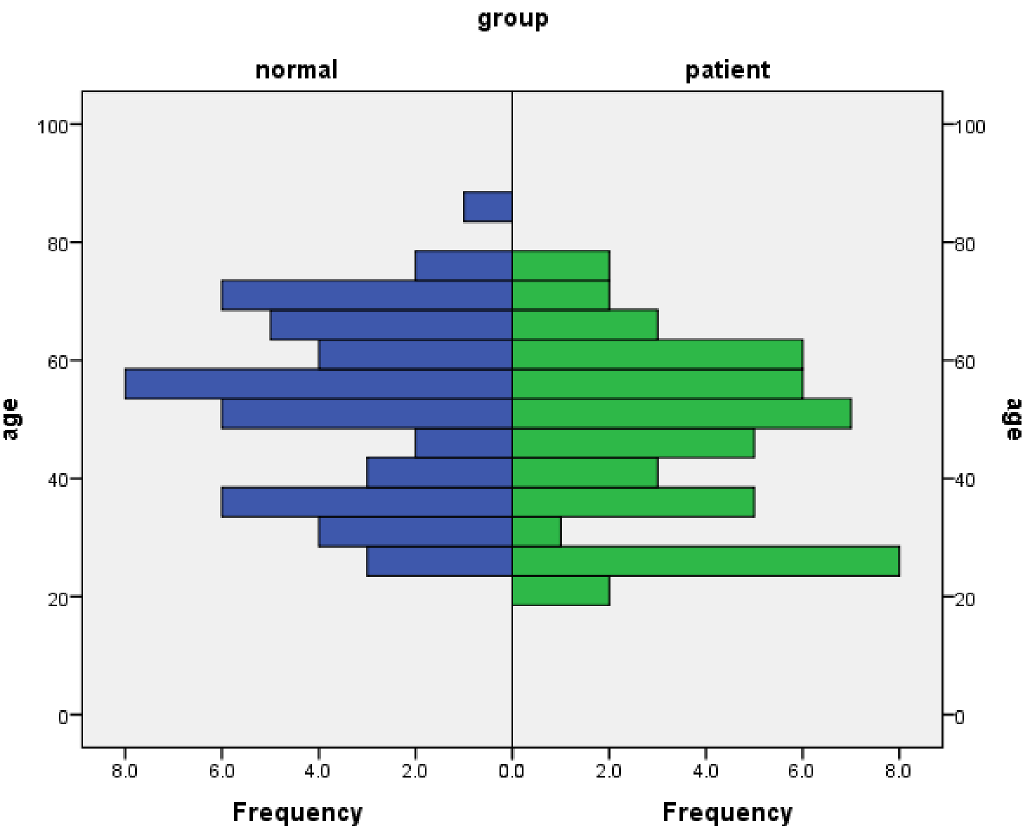

Figure 4. 1. The histograms show multimodal distribution with multiple peaks

The above table and histogram show that control and patients' group were both composed of 50 people: males and females. Their ages stretch between 21 to 85 years. The mean age for control group is 53 while that for pituitary patients is 47. Form statistical point of view using independent sample T test it was obvious that there was no significant difference between the two major groups, and we can say that they are comparable as far as age distribution is concerned (P value more than 0.05). Subgroups were comparable as well.

4.1.3. Projecting the Exact Site of Sellar Floor on Temporal Area

Fortunately, Radiant software can show an overlapping picture revealing both the Sella turcica and the temporal area with well demonstrated external features of the ears. In this way it was easy to put a marker on the skin at the temporal area and taking measurements of its coordinates in reference to the tragus in front of the external auditory meatus. The results were as shown below.

Table 4. 2. Description for the coordinates of temporal marker referring to sellar floor (A. In front of Tragus)

Groups and subgroups	Mean(SD)		Significance in statistical comparison
	Control	Patients	
overall	2.2 (0.6)	1.9(0.7)	0.03
male	2.2(0.6)	1.9(0.7)	NS
female	2.2(0.6)	1.86(0.7)	NS

Table 4. 3. Description for the coordinates of temporal marker referring to sellar floor (B. Above the Tragus)

Groups and subgroups	Mean(SD)		Significance in statistical comparison
	Control	Patients	
overall	2.75(0.5)	2.65 (0.6)	NS
male	2.9(0.5)	2.8(0.65)	NS
female	2.5(0.5)	2.5(0.4)	NS

SD standard deviation. NS non-significant P value more than 0.05

The mean of distances away from the tragus in the coronal plane anteriorly was 2.2 cm (0.9-3.5) in control group and 1.9 cm (0.5-3.5) in patients. On the other hand, In the control group the distance of the marker above the horizontal level of tragus was 2.75cm as a mean; stretching between 1.76 and 3.8 centimeters. While in patients' group the mean was 2.65 (1.5 to 3.9) cm.

Only the mean of the distances away from the tragus in the coronal plane showed a significant difference (P value 0.03) when the two major groups were statistically compared.

There is also a significant difference between genders in the control and patients' group when comparing the vertical distance above the tragus with P value less than 0.05 each. While investigating for differences in the means between the two male groups and the two female groups revealed that those groups were comparable.

4.1.4. Distance from Columella of the Nose to Sellar Floor

The distance from the base of the columella is considered the first point for advancing the instrument going trans-nasally toward the sellar floor. The line extending between them would be the trajectory of the instruments. This trajectory would intersect with the anterior wall of the sphenoid before entering the sphenoid sinus. We measured this line using a midsagittal view in nonenhanced CT scan for the head.

Table 4. 4. Distance between columella and most advanced point in the sellar floor

Groups and subgroups	Mean (SD)		Significance in statistical comparison
	Control	patients	
overall	8.7(0.5)	8.65(0.7)	NS
male	8.9(0.5)	8.8(0.7)	NS
female	8.5(0.4)	8.5(0.6)	NS

SD standard deviation. NS non-significant P value more than 0.05

The average was 8.7 (9.7-7.8) cm in control group and 7 (8.7-6.2) cm in patients with pituitary adenomas.

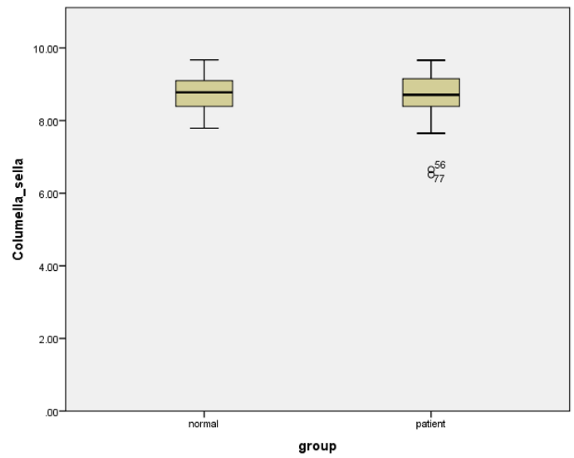

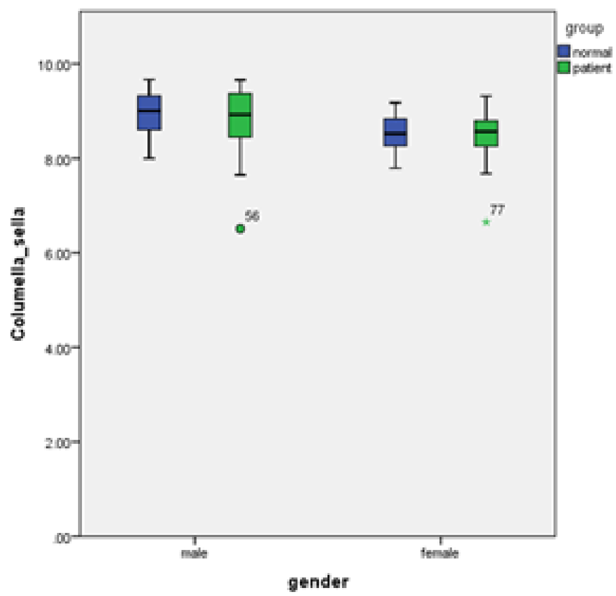

Figure 4. 2. Distance between columella and sellar floor in two major groups and subgroups

The outliers in the picture above appear with the patient group. The apparent numbers; 56 and 77 are numbers of patients in the original data. These boxplots are showing the maximum and minimum values in any group with the median and the extent of the middle 50% of values an any group. It shows how compact the values were and gives a graphical indicator of the variance of values.

As shown in the table above the groups were comparable. Interestingly, only the comparison between the two genders in the control group revealed a significant difference between the scores.

4.1.5. Distance from Columella to the Anterior Sphenoidal Wall

Using the same view, we can identify the point of intersection with the anterior sphenoidal wall. Measuring the distance between the base of columella to the anterior sphenoidal wall in both groups reveals the following average of 6.8(5.4-8) cm in control group and 7(6.2-8.7) cm in patients group as shown in the table below.

Table 4. 5. The distance between the columella and the point of intersection at anterior sphenoidal wall

Groups and subgroups	Mean (SD)		Significance in statistical comparison
	control	patients	
overall	6.8 (0.6)	7(0.6)	0.03
male	7 (0.6)	7(0.6)	NS
female	6.6 (0.5)	6.9(0.4)	0.01

SD standard deviation NS non-significant P value more than 0.05

Statistically, comparing the means between patients and control groups using independent sample T test revealed that the P value was 0.03. Since this value is below 0.05, we had to reject the null hypothesis and accept that the means are different significantly in comparison between these two groups.

The comparison between genders inside the same group and between females of the two groups also revealed a more significant difference with P values less than 0.05. But the result of the comparison between males in both groups showed a comparable result (P value was 0.2).

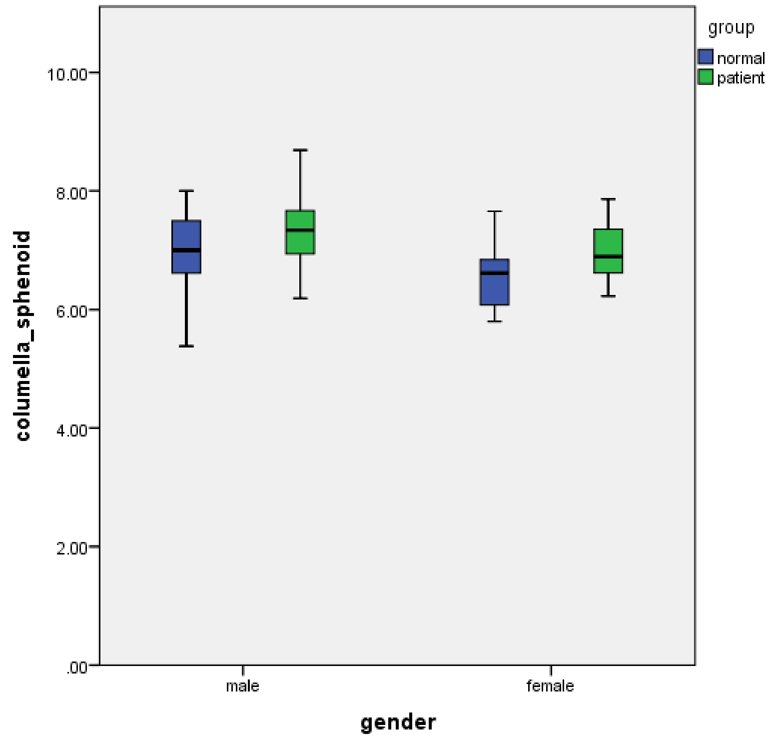

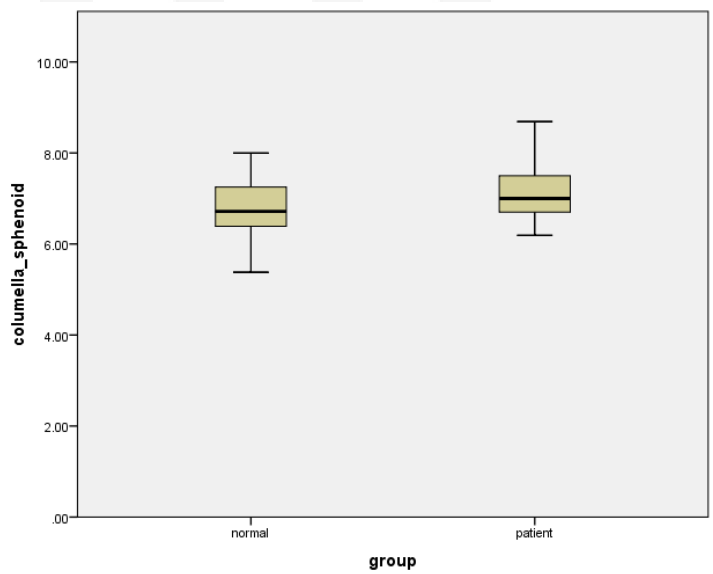

Figure 4. 3. Descriptive analysis with boxplots showing median, minimum, and maximum distribution in the two major groups and subgroups

4.1.6. Distance from the Intersection to Planum Sphenoidale

It would be of practical importance to see how much we are away from the anterior skull base by measuring the perpendicular distance between the point of intersection with the anterior sphenoidal wall and the planum sphenoidale. The results were as shown below.

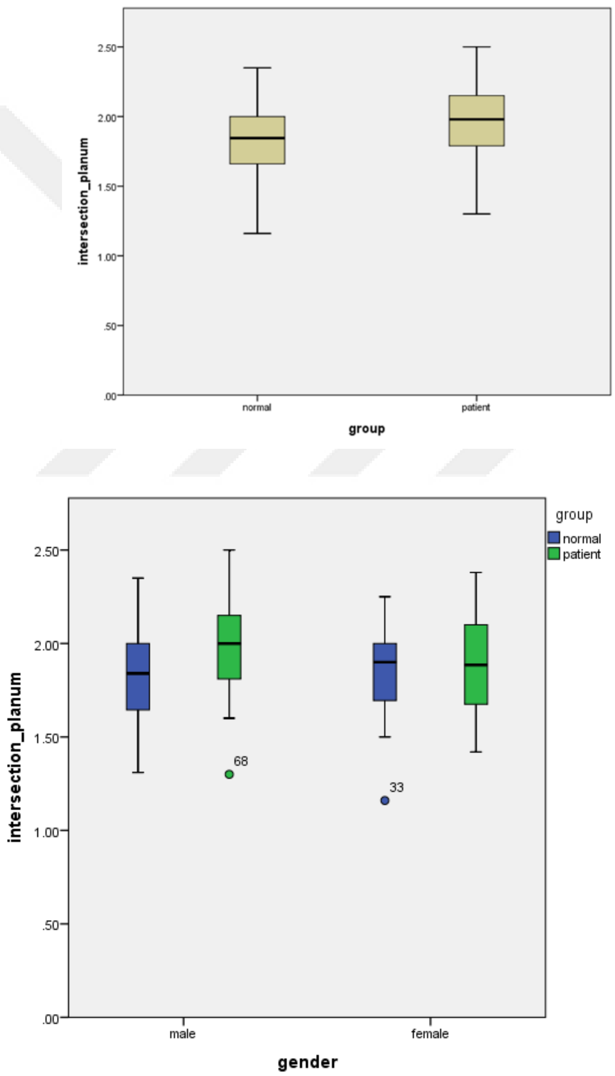

Figure 4. 4. The distance from the intersection to the skull base at planum sphenoidale median. minimum and maximum with the interquartile distribution

Table 4. 6. The distance from the intersection point to the skull base above

Groups and subgroups	Mean (SD)		Significance in statistical comparison
	Control	Patients	
overall	1.8(0.25)	1.9(0.27)	0.04
male	1.8(0.25)	1.98 (0.26)	0.02
female	1.85(0.26)	1.9(0.28)	NS

SD standard deviation NS non-significant P value more than 0.05

In control group we saw that the mean of these distances was 1.8 (1.2-2.35) cm while in diseased group it was 1.9 (1.3-2.5). Overall, the values in both groups extended between 1.2cm as a minimum to 2.5 cm maximum, with interquartile range of 0.36 cm for control and 0.37cm for patients.

With the use of independent sample T test, we investigated for the any significant difference between the distances in the two major groups. The resultant p value was 0.04 so that we are more than 95% confident that this difference is not a result of chance, and we could claim safely that the distances from the planum are significantly different.

Regarding the comparison between the subgroups, we found a significant difference only when comparing the two male groups with a p value less than 0.05, otherwise the comparison between the subgroups revealed that they are comparable.

4.1.7. Distance from the Intersection to Natural Ostium

Now we have reached to the point where we should investigate for the position of the intersection point in relation to the position of the natural ostium of the sphenoid wall. This ostium has been always regarded as a landmark that the operator should localize in approaching the sphenoid sinus. Determining the mean of the distance to the ostium starting from the intersection point revealed that it was 0.7, with standard deviation (SD) value of 0.3cm in control group and 0.8cm with SD of 0.4cm in patient group. There were 20% missing values due to lack of ostia. See table below.

Table 4. 7. The distance between the intersection point to the sphenoidal ostium in both major groups (Right side) left side

Groups and subgroups	Mean (SD)		Significance in statistical comparison
	Control	Patients	
overall male female	0.7 (0.3) 0.7(0.2) 0.67(0.3)	0.8(0.4) 0.8(0.4) 0.79(0.3)	NS NS NS

Table 4. 8. The distance between the intersection point to the sphenoidal ostium in both major groups (left side)

Groups and subgroups	Mean (SD)		Significance in statistical comparison
	Control	Patients	
overall male female	0.7(0.3) 0.75(0.3) 0.7(0.3)	0.8(0.4) 0.87(0.4) 0.75(0.3)	NS NS NS

NS non-significant P value more than 0.05

The overall values extended between 0.1 cm to 1.8 cm. From statistical perspective the values in the two major groups were comparable evident by having a p value more than 0.05. That applied also in comparison between the subgroups.

4.1.8. Orientation Before Hitting the Anterior Sphenoidal Wall

As the potential instrument reached the anterior wall of the sphenoid, we explored the relation between the intersection are with the landmarks at the posterior aspect of the nasal cavity the ethmoid cell and the superior turbinate.

Table 4. 9. The intersection area in relation to A. superior concha

Groups	Control	Patients	Statistical comparison
Total Males Females	(26)52% (14)52% (12)52%	(33)66% (16)62% (17)71%	NS NS NS

Table 4. 10. The intersection area in relation to B.ethmoid cell

Groups	Control	Patients	Statistical comparison
Total	(41)82%	84%	NS
Males	(21)78%	(22)85%	NS
Females	(20)87%	(20)83%	NS

NS non-significant P value more than 0.05

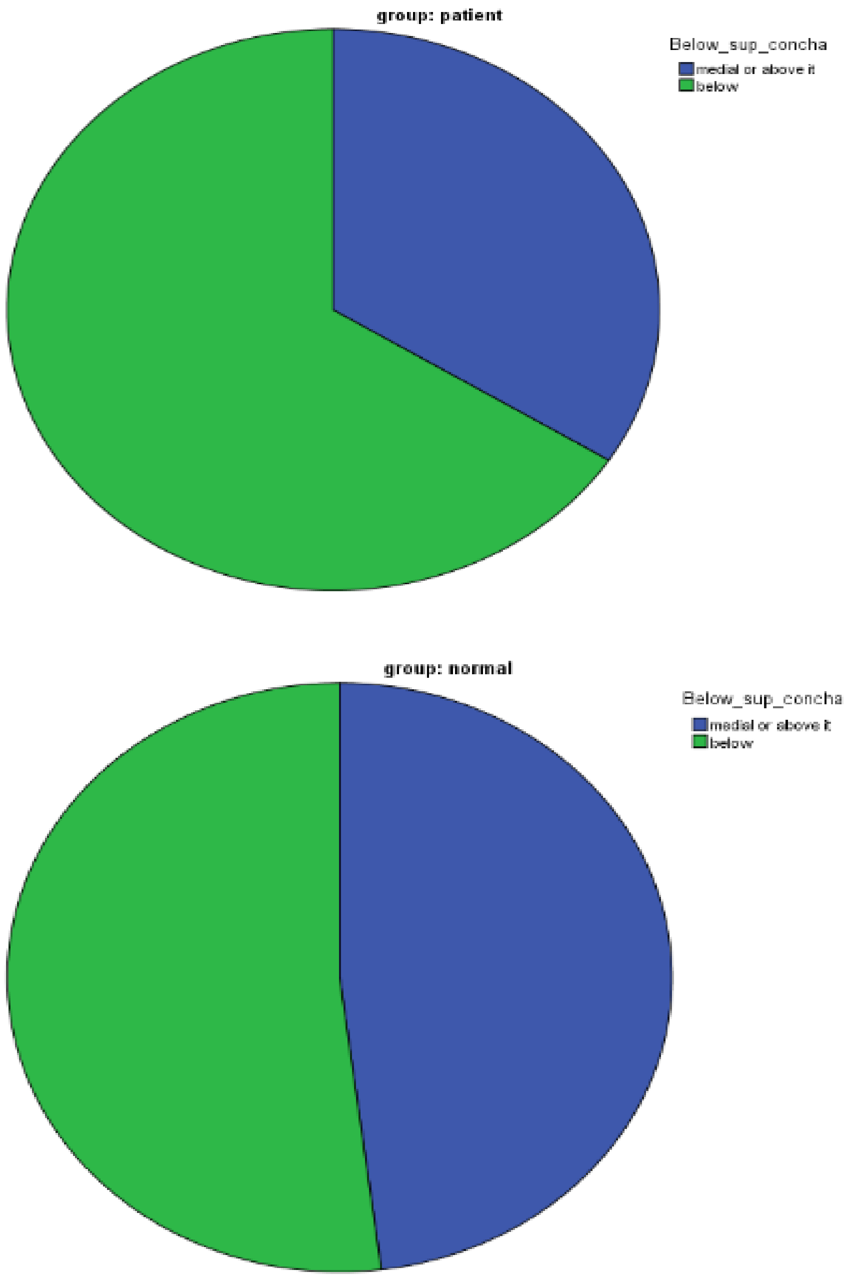

Figure 4. 5. The percentage of an intersection point below the superior concha

Slightly more than half of control cases showed that the line extending from base of columella to the sellar floor intersected the anterior sphenoidal wall below the superior chonca. Regarding the patient group, 66% of cases had the same intersection below the superior concha.

Table 4.7.B. is showing clearly that nearly the same percentage of control cases and that of the patient group had site of intersection below the ethmoid cell (82% in control and 84% in patients).

Chi square test was used for comparison betwee the groups . They were statistically comarable with no significant difference as evident by P value of more than 0.05.

In all cases , the path passed above the tail of the middle turbinate at the back of the nasal cavity.

4.1.10. Beaked Anterior Wall of Sphenoid

Peaked anterior wall means that it is more advanced anteriorly in the midline than laterally.This would make the sphenoethmoid recess even more restricted in diameters hiding the ostium even more laterally behind the superior turbinate.

Table 4. 11. The incidence of having peaked anterior wall of the sphenoid

Groups	Control	Patients	Statistical comparison
total	(44)88%	(39)78%	NS
males	(23)85%	(22)85%	NS
females	(21)91%	(17)71%	NS

NS non-significant P value more than 0.05

We can realize from this table that the majority of cases in both groups had beaked anterior wall and the groups were statistically comparable.

4.1.11. Posterior Inclination of the Anterior Sphenoidal Wall

The incidence of this feature extended between 10% in control cases to 26% in patients group.

Table 4. 12. The posterior inclination of the anterior sphenoidal wall

Groups	Control	Patients	Statistical comparison
Total	(5)10%	(13)26%	0.04
Males	(2)5%	(7)27%	0.00

Females	(3)13%	(6)25%	NS

NS non-significant P value more than 0.05

As evident in table 4.9., the two groups showed a significant difference in the frquency of cases with inclined sphenoidal wall as concluded from the Chi square test p value 0.04. Otherwise , only the comparison between males in the two groups showed a statistically significant difference.

4.1.12. Septa Leading to the Sella

The control group had 40% frquency of cases with a septum whether central or paracentral leading to sellar bulge. However, the patients with pituitary adenomas had a frequency of 65%. In statistically comparing between these two a p value of 0.01 was concluded from Chi square test.This value is obviously less than 0.05, so the difference was considered significant.

It was also evident from the table below that the incidence in the subgroups was different between genders in the same group and between the same gender in two groups. But when it comes to statistics, only the major two groups showed a statistically significant difference. Otherwise , the subgroups could be considered statistically comparable.

Table 4. 13. Intrasphenoidal septa leading to the sellar bulge

Groups	Control	Patients	Statistical comparison
Total	(20)40%	(32)65%	0.01
Males	(3)48%	(19)73%	NS
Females	(7)30%	(13)57%	NS

NS non-significant P value more than 0.05

4.1.13. Bulging over the Carotids and Optic Nerves

As apparent in the table below the frequency of having a radiologically obviously distinct optic and carotid bulgings extends between 12 to not more than 28% in the major groups whether in the right or the left side.See table below.

Table 4. 14. Obvious bulgings inside the sphenoid sinus (Over optic nerve)

The Observed variable	Control	Patients	Statistical comparison
Rt Optic Nerve Bulging			
Total	(8)16%	(14)28%	NS
Males	(2)7%	(9)35%	0.02
Females	(6)26%	(5)21%	NS
Left Optic Nerve Bulging.			
Total	(6)12%	(11)22%	NS
Males	(2)7%	(8)31%	0.03
Females	(4)17%	(3)13%	NS

Table 4. 15. Obvious bulgings inside the sphenoid sinus (Bulgings over carotid artery)

Groups	Control	Patients	Statistical comparison
Total	(11)22%	(13)28%	NS
Males	(1)4%	(9)38%	0.00
Females	(10)44%	(4)17%	NS

NS non-significant P value more than 0.05

When it came to the comparison between the major groups and subgroups, only genders inside the control group showed a significant difference with P value below 0.05 regarding the incidence of internal carotid bulgings. Also the comparison between males in the major groups showed significant differences with a p value way below 0.05. Otherwise, the groups were comparable.

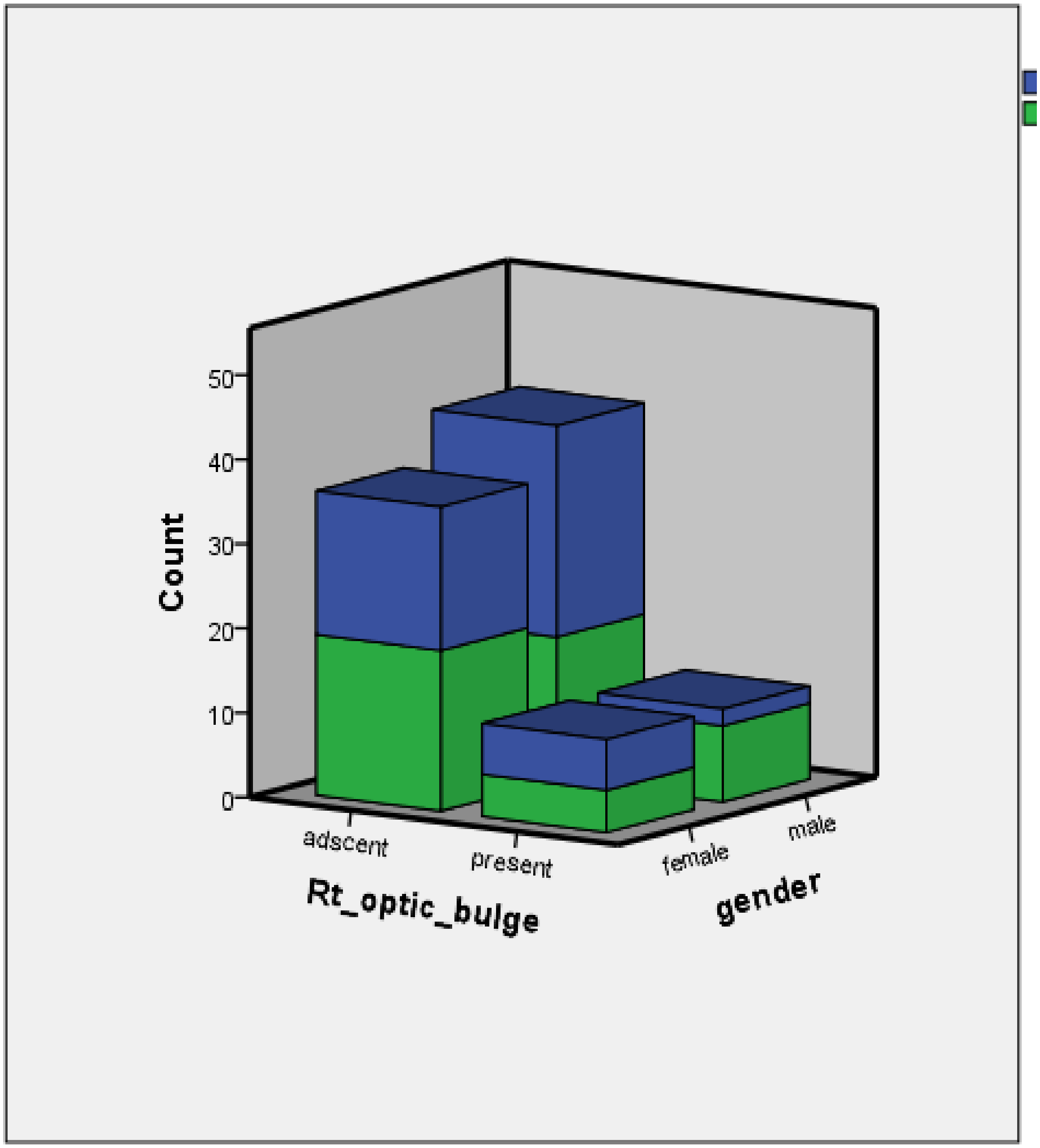

Figure 4. 6. The bulging of the right optic nerve inside the sphenoid sinus

4.1.14. Right and Left Opticocarotid Recesses

Normal group showed a fequency more than the patients in having an obvious lateral opticocarotid dimple lying lateral to the parasellar carotid below the final path of optic nerve towards the optic chiasm. In spite of that, this difference was found to be statistically insignificant. Even in the comparison between the subgroups we saw that they were compararable without any significant statistical differences.

Table 4. 16. The incidence of having obviuos lateral opticocarotid recess in both groups

The observed variable	Control group	Patients group	Statistical comparison
Obvious Right lateral optico-carotid recess			
total	(24)48%	(19)38%	NS
males	(11)41%	(11)42%	NS
females	(13)57%	(8)33%	NS
Obvious left lateral optico-carotid recess			
total	(26)52%	(20)40%	NS
males	(13)48%	(11)42%	NS
females	(13)57%	(9)38%	NS

NS non-significant P value more than 0.05

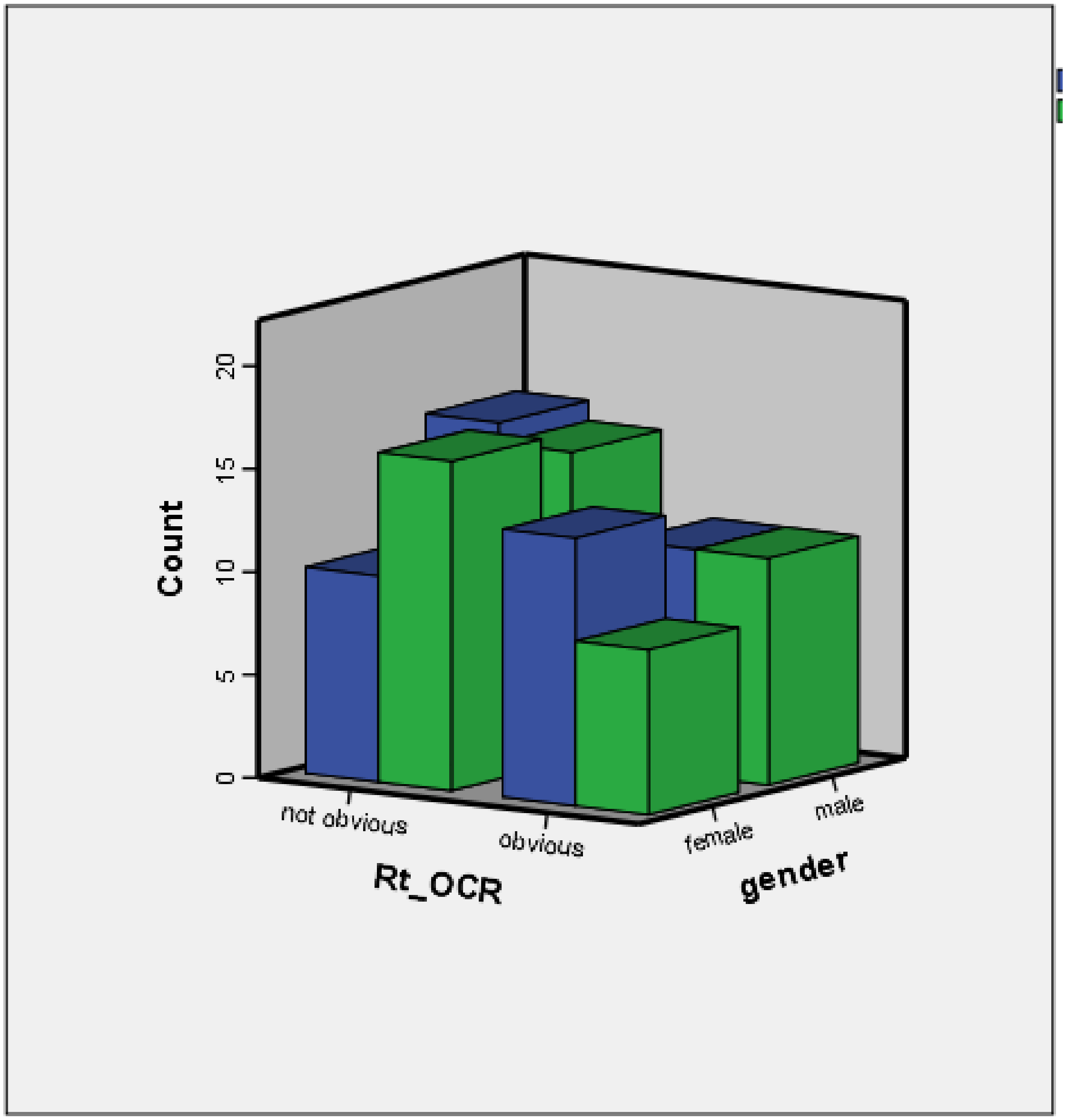

Figure 4. 7. Comparing between control and patients in having an obviuos opticocarotid recess OCR

4.1.15. Inter-Carotid Distance

As the carotids act as serpentines guarding the sellar bulge in which the pituitary gland rests, the operators have only the distance between these two vessels to reach the pituitary.

Table 4. 17. Inter carotid distance

Groups and subgroups	Mean (SD)		Significance in statistical comparison
	Control	patients	
overall	1.6(0.2)	1.85(0.3)	0.00
male	1.7(0.3)	1.86(0.3)	NS
female	1.6(0.2)	1.8(0.3)	0.00

SD standard deviation NS non-significant P value above 0.05

The control group showed a mean of 1.6 (with a minimum of 1 to a maximum of 1.99) cm, while in the patient group the mean was 1.85 (1-2.4) cm.

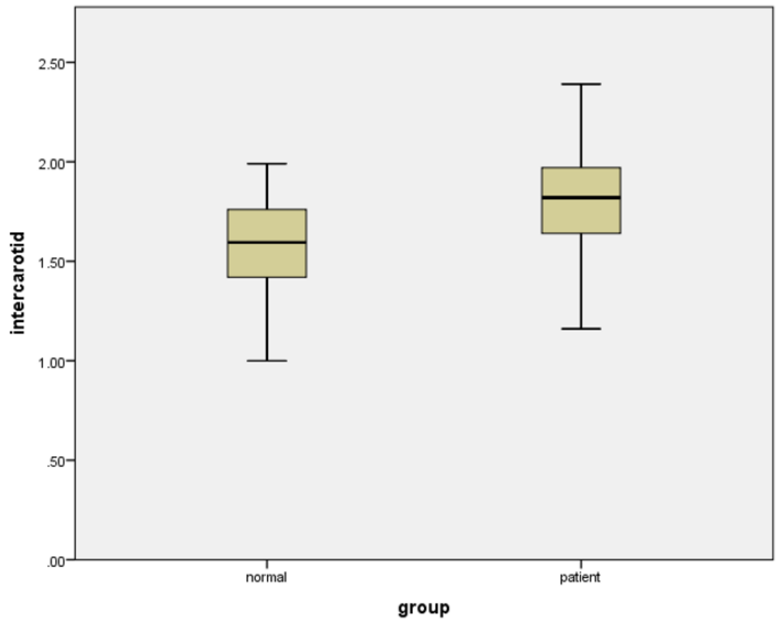

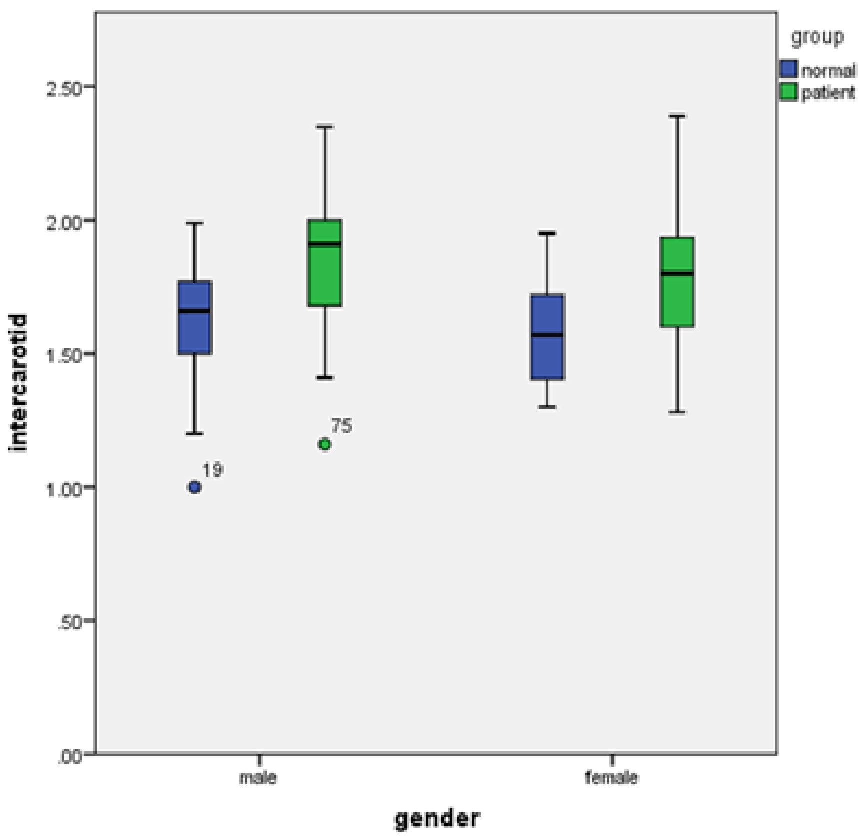

Figure 4. 8. Descriptive values (median, maximum and minimum) in both major group and subgroups for inter-carotid distance alt the level of sellar floor

The boxplots above reveal that the condensation of values in patient group is in a higher level compared with the control group.

Statistically speaking, there were significant differences between the values of both major groups (P0.00), between genders in control group (P0.01) and between females in both major groups (P0.00).

4.1.16. Pneumatization of Anterior Clinoid Process

The incidence of pneumatization of the anterior clinoid in our series extends between 14% in control group to not more than 22% in patients group. the differences between the major groups and the between the subgroups are not statistically significant.

Table 4. 18. Incidence of pneumatization of the anterior clinoid process

Pneumatization of Anterior Clinoid	Control	Patients	Statistical comparison
Right Side			
Total	(7)14%	(11)22%	NS
Males	(3)11%	(7)27%	NS
Females	(4)17%	(4)17%	NS
Left Side			
Total	(7)14%	(8)16%	NS
Males	(3)11%	(6)23%	NS
Females	(4)17%	(2)8%	NS

NS non significant P value above 0.05

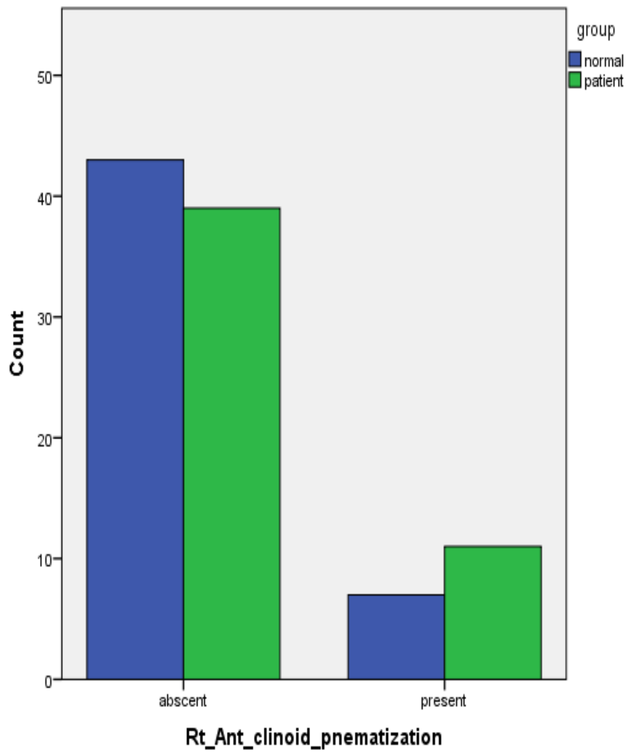

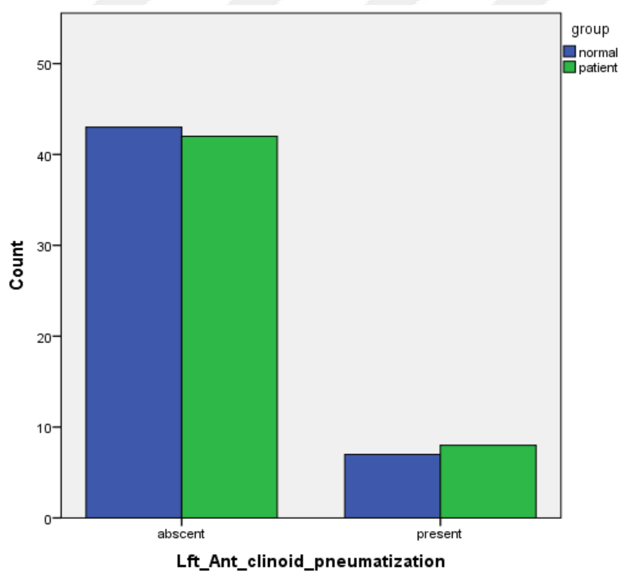

Figure 4. 9. Pneumatization of right and left anterior clinoid

4.1.17. Correlations

The correlation by definition refers to the degree of association or relationship between two random variables but by itself it does not imply that one variable causes the other. We had 3 options for this type of relationships; Prearson parametric test for continuous variables and its non parametric counterpart spearman test for non normally distributed variables. On the other hand, we have chi square test for nominal variables.In case of investigating a relationship between a nominal and an interval (continuous)variable, we have chosen Eta cofficient. All the above tests including Chi square (after adding Phi test) could investigate the strength of correlation .

4.1.18. Ant.Clinoid Pneumatization and Opticocarotid Recess Correlation

With C|hi sqaure test we investigated the correlation between having an obvious opticocarotid recess and pneumatization of the ipsilateral anterior clinoid process .Phi test was included to show the strngth of correlation.for the right side in control group ,the correlation was significant as the P value was 0.04 but the Phi test result (0.3) indicated that the correlation was weak. However, correlation in the right side in patients group was stronger (P value 0.00 and with Phi 0.5). The charts below clearly showed the difference between the two major groups with stronger correlation in patients group.

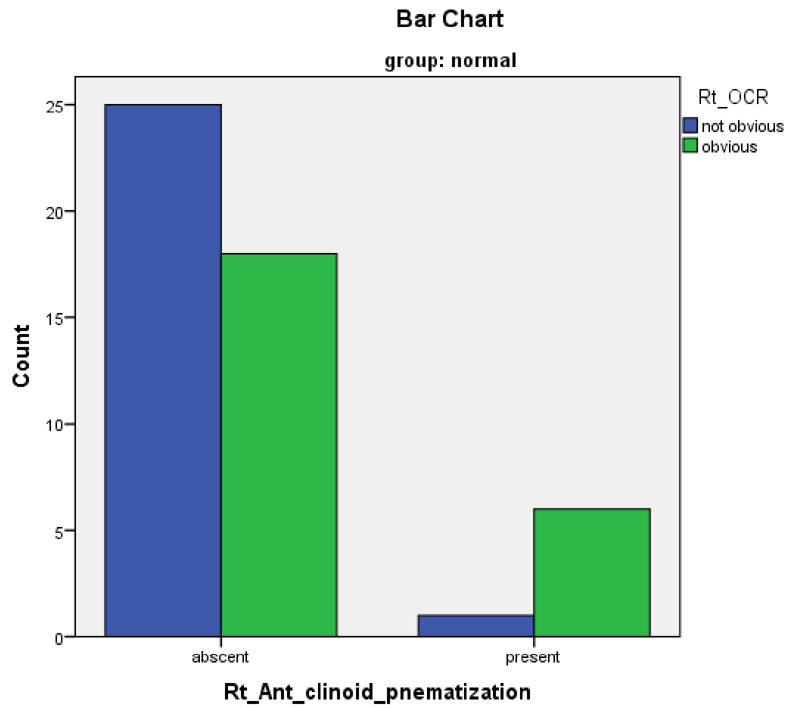

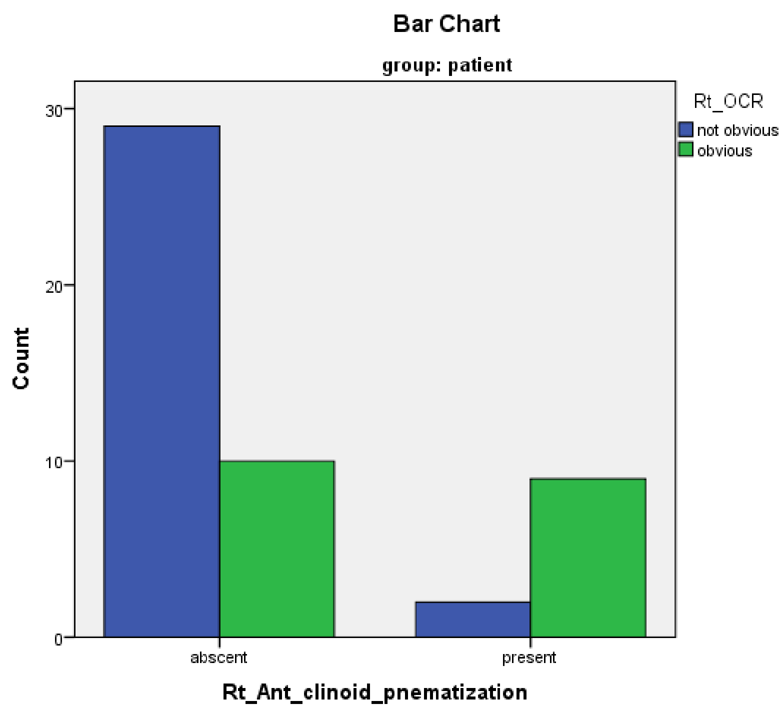

Figure 4. 10. Bar chart showing correlation between ant.clinoid pneumatization and opticocarotid recess. (OCR opticocarotid recess)

Left sided correlations were also significant with a strength of 0.4 in Phi test in both groups.

4.1.19. Age and Intercarotid Correlation

The correlation between age and the inter-carotid distance was studies using Pearson correlation coefficient. The two tailed significance was above 0.05 in both groups meaning that there was no significant correlation between these two variables: age and inter-carotid distance.

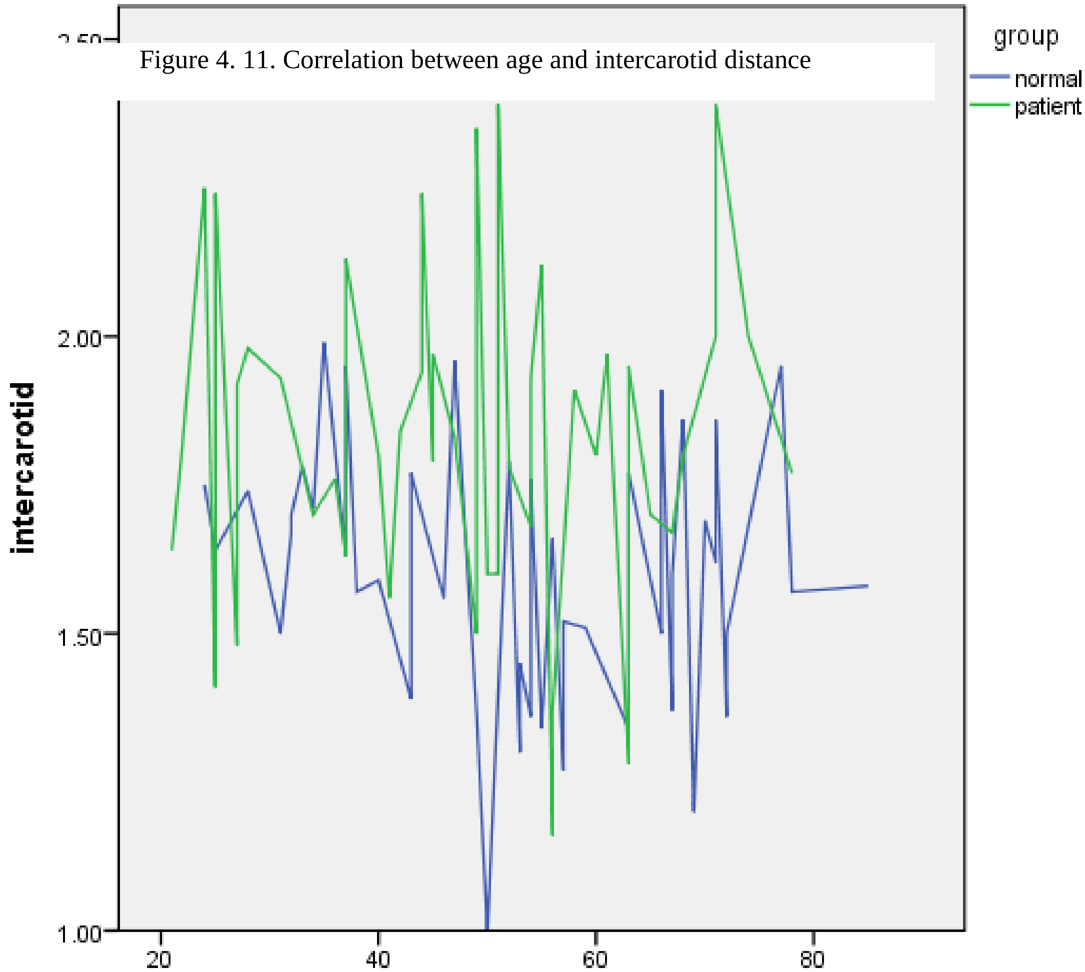

Figure 4. 11. Correlation between age and intercarotid distance

We can see from the graph above that although the patient group shows generally higher values but the mode of the two graphs is obviously hectic with no significant difference between the extreme age groups in the selected individuals.

4.1.20. Intercarotid and Columella-Sella Distances Correlation

The above graph with Pearson coefficient indicated that there is no significant correlation between inter-carotid and columella-Sella distances. Moreover, we could observe from the graph below that the values of columella-Sella distance is bouncing between 8 and less than 10 cm as the inter-carotid distance is moving from 1 to more than 2. 5 cm.

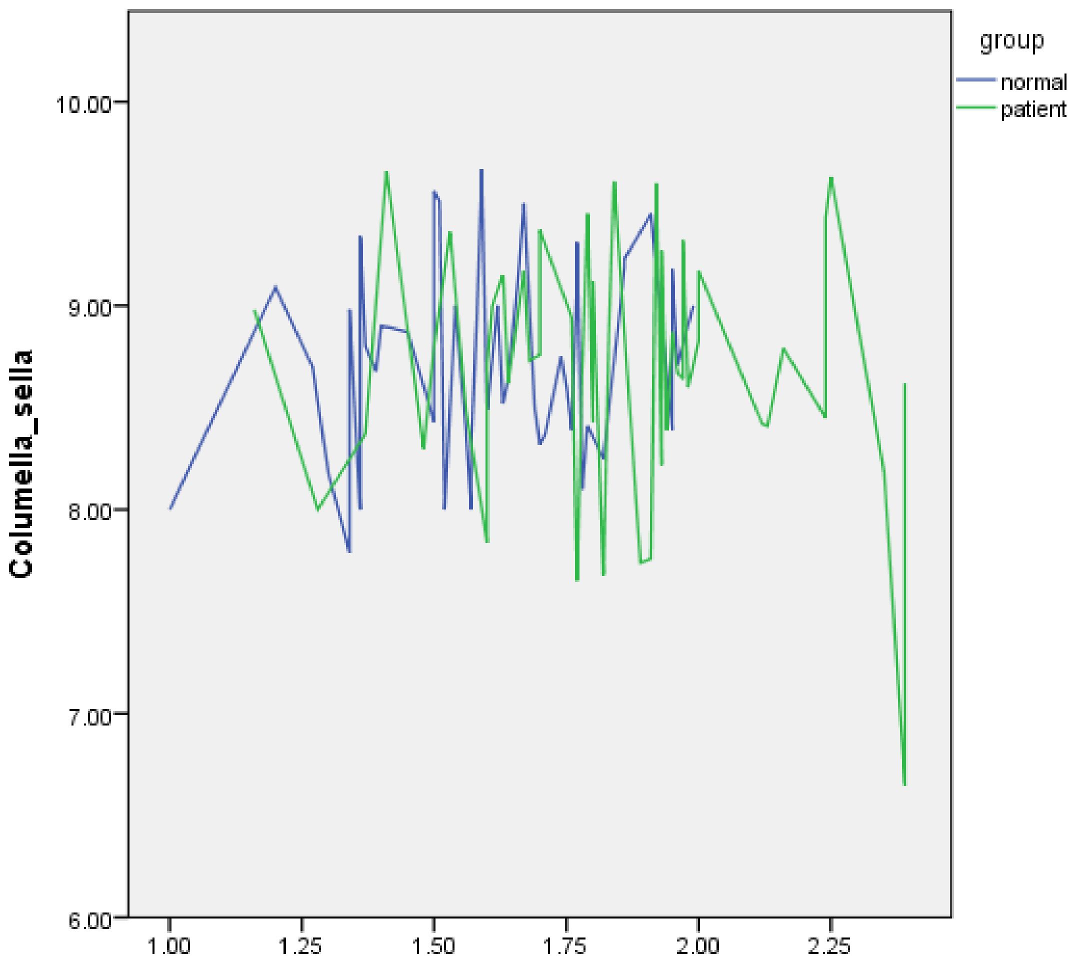

Figure 4. 12. Correlation between intercarotid distance and the distance between the columella and sellar floor

4.2. DISCUSSION

Sophisticated neuroimaging and neuro-navigation is in no way a substitute to surgeon's extensive knowledge in relevant surgical anatomy. In contrast, it represents an opportunity to go in depth in identifying microscopical relevant anatomical details. The present study evaluated the ability of the widely available preoperative CT scan to identify a set of findings other than the pathology itself. This set includes the landmarks related to the shortest path from outside at the entrance to the nose till reaching the sellar base passing through the sphenoid sinus.

These landmarks are important in keeping the surgeon oriented during this passage, avoiding going astray whether laterally away from the midline, superiorly towards the planum or inferiorly towards the clivus. They also aid in identifying the site of e important neurovascular structures nearby, especially internal carotid artery and optic nerves

The morphometry of the surgical corridor would be critical in identifying the potential working space and the limits for safe range of instruments' motion.

In bottom line, we want to use the widely available preoperative CT to identify the practically feasible shortest and safest corridor toward the sellar floor while maintaining the midline orientation without even using intraoperative navigation device. This study was aiming at helping surgeons in training and we hope that it would have a positive impact on the practice of radiological reporting, archiving, and transferring relevant surgical experiences.

The core landmarks for the nasal route toward the Sella turcica passing through the sphenoid sinus could be fairly identified to make a simple agreed upon roadmap using multi-planner CT scan and widely available software. This would aid in creating a common language between the departments involved in caring for such patients.

4.2.1. General Profile

Time limit for the selection was from 2014 to 2020, because the documents before this date were scarce in the electronic bank of data in our teaching hospital. So, we found ourselves obliged to select from within this limit.

Two groups 50 patients each. Gender distribution is approximately the same. All are adults passing the age of 15 which is considered the age of complete development of sphenoid sinus (Banu et al., 2014).

Our study concentrated on adults as they are the best age group for a beginner surgeon to avoid difficulties imposed by underdeveloped poorly pneumatized sphenoid sinus. In this way, the identification of the landmarks would be relatively more straightforward job.

4.2.2. Projection of Sellar Floor on the Lateral Surface of the Scalp

Tragus was used as an external landmark to measure the exact site of the sellar floor as projected on the lateral surface of the head at the temporal area. We referred to the tragus in pinpointing the site of the marker as in front and above the tragus. It would be easy to refer to this marker with any attempt to reintroduce the instruments. Campero et al. used the external acoustic meatus instead of the tragus as a reference point(2009).

Knowing that the straight instruments need a straight bath to reach the sella, we can argue against the use of what was called spheno-sellar point recommended by Campero et al. as it is directed away from the straight line heading to sellar floor according to the picture below (2009).

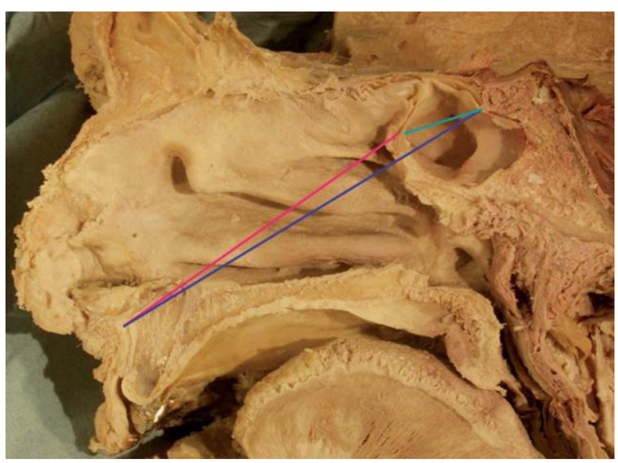

Figure 4. 13. The difference in the trajectory of the surgical path when the ostium is included (Campero and Rhoton 2009)

Anyway, and in line with their conclusion we also saw that this is a fast, reliable and very simple way to plan for transsphenoidal surgery, and their use may avoid complications associated with misdirection.

4.2.3. Angle of the Operative Path with the Nasal Floor

Radiant software could be used to show the exact location of the sella projected on the lateral surface of the skull at the temporal area as discussed above. In this way there would be no need to measure any angles between the path of the instruments and another reference line as the nasal floor or an imaginary line connecting between external landmarks as Wang et al. suggested who used a refence line linking the glabella and the external occipital tubercle (2010). Putting a marker that could be sensed by touch at the exact site of sellar projection would be enough to direct the instruments during their repetitive nasal introduction. In this way, selecting the proper angle need no sophisticated equipment.

Wang et al. suggested that it would be more practical to position the head in a way that makes the path toward the sella perpendicular or parallel to the floor (2010). But using this external marker at the head itself makes the operator freer to choose any position feasible.

4.2.4. Distance from Columella to the Sellar Floor

In harmony with the observation of Wang, et al (2010) who demonstrated that the mean depth to the sellar floor were not significantly different in sellar tumor and in control group (86.01 ± 4.99 mm and 85.34 ± 4.96 mm respectively, $p > 0.05$). We also reached the same conclusion using T test to compare between the two groups. Our explanation is that the surgical intervention nowadays usually ordered with microadenomas with normal or nearly normal diameters, or the adenoma is actually extending upward towards the brain. Even with an expanded sella, the infra-sellar adenomas were found to be 17% (Wang et al., 2016).

In contrary to Banu et al. point of view who claimed that skull base lesions have a significant impact on the skull base measurements in pediatric age group (2014), we did not notice a significant change in this distance between control and patients' group, as most differences in sphenoid sinus morphological features occur during early childhood.

In study conducted by Kim et al. the mean distances from the base of the columella to the sellar floor was 86.26±4.57 in age group older than 15 years and showed the smallest degree of variation with no further increases were evident after this age(2013). Interestingly we found nearly the same results in control cases with statistically insignificant difference with the patients as mentioned above.

There were no significant differences in the measurements between males and females as Kim et al., (2013) we found them consistent among individuals. But we noticed intersexual differences inside control group only.

Lazaridis et al. demonstrated that this distance was greater in males (2010). Regarding our results we also found that the mean values of males in control and patients' group were greater than that of females, although those differences were only significant in control group.

We can justify using this path from the columella to the sellar floor by referencing to Chumnanvej et al. who designed what he called the shortest and the safest distance to the sellar floor for the robotic arm made for transsphenoidal approach to the sella. He used the straight line extending between the anterior nasal spine and the base of sella (Chumnanvej et al., 2019).

4.2.5. Distance from Columella to the Anterior Sphenoidal Wall

Uygun et al. measured the distance between superior margin of the upper labial philtrum and top of spheno-vomerine joint and found the means between 6.66 cm for females and 7.44 cm for males (2016). We chose the same point, as the superior margin of the upper labial philtrum is exactly at the base of the columella. We also got approximately the same value for females in control group (6.6 cm) but slightly more 6.9 in patients' group. Our means for males in both groups was 7 cm.

Kim et al. also found the mean distances from the base of the columella to the anterior wall of the sphenoid sinus around 7(2013). They emphasized that the mean came with small degree of variance evident from ±0.4cm standard deviation.

Lazaridis et al also showed that the mean distance between the subspinale (inferior–posterior edge of the anterior nasal spine) and the anterior sphenoid wall was 62.3 SD 4.6 mm for the sellar type of sinus (2010).

As Banu et al. (2014) agreed upon the conclusion of Lazaridis et al. (2010) who found that the distance to the anterior sphenoidal wall would be the only significantly different distance between genders. Banu also concluded that development of sphenoid sinus and its final pneumatization is sex independent process.

We also discovered that there were intersexual significant differences in both control and patients group evident by p values less than 0.05.

We should take into consideration that the interpersonal differences and choosing different reference points may be the cause behind the differences in the values that appeared in different articles.

On the other hand, the pituitary adenoma in adult with a developed sinus is difficult to be considered as a factor in changing the morphology of the anterior sphenoidal wall. Still, we should investigate deeper in cases with evidence of elevated growth hormone level from a pituitary adenoma as it may change the composition of bones in patients affected by this type of hormonally active tumors.

4.2.6. Distance from the Intersection to the Planum Sphenoidale

The smallest recorded value for this distance was 1.2 cm and the maximum was 2.5 cm although the difference between the means was considered significant in the T test but most of the values were clustered around the means (1.8 cm for control and 1.9 for patients) evident in a variance of 0.07 each with interquartile range of 0.36 cm for control and 0.37 cm for patients. However, as the maximum value in the patient group was more than that of the control group, we can assume that the downward extension of the enlarged sella might lower the path toward the sella making the intersection point even lower than the control counterpart.

So, we have slightly less than 2 cm distance away from the skull base to enter the sphenoid sinus safely. This of course is an advantage to move in a safe path without getting a fracture at the roof of the nose with subsequent CSF leak.

4.2.7. Orientation Before Hitting the Anterior Sphenoidal Wall

4.2.7.1. Intersection Point Relation with the Ostium

Kim, et al. favored MRI over CT in studying the path between the base of the columella and the base of the Sella (2013). Interestingly, they ignored the relation of this path with the natural ostium. Taking into consideration the significant variations in the shape and position of the natural ostium as shown by Ismail et al (2018) we can assume that the natural ostium is irrelevant to the surgical path. In contrary to Kim et al. (2013) with the use of CT scan we had the opportunity to pinpoint the site of the ostium and to measure the distance between it and the potential surgical path under investigation.

All the studied individuals in control and patients group showed that the calculated site of entrance to the sphenoidal sinus lied below the natural ostium and even below the bulk of ethmoid sinuses that reside in front of the sphenoid sinus. In this way, the surgeon will not be obliged to have his instruments inside the confined gutter created between the midline nasal septum and the ethmoid bullae laterally.

The ostium of the sphenoid sinus lies above the path toward the sella turcica. Although it is an already natural aperture leading to the interior of the sphenoid sinus but searching for it during operation would complicate the procedure and it makes a drift from the straight line connecting between the exterior and the target of this type of operation which is the floor of sella turcica.

Taking Wuet al. (2011) as an example we had an impression from the literature review that many articles were not concerned with the exact practical implication of the plenty of measurements related to the sphenoid ostium they had chosen to study. Instead, they refer to these extensive measures about the ostium as important in avoiding the surgical complications without telling us how we can consider it relevant. Moreover, with cases that have no clearly identified ostia the whole measurements would be irrelevant.

4.2.7.2. Branches Of Sphenopalatine (SP) Artery

The entry site in our study lied below the natural ostium of the sphenoid, so we should always remember that this is the site from the branches of the sphenopalatine artery to run medially from the sphenopalatine foramen lying just posterior to the tail of the middle concha reaching toward the posterior nasal septum.

4.2.7.3. Sphenosellar Point

Campero et al. selected a point in the anterior wall of the sphenoid created by the intersection of one horizontal line extending from the floor of the sella to another vertical line tangential to the anterior sphenoidal wall and called it spheno-sellar point (2009). This point would be different from our point of transection with the sphenoidal sinus since we have stretched our line between the base of columella and the most advanced point in the sellar floor. This act would create another point of intersection with the anterior sphenoidal wall.

D'Souza et al also pointed out that it is not always easy to locate the ostium during endoscopy (2013). Moreover, others emphasized that there was no need to reach for the ostium for sphenoidotomy (Cappabianca et al., 2012). Dutta elaborated on this critical point saying that the lower third of superior turbinate (ST) may need to be resected to visualize the natural sphenoid ostium (2020), which lies lateral to ST in 17% patients according to their data. They also warned that manipulating the ST might injure the cribriform plate resulting in cerebrospinal fluid rhinorrhea. After all we may reach the conclusion that locating the natural ostium for sphenoidotomy is not mandatory. In addition to that Yilmaz, Nesibe in her article (2016) found that the ostium even absents in 10% of the studied individual.

4.2.7.4. Relation with Middle and Superior Conchae

Data clearly suggests that it is possible to advance the instrument safely till reaching the anterior sphenoidal wall. The middle and superior conchae are obvious landmarks to use for this purpose. These landmarks would show the normal supero-inferior coordinate for the instrument, while the posterior part of the nasal septum would insure the midline orientation.

As we studied the relation of the intersection site with the tail of the middle concha, we concluded that in all cases the trajectory should pass above the posteriorly situated tail of middle concha before hitting the anterior wall of the sphenoid sinus.

More than half of the control cases and 66% of the patients had their intersection site below the superior concha. This would leave very limited place for mistakenly drifting away from the recommended path. For the remaining percentage of cases the intersection would be hidden inside the gutter created by the superior concha laterally and the nasal septum medially. Even with these cases it is possible to start drilling bone below the superior concha then moving upward slowly putting the sellar floor under vision and heading toward it.

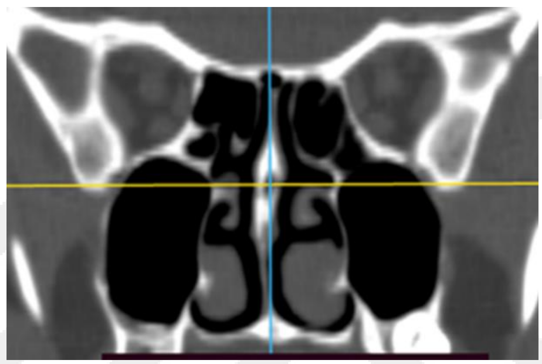

Figure 4. 14. Shows the intersection point at the anterior wall of the sphenoid below the superior concha and ethmoid cell

4.2.7.5. Relation with the Ethmoid Sinus

According to our data, the relation between the intersection and the ethmoid cells indicated that most of our cases in the patient and control groups have the intersection point below the level of ethmoid. So, we could conclude that it would be below the gutter formed between the posterior part of nasal septum and the lateralty situated ethmoid sinus.This confined space which is the sphenoethmoidal recess would be even more restricted when having an advanced anterior wall.So having the intersection below this restricted area would make the opertor free from tedious dissection in a limited space that definitely increases time of the operation and decreases safety.

4.3. Characteristics of the Anterior Wall of the Sphenoid

4.3.1. Beaked Anterior Wall of Sphenoid Sinus

A significant percentage of the sphenoidal anterior walls are having a beak anteriorly. This keel would make reaching the inside of the sinus even easier as it represents an anteriorly advanced sphenoid sinus.

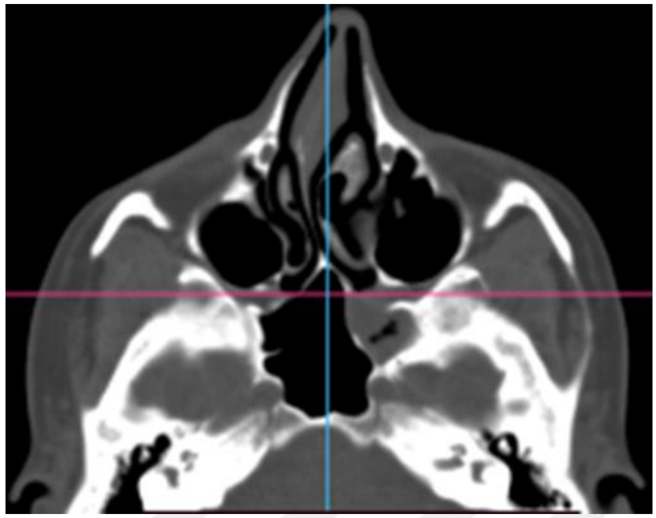

Figure 4. 15. Anterior wall of the sphenoid protruding anteriorly at the intersection point

Most of the anterior walls where more advanced at the midline with a keel like protrusion. Uygun et al. indicated that this beak is dictated by the angle between the alae of vomer (2016). They estimated the incidence to be around 74% for both genders. in another word, the anterior wall is sloping posteriorly from medial to lateral direction. In these situations, sticking to the midline would ensure hitting the anterior wall earlier without manipulating laterally behind the superior conchae. Wei et al. called it the 'bow sign' and said that it is the most important landmark indicating the correct direction for approaching the sellar floor appropriately (2013). They emphasized that this 'bird beak' is the best place to enter the sphenoid sinus (Wei et al., 2013).

4.3.2. Orientation of the Anterior Wall

Most of the cases whether in control or in patient group showed vertical type of anterior wall of sphenoid. On the other hand, the posteriorly inclined walls showed an extraordinarily strong relation with the presence of posterior spheno-ethmoidOnodi cell making this sing a very important aid to exclude or confirm the presence of Onodi cell preoperatively using CT scan. The operator should be prepared for a possibility of bulged and exposed optic nerve in such cases. In cases with inclined wall and Onodi cell assuming a lower approach if applicable is more strongly indicated to avoid the possible danger of entering the onodi cell and injuring the optic nerve and even entering the middle fossa mistakenly instead of sellar fossa as the operator would be confused with the landmarks inside the ethmoid maze.

Although our patients' group showed more cases of Onodi in statistical comparison with the control, but it is difficult to conclude that this is an effect of the adenoma itself since pneumatization is a developmental process that takes place earlier in life.

As expected, the posteriorly incline anterior wall of the sphenoid was indicative of the posterior extension of the ethmoid cell overriding sphenoid sinus especially affecting its lateral wall and the roof. This would be another benefit having a working path relatively distant from the skull base avoiding an inadvertent breach into ethmoid cell. In order to be on the safe side; it is highly recommended to stay strictly along the nasal septum close to the midline and lower enough to reach the sellar floor below even the onodi cell.

The scanned literature showed an incidence that extended between 22% according to Kaplanoglu (2013) to not more than 12% (Halil Arslan et al., 1999). Others had found 5.7% of cases studied with such a variant (Sildiroglu, 2015). We should make it clear that this incidence sometimes was concluded from extremely limited number of cases as Mutlu et al., who found the prevalence of 7.2% calculated from only 5 cases (2001).

4.4. Sellar Pneumatization

Our two sets of samples had only individuals with sellar type of pneumatization. Although it is know that this type of pneumatization is the most common type in sphenoid sinus according to Nesibe (2016) and García-Garrigós et al. (2015) who estimated its incidence as approximately 76% of the population , we could not be sure if the cases for transsphenoidal approach were already selected upon the criteria of having this type of pneumatization since it is the best type from practical point of view in having more obvious landmarks and need not much drilling of bony layers before reaching the sellar floor. In spite of that and taking the conclusion of Kim et al. into consideration which stated that pneumatization may not change distances and angles (2013), we could claim that our collected data is still generally valid across multiple types of pneumatization whether concha, presellar and sellar (Carrabba et al., 2013).

Banu et al found that differences in sphenoid volume is most likely related to changes in the width of the sinus more than the length or the height (2014). Kikuchi even saw no relation between lateral and sagittal plane pneumatization (2015).

Our target in the transsphenoidal approach to the pituitary tumor is to find the midline situated sellar bulge beneath the pituitary fossa. As we mentioned above the morphology of the bulge would be different according to the degree of pneumatization of sphenoid. However, we were able to define the sellar bulge in midsagittal cut in all cases.

4.5. Septal Attachment to Sella

Incidence of septal attachment related to the sella was 65% in patients' group. Obviously, it was more than the control group (40%). Ismail et al declared that most of inter-sphenoid septations (67%) had paramedian orientation (2018). While only 13% presented with a typical isolated midline septation (Fernandez-Mirandaet al. ,2009). Ahmadipouret al. found that the incidence of midline septum was 23 % only (2016).

Anyways, whether the midline septum was in strictly median or paramedian position the operator could use it to ensure the orientation towards the sellar bulge inside the sphenoid sinus. When statistically investigated with Chi square test the difference between the incidence of this type of septation in patients was significantly different from that of normal group. There is no obvious explanation why we got this difference as the adenoma per se is not a convincing cause behind having a specific pattern of septations.

As Zada et al. (2011) indicated, complexity and variability of septa would open the possibility of having any combination of septal configuration. There is a possibility of involving the internal carotid artery and optic canal in the attachment of the septa away from the midline towards the lateral wall of the sphenoid sinus. Moreover, the presence of very thin or even a dehiscent bone may complicate the situation. So, it would be of practical use to be aware that the drift of the septum from the midline would increase the risk of having a septum attached to the critical neurovascular structures behind the lateral wall of the sphenoid sinus (Unlu et al., 2008).

4.6. Bulging over the Carotids and Optic Nerves

The incidence of these bulges did not pass the fourth of cases in our major groups with no statistically significant difference in comparison between them. That was an unfortunate situation since it is so important to orient the operator with these para-sellar protuberances which are considered as indicators for midline by (Zada et al., 2011).

Yeung et al. called carotid artery bulging Teddy Bear sign (2018). Twigg et al. claimed that this ‘teddy bear’ sign in axial CT indicates that the carotid arteries will be identifiable intra-operatively (2017). This claim is yet to be proved in our cases before making this generalization.

Sildiroglu et al. observed optic nerve protrusion using CT scan in 30 patients (13.1%) and carotid artery protrusion in 29 patients (12.7%) (2015), while Halil Arslan reported carotid artery bulging into the sphenoid sinus in only 8% of his cases (1999). As Wei et al. indicated, para-sellar carotid bulge could be observed after tilting the microscope slightly to the left or right (2013). They explained that when these bulges could be observed intraoperatively bilaterally, they will give an extra insurance that the Sella is the space lying between them.

Interestingly, Unlu et al. found in their cadaveric study that the optic nerve and the carotid prominences along with the optico-carotid recess and the pituitary bulge in the midline were identifiable on both sides (2008). Ismail et al. confirmed the same findings that these landmarks were well-defined in sellar type pneumatization (2018).

This discrepancy between the CT, cadavers and intraoperative findings draws the attention to the importance of investigating for these landmarks in a study that at least include the CT and the operative findings to investigate how much we could lean from the CT scan in anticipating the observation of these bulges intraoperatively.

4.7. Lateral Optico-Carotid Recess

Having an obvious opticocarotid recess is a blessing for the operator since it would make it clear to see the optic bulge above and the carotid bulge below and medial. This recess corresponds to the optic strut base and the clinoid segment of the carotid artery would be immediately lying medial to it aiding in the intraoperative localization of the carotid artery segments (Peris-Celdaet al., 2013). Güler claimed that the segment of the optic nerve above the optico-carotid recess which is considered the medial and inferior proximal portions of this nerve is more prone to injury caused by traction or compression (2019). So better to identify this portion before any manipulation. In our study we could only identify this landmark in less than half of the cases using CT scan despite the confirmation from Unlu et al (2008) and Ismailet et al (2018) that this landmark is well-defined in sellar type pneumatization in cadevers. Taking this discrepancy into consideration, we think that the match between the radiological finding and the surgical scene is of utmost importance to evaluate the credibility of CT scan in identifying this important landmark.

4.8. Pneumatization of the Anterior Clinoid

Sildiroglu et al. found that pneumatization of the anterior clinoid process in 32 patients was14% (2015). This frequency has been reported in our series for control group. Although the patients reported higher values, but the difference was not statistically significant.

As this type of pneumatization was found to be highly correlated with the presence of optico-carotid recess, we would like to extend our investigation later to see if this is in harmony with the actual scenes during the operations to see if we can predict the presence of the lateral optico-carotid dimple from observing the anterior clinoid pneumatization.

4.9. Inter-Carotid Distance at the Anterior Point of the Sellar Floor

Banu et al. concluded that inter-carotid distance is significantly different only in the extreme age group when pediatric age is considered (2014). That was not the case in our groups weather patients or control.

Banu et al also indicated that **Nare-sellar distance** can be used to assess global skull base development because it highly correlates with the **inter-carotid distance** in both the normal population and in patients harboring skull base lesions (2014). Our selected cases did not reveal the same result. Banu group was studying pediatric age group in which the sphenoid sinus was still developing. we can conclude that after passing the age of full development of the sphenoid sinus the measurements related to the sphenoid would not be intimately interrelated.

Carrabba et al. discovered that the inter-carotid distance decreases with growth hormone- secreting adenomas and acromegaly (2013). Sacher called the carotids approaching the midline in acromegaly ‘kissing carotid’ (1986). Newman et al. showed that the internal carotid approached within 4 mm of the midline in 1.3% of cases (2020).

In contrary to what Ahmadipour et al. found in 2016, our data showed that the overall mean of this distance for patients were larger than control group (1.85cm SD .3 for patients and 1.6cm SD .22 for control). May be the enlargement of the sella in response to the expanding adenoma was behind this increase in the diameter between these two groups. The difference was found to be highly significant with P value of 0.00 as shown in table (4.13). However, as we mentioned above in acromegaly the reverse would be expected having the carotid approaching the midline making the gate between them more restricted which would increase the difficulty in reaching the pituitary adenoma.

We should be remembering that even with pituitary macroadenoma there are factors in the unique anatomy of sphenoid that may prevent the tumor from growing downward into the sphenoid sinus. In these situations, the tumor may choose to extend into the suprasellar space away from the sphenoid keeping the measurements strangely near normal (Ramakrishnan et al., 2013).

Wang et al (2010) found the distance at the cavernous sinuses in the patients with sellar tumors to be 22.68 ± 5.03 mm way greater than in the control group (15.89 ± 3.11 mm) ($p < 0.01$). These variations were expected since the arteries take serpentine course, and the distance would vary according to the level of measurements with the possibility of change because of having expanded tumor. In their article, Ismail et al.had the para-sellar inter-carotid distance 13.8±2.8 mm (range: 9-19 mm) while it was 13.3±3.3 mm (range: 7-18 mm) at the Paraclival level (2018).

Unluet al. took the measurement at the same level that we have chosen at the lower margin of the pituitary and reached nearly the same results that we found in patient group i.e18 SD 3.1 mm (2008).

In the bottom line, the surgeon would not have more than 2.5 cm to get into the pituitary passing the sellar bulge between the two carotids.

4.10. Limitations

In pursuing higher level of credibility, we would like to reveal some limitations we came across during the conduct of the study. Knowing that despite these obstacles, conclusions drawn from the study could be safely considered valid and in harmony with basic objectives of the study.

4.10.1. Design

This study was limited by its retrospective nature, single-site perspective.

4.10.2. Size of the Samples

Small sample size hinders the generalizability of the findings. Taking into consideration that every patient has his unique way of sphenoidal pneumatization, so we can conclude that increasing the size of the sample surely would reveal even more types of variations. Despite that, our result showed that the landmarks have a predictable fashion and could be used repeatedly as a strong indicator for the neural or vascular structure lurking behind.

4.10.3. Age Group

Future studies may benefit from a larger sample size including younger ages with less developed sphenoid sinus.

4.10.4. Inclusion Criteria

We excluded patients with history of nasal surgery or significant facial pathological changes from the study. Moreover, many patients' data in the electronic archive of the hospital has been lost completely. This has limited the available participants matching criteria of selection.

4.10.5. Limitation in Selection of Landmarks

While we concentrated on anatomical landmarks relevant to sellar approach, there are other landmarks that should be studied for extended approach to the skull base via transsphenoidal route.

4.10.6. Inherent Limitations of CT Scan

In comparison with other neuroimaging as MRI, CTscan has some limitation especially in identification of the intra-cavernous internal carotid artery in case of non-contrast study. Inability to identify the internal carotid artery borders, in case of bony dehiscence or because of blending with the sellar tumor, was an important shortcoming that hinder measurement of intercarotid distance at all levels.

4.10.7. Language Restriction

We imposed restrictions on language and publication date as only English publications that dated back to 1990 were chosen.

4.10.8. Limitations of the Software

More sensitive software application tailored for optimal visualization of the sphenoidal details in 3D mode is highly indicated for advanced data collection and analysis. The latest version of SPSS is not available on the web site of our university and the only way to get it was by using a trial version from ibm.com.

4.10.9. Absence of Correlations with Operative Findings

Correlating radiological findings with the operative scene would have increased the usefulness of the CT findings in recognizing the landmarks during operation.

4.11. Impact of Limitations on Achieving Research Goals

We aimed at using the accessible armamentarium in one specific hospital in accomplishing the work safely and effectively. The practicality of our results is yet to be tested clinically, as it depends on expertise, training, and facilities at our institution. That may differ from those at other institutions which may limit the ability to generalize our recommendations.

Despite the stated limitations, findings are nonetheless valid for the purpose of answering the research questions. As we came across many articles related to the same subject, we claim that our study has its own unique approach in aiming at constructing a consensus between the specialties involved in the management of patients with pituitary adenomas using an easily reproducible protocol and widely available non-invasive test as CT scan.

4.12. Future Work

- We would like to strengthen the practical impact of our study with future similar studies that include a correlation with intraoperative findings with prospective study using the surgical videos.
- Also, we would like to evaluate the practicality of the checklist we created in this study as a template for the radiologists to use during their analysis and reporting of CT findings for a referred patient.

5. CONCLUSION AND RECOMMENDATIONS

Detailed preoperative analysis of the path toward the Sella passing through sphenoid sinus using CT scan is crucial for surgeons before performing a transsphenoidal surgery. This procedure would make it easy for the surgeon to anticipate in advance the structures that would be encountered during surgery. Moreover, limits of dissection would be more obvious for the operator to refrain from avoidable iatrogenic lesion while making his way through this corridor without using expensive intraoperative navigation device.

Adding this new purpose in using the CT scan will establish a consensus for future preoperative planning in using landmarks checklist to ensure safe operative route. Establishing this routine would later enrich the medical library with our own experience. Eventually, this would aid in sharing and transferring experience to new generations of surgeons more easily.

The set of anatomic landmarks and their relationship with the adjacent neurovascular critical structures should be reported by the radiologist. This would aid in constructing interdisciplinary consensus. This practice is highly indicated even with the use of intraoperative surgical navigation. However, taking into consideration that limited resources is a universal phenomenon so better to adapt the practice of getting more from the available limited tools.

Multiplanar images bone window thin cut CT is a useful adjunct in creating preoperative roadmap for intranasal transsphenoidal approach. Axial and coronal images obtained by direct acquisition or by reconstructions are necessary to show the position of the parameters, detect sphenoid variations and choose the best possible corridor, angle, and limits of working zone.

REFERENCES

A. Neubauer, S. Wolfsberger, M. -. Forster, L. Mroz, R. Wegenkittl and K. Buhler, "Advanced virtual endoscopic pituitary surgery," in IEEE Transactions on Visualization and Computer Graphics, vol. 11, no. 5, pp. 497-507, Sept.-Oct. 2005.

Achey, Rebecca and Karsy, Michael and Azab, Mohammed and Scoville, Jonathan and Kundu, Bornali and Bowers, Christian and Couldwell, William. (2019). Improved Surgical Safety via Intraoperative Navigation for Transnasal Transsphenoidal Resection of Pituitary Adenomas. Journal of Neurological Surgery Part B: Skull Base. 80. 10.1055/s-0039-1677677.

Adin, M. E., Ozmen, C. A., and Aygun, N. (2019). Utility of the Vidian canal in endoscopic skull base surgery: detailed anatomy and relationship to the internal carotid artery. *World Neurosurgery*, 121, e140-e146.

Agbetoba, A., Luong, A., Siow, J. K., Senior, B., Callejas, C., Szczygielski, K., and Citardi, M. J. (2017, February). Educational utility of advanced three-dimensional virtual imaging in evaluating the anatomical configuration of the frontal recess. In *International forum of allergy & rhinology* (Vol. 7, No. 2, pp. 143-148).

Ahmadipour, Y., Lemonas, E., Maslehaty, H., Goericke, S., Stuck, B. A., El Hindy, N., ... and Mueller, O. (2016). Critical analysis of anatomical landmarks within the sphenoid sinus for transsphenoidal surgery. *European Archives of Oto-Rhino-Laryngology*, *273*(11), 3929-3936.

Ahmed, S., Elsheikh, M., Stratton, I. M., Page, R. C., Adams, C. B., and Wass, J. A. (1999). Outcome of transphenoidal surgery for acromegaly and its relationship to surgical experience. *Clinical Endocrinology,* 50(5), 561–567.

Aktas, U., Yilmazlar, S., and Ugras, N. (2013). Anatomical restrictions in the transsphenoidal, transclival approach to the upper clival region: a cadaveric, anatomic study. Journal of cranio-maxillo-facial surgery: official publication of the European Association for Cranio-Maxillo-Facial Surgery, 41(6), 457–467.

Albano, L., Parisi, V., Acerno, S., Barzaghi, L. R., Losa, M., and Mortini, P. (2019). Sublabial transsphenoidal microsurgical technique to treat congenital transsphenoidal encephalocele: a technical note. *Neurosurgical Review*, 42(2), 571-575.

Arbolay, O. L., González, J. G., González, R. H., & Gálvez, Y. H. (2009). Extended endoscopic endonasal approach to the skull base. *min-Minimally Invasive Neurosurgery*, *52*(03), 114-118.

Mert, A., Micko, A., Donat, M., Maringer, M., Buehler, K., Sutherland, G. R., and Wolfsberger, S. (2014). An advanced navigation protocol for endoscopic transsphenoidal surgery. *World neurosurgery*, *82*(6), S95-S105.

Banu, M. A., Guerrero-Maldonado, A., McCrea, H. J., Garcia-Navarro, V., Souweidane, M. M., Anand, V. K., and Greenfield, J. P. (2014). Impact of skull base development on endonasal endoscopic surgical corridors. *Journal of Neurosurgery: Pediatrics*, *13*(2), 155-169.

Bolger, W. E., Keyes, A. S., & Lanza, D. C. (1999). Use of the superior meatus and superior turbinate in the endoscopic approach to the sphenoid sinus. *Otolaryngology--Head and Neck Surgery*, *120*(3), 308-313.

Bora, S. K., Suri, A., Khadgawat, R., Tandon, N., Suri, V., Sharma, M. C., ... and Kale, S. S. (2020). Management of Cushing's disease: Changing trend from microscopic to endoscopic surgery. *World Neurosurgery,* 134, e46-e54.

Budu, V., Mogoanta, C. A., Fanuta, B., and Bulescu, I. (2013). The anatomical relations of the sphenoid sinus and their implications in sphenoid endoscopic surgery. *Rom J Morphol Embryol*, *54*(1), 13-6.

Campero, A., Socolovsky, M., Torino, R., Martins, C., Yasuda, A., & Rhoton Jr, A. L. (2009). Anatomical landmarks for positioning the head in preparation for the transsphenoidal approach: the spheno-sellar point. *British journal of Neurosurgery*, *23*(3), 282-286.

Cappabianca, P., Cavallo, L. M., Esposito, I., & Solari, D. (2012). Sellar/tuberculum approach. In *Endoscopic Approaches to the skull base* (Vol. 26, pp. 41-59). Karger Publishers.

Carrabba, G., Locatelli, M., Mattei, L., Guastella, C., Mantovani, G., Rampini, P., and Gaini, S. M. (2013). Transphenoidal surgery in acromegalic patients: anatomical considerations and potential pitfalls. *Acta Neurochirurgica*, *155*(1), 125-130.

Chumnanvej, S., Pattamarakha, D., Sudsang, T., and Suthakorn, J. (2019). Anatomical Workspace Study of Endonasal Endoscopic Transsphenoidal Approach. *Open Medicine,* 14, 537 - 544.

Cusimano, M. D., Di Ieva, A., Lee, J., and Anderson, J. (2013). Canula-assisted endoscopy in bi-portal transphenoidal cranial base surgery. *Acta Neurochirurgica*, 155(5), 909-911.

Dasar, U., and Gokce, E. (2016). Evaluation of variations in sinonasal region with computed tomography. *World Journal of Radiology*, *8*(1), 98.

Szolar, D., Preidler, K., Ranner, G., Braun, H., Kern, R., Wolf, G., and Ebner, F. (1994). Magnetic resonance assessment of age-related development of the sphenoid sinus. *The British journal of radiology*, *67*(797), 431-435.

Daniel L. Barrow, M.D., George T. Tindall, M.D., (1990) Loss of Vision after Transsphenoidal Surgery, *Neurosurgery,* 27 (1), 60–68.

Dasar, U., and Gokce, E. (2016). Evaluation of variations in sinonasal region with computed tomography. *World Journal of Radiology,* 8(1), 98–108.

DeLano, M. C., Fun, F. Y., and Zinreich, S. J. (1996). Relationship of the optic nerve to the posterior paranasal sinuses: a CT anatomic study. AJNR. *American Journal of Neuroradiology*, 17(4), 669–675.

Dessi, P., Moulin, G., Castro, F., Chagnaud, C., and Cannoni, M. (1994). Protrusion of the optic nerve into the ethmoid and sphenoid sinus: prospective study of 150 CT studies. *Neuroradiology*, 36(7), 515–516.

Deutschmann, M. W., Yeung, J., Bosch, M., Lysack, J. T., Kingstone, M., Kilty, S. J., and Rudmik, L. R. (2013). Radiologic reporting for paranasal sinus computed tomography: A multi-institutional review of content and consistency. *The Laryngoscope*, 123(5), 1100-1105.

Drake, R., Vogl, A. W., and Mitchell, A. W. (2009). Gray's anatomy for students E-book. Elsevier Health Sciences.

Dutta, M. (2020). Unaltered, Endoscopic View of the Sphenoethmoid Recess Through the Second Pass. Ear, Nose and Throat Journal.

ELKammash, T. H., Enaba, M. M., and Awadalla, A. M. (2014). Variability in sphenoid sinus pneumatization and its impact upon reduction of complications following sellar region surgeries. *The Egyptian Journal of Radiology and Nuclear Medicine*, 45(3), 705-714.

Ellis, H. (2002). Medico-legal litigation and its links with surgical anatomy. *Surgery (Oxford)*, *20*(8), i-ii.

Eordogh, M., Grimm, A., Gawish, I., Patonay, L., Reisch, R., Briner, H. R., and Baksa, G. (2018). Anatomy of the sphenopalatine artery and its implications for transnasal neurosurgery. *Rhinology*, *56*(1), 82-88.

Error, M., Ashby, S., Orlandi, R. R., and Alt, J. A. (2018). Single-blinded prospective implementation of a preoperative imaging checklist for endoscopic sinus surgery. *Otolaryngology–Head and Neck Surgery*, 158(1), 177-180.

Eweiss, A.Z., Ibrahim, A.A. and Khalil, H.S. (2012). The safe gate to the posterior paranasal sinuses: reassessing the role of the superior turbinate. *Eur Arch Otorhinolaryngol*, 269, 1451–1456.

Farımaz, M., Çelik, H. H., Ergun, K. M., Akgöz, A., and Urfalı, B. (2019). The morphometry of the cavernous part of the internal carotid artery. *Folia Morphologica*, 78(1), 54-62.

Fernandez-Miranda, J. C., Prevedello, D. M., Madhok, R., Morera, V., Barges-Coll, J., Reineman, K., ... and Kassam, A. B. (2009). Sphenoid septations and their relationship with internal carotid arteries: anatomical and radiological study. *The Laryngoscope*, 119(10), 1893-1896.

Frank G, Pasquini E, Farneti G, Mazzatenta D, Sciarretta V, Grasso V, Faustini Fustini M:(2006) The Endoscopic versus the Traditional Approach in Pituitary Surgery. *Neuroendocrinology*; 83:240-248.

Ganjaei, K. G., Soler, Z. M., Mappus, E. D., Worley, M. L., Rowan, N. R., Garcia, G. J., and Schlosser, R. J. (2019). Radiologic changes in the aging nasal cavity. *Rhinology*, 57(2), 117.

García-Garrigós, E., Arenas-Jiménez, J. J., Monjas-Cánovas, I., Abarca-Olivas, J., Cortés-Vela, J. J., De La Hoz–Rosa, J., and Guirau-Rubio, M. D. (2015). Transsphenoidal approach in endoscopic endonasal surgery for skull base lesions: what radiologists and surgeons need to know. *Radiographics,* 35(4), 1170-1185.

Gotlib, T., Kuźmińska, M., Sokołowski, J., Dziedzic, T., and Niemczyk, K. (2018). The supreme turbinate and the drainage of the posterior ethmoids: a computed tomographic study. *Folia Morphologica*, 77(1), 110-115.

Goudakos, J. K., Markou, K. D., & Georgalas, C. (2011). Endoscopic versus microscopic trans-sphenoidal pituitary surgery: a systematic review and meta-analysis. *Clinical Otolaryngology*, *36*(3), 212-220.

Güldner, C., Pistorius, S. M., Diogo, I., Bien, S., Sesterhenn, A., and Werner, J. A. (2012). Analysis of pneumatization and neurovascular structures of the sphenoid sinus using cone-beam tomography (CBT). *Acta Radiologica*, 53(2), 214-219.

Güler, T. M., Yılmazlar, S., & Özgün, G. (2019). Anatomical aspects of optic nerve decompression in transcranial and transsphenoidal approach. *Journal of Cranio-Maxillofacial Surgery*, *47*(4), 561-569.

Guo, Z., Liu, C., Hou, H., Li, R., Su, J., Zhang, F., Xing, G., Qian, L., Qiu, J., Xie, Y., and Zhu, N. (2018). Preoperative Computed Tomography (CT) Evaluation of Anatomical Abnormalities in Endonasal Transsphenoidal Approach in Pituitary Adenoma. Medical science monitor: *International Medical Journal of Experimental and Clinical Research*, 24, 1268–1275.

Gupta, T., Aggarwal, A., & Sahni, D. (2013). Anatomical landmarks for locating the sphenoid ostium during endoscopic endonasal approach: a cadaveric study. *Surgical and radiologic anatomy*, *35*(2), 137-142.

Arslan, H., Aydınlıoğlu, A., Bozkurt, M., and Egeli, E. (1999). Anatomic variations of the paranasal sinuses: CT examination for endoscopic sinus surgery. *Auris Nasus Larynx*, *26*(1), 39-48.

Hamberger, C. A., Hammer, G., Norlen, G., and Sjogren, B. (1961). Transantrosphenoidal hypophysectomy. *Archives of Otolaryngology*, 74(1), 2-8.

Hamid, O., El Fiky, L., Hassan, O., Kotb, A., and El Fiky, S. (2008). Anatomic Variations of the Sphenoid Sinus and Their Impact on Trans-sphenoid Pituitary Surgery. Skull base: official journal of North American Skull Base Society ... [et al.], 18(1), 9–15.

Hammer, G., and Rådberg, C. (1961). The sphenoidal sinus: an anatomical and roentgenologic study with reference to transsphenoid hypophysectomy. *Acta radiologica*, (6), 401-422.

Hiyama, T., Shiigai, M., Masumoto, T., and Minami, M. (2015, March). The sphenoid sinus: clinical imaging anatomy and pathology. European Congress of Radiology 2015.

Ismail, M., Abdelhakb, B., and Michela, O. (2018). Endoscopic sphenoid sinus anatomy in View of Transsphenoidal Surgery: Standardized Way-point Cadaver Dissection. *Egyptian Journal of Ear, Nose, Throat and Allied Sciences*, *19*(2), 38-44.

Jane, J. A., Jr., Han, J., Prevedello, D. M., Jagannathan, J., Dumont, A. S., and Laws, E. R., Jr. (2005). Perspectives on endoscopic transsphenoidal surgery, Neurosurgical Focus FOC, 19(6), 1-10. Retrieved Mar 30, 2021.

Wang, J., Bidari, S., Inoue, K., Yang, H., and Rhoton Jr, A. (2010). Extensions of the sphenoid sinus: a new classification. *Neurosurgery*, *66*(4), 797-816.

Johnson, D. M., Hopkins, R. J., Hanafee, W. N., and Fisk, J. D. (1985). The unprotected parasphenoidal carotid artery studied by high-resolution computed tomography. *Radiology*, *155*(1), 137-141.

Sievers, K. W., Greess, H., Baum, U., Dobritz, M., and Lenz, M. (2000). Paranasal sinuses and nasopharynx CT and MRI. *European Journal of Radiology*, *33*(3), 185-202.

Kabil, M. S., Eby, J. B., and Shahinian, H. K. (2005). Fully endoscopic transnasal versus transseptal transphenoidal pituitary surgery. *Neurosurgery Quarterly*, *15*(3), 190-196.

Kajoak, S. A., Ayad, C. E., Balla, E. A. A., Najmeldeen, M., Yousif, M., and Musa, A. (2014). Characterization of sphenoid sinuses for Sudanese population using computed tomography. *Global journal of health science*, *6*(1), 135.

Kaplanoglu, H., Kaplanoglu, V., Toprak, U., and Hekimoglu, B. (2013). Surgical measurement of the sphenoid sinus on sagittal reformatted CT in the Turkish population. *The Eurasian journal of medicine*, *45*(1), 7-15.

Karkas, A., Zimmer, L. A., Theodosopoulos, P. V., Keller, J. T., and Prades, J. M. (2020). Endonasal endoscopic approach to the pterygopalatine and infratemporal fossae. *European Annals of Otorhinolaryngology, Head and Neck Diseases*.

Kikuchi, R., Toda, M., Tomita, T., Ogawa, K., and Yoshida, K. (2015). Analysis of sphenoid sinus lateral pneumatization for endonasal endoscopic surgery. *Surgical neurology international*, Int 27-Oct-6:166.

Kim, H. U., Kim, S. S., Kang, S. S., Chung, I. H., Lee, J. G., and Yoon, J. H. (2001). Surgical anatomy of the natural ostium of the sphenoid sinus. *The Laryngoscope*, 111(9), 1599-1602.

Kim, Y. H., Kim, J. E., Kim, M. J., and Cho, J. H. (2013). New landmark for the endoscopic endonasal transsphenoidal approach of pituitary surgery. *Journal of Korean Neurosurgical Society*, 53(4), 218.

Komotar, R. J., Starke, R. M., Raper, D. M., Anand, V. K., and Schwartz, T. H. (2012). Endoscopic endonasal compared with microscopic transsphenoidal and open transcranial resection of giant pituitary adenomas. *Pituitary*, *15*(2), 150-159.

Koren, I., Hadar, T., Rappaport, Z. H., and Yaniv, E. (1999). Endoscopic transnasal transsphenoidal microsurgery versus the sublabial approach for the treatment of pituitary tumors: endonasal complications. *The Laryngoscope*, *109*(11), 1838–1840.

Laws Jr, E. R., Cohen-Gadol, A. A., Schwartz, T. H., and Sheehan, J. P. (Eds.). (2017). Transsphenoidal Surgery: Complication Avoidance and Management Techniques. Springer.

Lazaridis, N., Natsis, K., Koebke, J., and Themelis, C. (2010). Nasal, sellar, and sphenoid sinus measurements in relation to pituitary surgery. *Clinical Anatomy*, 23(6), 629-636.

Lekgwara, P., Kelly, A., and Younus, A. (2019). Surgical considerations in the endoscopic endonasal transphenoidal approach for giant pituitary adenomas: A single surgeons' experience over a decade. *Interdisciplinary Neurosurgery*, 17, 138-142.

Li A, Liu W, Cao P, Zheng Y, Bu Z, Zhou T. (2017) Endoscopic Versus Microscopic Transsphenoidal Surgery in the Treatment of Pituitary Adenoma: A Systematic Review and Meta-Analysis. *World Neurosurg*. 101:236-246.

Liu, J. K., Das, K., Weiss, M. H., Laws, E. R., Jr, and Couldwell, W. T. (2001). The history and evolution of transsphenoidal surgery, *Journal of Neurosurgery*, 95(6), 1083-1096.

Locatelli, M., Di Cristofori, A., Draghi, R., Bertani, G., Guastella, C., Pignataro, L., and Carrabba, G. (2017). Is complex sphenoidal sinus anatomy a contraindication to a transsphenoidal approach for resection of sellar lesions? Case series and review of the literature. *World neurosurgery*, 100, 173-179.

Lubbe, D., and Semple, P. (2008). Pre-operative assessment of patients undergoing endoscopic, transnasal, transsphenoidal pituitary surgery. *The Journal of Laryngology and Otology*, 122(6), 644-646.

Marcati, E., Andaluz, N., Froelich, S. C., Zimmer, L. A., Leach, J. L., Fernandez-Miranda, J. C., and Keller, J. T. (2018). Paratrigeminal, Paraclival, precavernous, or all of the above? a circumferential anatomical study of the C3-C4 transitional segment of the internal carotid artery. *Operative Neurosurgery*, *14*(4), 432-440.

Meybodi, A. T., Moreira, L. B., Little, A. S., Lawton, M. T., and Preul, M. C. (2018). Anatomical assessment of the endoscopic endonasal approach for the treatment of paraclinoid aneurysms. *Journal of Neurosurgery*, 131(6), 1734-1742.

Mutlu, C., Unlu, H. H., Goktan, C., Tarhan, S., and Egrilmez, M. (2001). Radiologic anatomy of the sphenoid sinus for intranasal surgery. *Rhinology*, 39(3), 128–132.

Naim-Ur-Rahman, and Jamjoom, Abdulhakim and Jamjoom, Zain. (1996). Modified coronal computerized tomographic cuts for transsphenoidal surgery. Technical note. *Neurosurgical Review*. 19. 85-8. 10.1007/BF00418075.

Fatemi, N., Dusick, J. R., de Paiva Neto, M. A., & Kelly, D. F. (2008). The endonasal microscopic approach for pituitary adenomas and other parasellar tumors: a 10-year experience. *Operative Neurosurgery*, *63*(suppl_4), ONS244-ONS256.

Nesibe YILMAZ (2015). Detailed anatomical analysis of the sphenoidal sinus and ostium of sphenoidal sinus by the cone-beam computed tomography.

Newman, H., Milne, N., and Lewis, S. B. (2020). Neurosurgical Anatomy of the Internal Carotid Artery: Magnetic Resonance Imaging Study of the Sellar Region. *World neurosurgery*, 133, e711-e715.

Nunes, C. F., Prevedello, D. M. S., Carrau, R. L., da Fonseca, C. O. P., and Landeiro, J. A. (2016). Morphometric analysis of the medial opticocarotid recess and its anatomical relations relevant to the transsphenoidal endoscopic endonasal approaches. *Acta neurochirurgica*, 158(2), 319-324.

Pádua, F. G., and Voegels, R. L. (2008). Severe posterior epistaxis–endoscopic surgical anatomy. *The Laryngoscope*, 118(1), 156-161.

Palmer, J. N., and Chiu, A. G. (2013). Atlas of Endoscopic Sinus and Skull Base Surgery: Expert Consult-Online and Print. Elsevier Health Sciences.

Jiang, P. F., Dai, X. Y., Lv, Y., Liu, S., and Mu, X. Y. (2015). Imaging study on the optic canal using sixty-four-slice spiral computed tomography. *International journal of clinical and experimental medicine*, *8*(11), 21247.

Peris-Celda, Maria and Kucukyuruk, Baris and Monroy-Sosa, Alejandro and Funaki, Takeshi and Valentine, Rowan and Rhoton Jr., M.D., Albert L. (2013). The Recesses of the Sellar Wall of the Sphenoid Sinus and Their Intracranial Relationships. Neurosurgery. 73. 10.1227/NEU.0b013e31828ce2f2.

Perondi, G. E., Isolan, G. R., de Aguiar, P. H. P., Stefani, M. A., and Falcetta, E. F. (2013). Endoscopic anatomy of sellar region. *Pituitary*, 16(2), 251-259.

Phillips, N., and Nix, P. (2016). How I do it-endoscopic endonasal approach for pituitary tumour. *Acta neurochirurgica*, 158(10), 1983-1985.

Pirinc, B., Fazliogullari, Z., Guler, I., Dogan, N. U., Uysal, I. I., and Karabulut, A. K. (2019). Classification and volumetric study of the sphenoid sinus on MDCT images. *European Archives of Oto-Rhino-Laryngology*, *276*(10), 2887-2894.

Rahmati, A., Ghafari, R., and AnjomShoa, M. (2016). Normal Variations of Sphenoid Sinus and the Adjacent Structures Detected in Cone Beam Computed Tomography. *Journal Of Dentistry* (Shiraz, Iran), 17(1), 32–37.

Ramakrishnan, V. R., Suh, J. D., Lee, J. Y., O'Malley, B. W., Jr., Grady, M. S., and Palmer, J. N. (2013). Sphenoid sinus anatomy and suprasellar extension of pituitary tumors, *Journal of Neurosurgery JNS*, 119(3), 669-674.

Renn, W. H., and Rhoton, A. L., Jr. (1975). Microsurgical anatomy of the sellar region, *Journal of Neurosurgery*, 43(3), 288-298. Retrieved Mar 24, 2021.

Rhoton A. L., Jr (2002). The sellar region. *Neurosurgery*, 51(4 Suppl), S335–S374.

Sacher, M., Som, P. M., Shugar, J. M., and Leeds, N. E. (1986). Kissing intrasellar carotid arteries in acromegaly: CT demonstration. *Journal of computer assisted tomography*, *10*(6), 1033-1035.

Schulze, F., Bühler, K., Neubauer, A., Kanitsar, A., Holton, L., & Wolfsberger, S. (2010). Intra-operative virtual endoscopy for image guided endonasal transsphenoidal pituitary surgery. *International journal of computer assisted radiology and surgery*, *5*(2), 143-154.

Secchi, M. M. D., Dolci, R. L. L., Teixeira, R., and Lazarini, P. R. (2018). An analysis of anatomic variations of the sphenoid sinus and its relationship to the internal carotid artery. *International archives of otorhinolaryngology*, 22(2), 161-166.

Sildiroglu, Onur and Sivrioglu, Ali and Kara, Kemal and Salihoglu, Murat and Sonmez, Guner and Ozturk, Ersin and Cuce, Ferhat and Saglam, Muzaffer and Mutlu, Hakan. (2015). Variations of the sphenoid sinus in Turkish population and importance in surgical planning: A CT study. *Gulhane Medical Journal*. 57. 1. 10.5455/gulhane.187255.

Solari, Domenico and Villa, Alessandro and De Angelis, Michelangelo and Esposito, Felice and Cavallo, Luigi and Cappabianca, Paolo. (2012). Anatomy and Surgery of the Endoscopic Endonasal Approach to the Skull Base. *Translational medicine @ UniSa*. 2. 36-46.

Szolar, D., Preidler, K., Ranner, G., Braun, H., Kern, R., Wolf, G., ... & Ebner, F. (1994). Magnetic resonance assessment of age-related development of the sphenoid sinus. *The British journal of Radiology*, *67*(797), 431-435.

Terra, E. R., Guedes, F. R., Manzi, F. R., and Boscolo, F. N. (2006). Pneumatization of the sphenoid sinus. *Dentomaxillofacial Radiology*, *35*(1), 47-49.

Twigg, V., Carr, S. D., Balakumar, R., Sinha, S., and Mirza, S. (2017). Radiological features for the approach in trans-sphenoidal pituitary surgery. *Pituitary*, 20(4), 395–402.

Unlu, A., Meco, C., Ugur, H. C., Comert, A., Ozdemir, M., and Elhan, A. (2008). Endoscopic anatomy of sphenoid sinus for pituitary surgery. *Clinical Anatomy*, *21*(7), 627-632.

Uygun, S., Surucu, H. S., Tatar, I., Ozgen, B., Tunali, S., and Berker, M. (2016). Descriptive analysis of sphenovomerine suture and its importance in neurosurgery. *Journal of Craniofacial Surgery*, *27*(7), 1858-1861.

Uzun, A., and Ozdemir, F. (2014). Morphometric analysis of nasal shapes and angles in young adults. *Brazilian Journal of Otorhinolaryngology*, 80(5), 397-402.

Vuksanovic-Bozaric, A., Vukcevic, B., Abramovic, M., Vukcevic, N., Popovic, N., and Radunovic, M. (2019). The pterygopalatine fossa: morphometric CT study with clinical implications. *Surgical and Radiologic Anatomy*, 41(2), 161-168.

Wang, C., Pan, Y., Lu, Y., and Ding, X. (2010). Clinical significance of MRI-aided measurements in the transsphenoidal approach in Chinese adults. *Journal of Clinical Neuroscience*, 17(12), 1523-1526.

Wang, S. S., Wei, L., Jing, J. J., and Zhang, S. M. (2016). Three-dimensional reconstruction and morphological characterization of pituitary macroadenomas. *Archives of medical science*: AMS, 12(3), 576–586.

Wei, L. F., Zhang, J., Chen, H. J., and Wang, R. (2013). Value of anatomical landmarks in single-nostril endonasal transnasal-sphenoidal surgery. *Experimental and therapeutic medicine*, *5*(4), 1057-1062.

Wiebracht, N. D., & Zimmer, L. A. (2014). Complex anatomy of the sphenoid sinus: a radiographic study and literature review. *Journal of Neurological Surgery Part B: Skull Base*, *75*(6), 378-382.

Wu, H. B., Zhu, L., Yuan, H. S., & Hou, C. (2011). Surgical measurement to sphenoid sinus for the Chinese in Asia based on CT using sagittal reconstruction images. *European Archives of Oto-Rhino-Laryngology*, *268*(2), 241-246.

Yeung, W., Twigg, V., Carr, S., Sinha, S., and Mirza, S. (2018). Radiological "Teddy Bear" Sign on CT Imaging to Aid Internal Carotid Artery Localization in Transsphenoidal Pituitary and Anterior Skull Base Surgery. *Journal of neurological surgery*. Part B, Skull base, 79(4), 401–406.

Zada, G., Agarwalla, P. K., Mukundan, S., Dunn, I., Golby, A. J., and Laws, E. R. (2011). The neurosurgical anatomy of the sphenoid sinus and sellar floor in endoscopic transsphenoidal surgery. *Journal of neurosurgery*, *114*(5), 1319-1330.

Zufiría, L. O., Alobid, I., Berenguer, J., Valduvieco, I., and Verger, E. (2015, March). Imaging of the anterior and central skull base as a guide for endoscopic skull surgery. European Congress of Radiology 2015.

ETHICAL DECISION

T.C.
ONDOKUZ MAYIS ÜNİVERSİTESİ
KLİNİK ARAŞTIRMALAR ETİK KURULU

Sayı: B.30.2.ODM.0.20.08/1023-1072

21.01.2020

Sayın Doç.Dr. Mennan ECE PİRZİRENLİ

Etik Kurulumuza sunmuş olduğunuz **Sella Turcica Bölgesine Transsfenoidal Girişimlerle İlgili Kranial Yapıların Nörogörüntüleme Tekniği İle Morfometrik Analizi** başlıklı OMÜ KAEK 2019/895 Karar nolu Radyoloji çalışması nitelikli araştırma projeniz amaç, gerekçe, yaklaşım ve yöntemle ilgili açıklamaları açısından Klinik Araştırmalar Etik Kurulu yönergesine göre incelenmiş ve etik açıdan bir sakınca olmadığına, çalışmanın süresi 6 ayı geçerse 6 aylık bildirimlerinin yapılmasına, çalışma tamamlandıktan sonra sonucunun tarafımıza en geç üç(3) ay içerisinde bildirilmesine 26.12.2019 tarihli Etik kurulumuzda oy birliği ile karar verilmiştir.

Bilgilerinize arz/rica ederim.

Prof.Dr.Ramis ÇOLAK
Klinik Araştırmalar Etik Kurulu Başkanı

Ondokuz mayıs Üniversitesi Klinik Araştırmalar Etik Kurulu Tel.(0362)3121919/2782 -4576007 Omutaek@gmail.com
Eski Diş Hekimliği Fakültesi 2 Kat Atakum/SAMSUN

CURRICULUM VITEA

Haidar graduated from Baghdad medical school in 1991.
In 2000 board certified neurosurgeon in Iraq
Worked In Iraq and Yemen as neurosurgeon till 2015.
Moved to Turkey and engaged in PhD program in OMU in Samsun in 2016.
interested now in teaching surgical anatomy to new generations of surgeons.

Email : 16220634@stu.omu.edu.tr
ORCID Number: 0000-0002-0387-9343